

**ANL-HEP-TR-03-120**

**HIGH ENERGY PHYSICS DIVISION  
SEMIANNUAL REPORT OF  
RESEARCH ACTIVITIES**

**January 1, 2003 – June 30, 2003**



**ARGONNE NATIONAL LABORATORY**

**Argonne, Illinois**

**Operated by THE UNIVERSITY OF CHICAGO for the**

**U.S. DEPARTMENT OF ENERGY**

**under Contract W-31-109-Eng-38**

Argonne National Laboratory, a U.S. Department of Energy Office of Science laboratory, is operated by The University of Chicago under contract W-31-109-Eng-38.

DISCLAIMER

This report was prepared as an account of work sponsored by an agency of the United States Government. Neither the United States Government nor any agency thereof, nor The University of Chicago, nor any of their employees or officers, makes any warranty, express or implied, or assumes any legal liability or responsibility for the accuracy, completeness, or usefulness of any information, apparatus, product, or process disclosed, or represents that its use would not infringe privately owned rights. Reference herein to any specific commercial product, process, or service by trade name, trademark, manufacturer, or otherwise, does not necessarily constitute or imply its endorsement, recommendation, or favoring by the United States Government or any agency thereof. The views and opinions of document authors expressed herein do not necessarily state or reflect those of the United States Government or any agency thereof.

Available electronically at <http://www.doe.gov/bridge>

Available for a processing fee to U.S. Department of Energy and its contractors, in paper, from:

U.S. Department of Energy  
Office of Scientific and Technical Information  
P.O. Box 62  
Oak Ridge, TN 37831-0062  
phone: (865) 576-8401  
fax: (865) 576-5728  
email: [reports@adonis.osti.gov](mailto:reports@adonis.osti.gov)

Argonne National Laboratory  
9700 South Cass Avenue  
Argonne, Illinois 60439

**HIGH ENERGY PHYSICS DIVISION  
SEMIANNUAL REPORT OF  
RESEARCH ACTIVITIES**

*January 1, 2003 – June 30, 2003*

Prepared from information gathered and edited by  
The Committee for Publications and Information:

Members: P. Malhotra  
J. Norem  
R. Rezmer  
R. Wagner

**December 2003**



## **Abstract**

This report describes the research conducted in the High Energy Physics Division of Argonne National Laboratory during the period of January 1 through June 30, 2003. Topics covered here include experimental and theoretical particle physics, advanced accelerator physics, detector development, and experimental facilities research. Lists of Division publications and colloquia are included.

## Table of Contents

<b>I.</b>	<b>EXPERIMENTAL RESEARCH PROGRAM</b> .....	1
	<b>A. EXPERIMENTS WITH DATA</b> .....	1
	1. Medium Energy Polarization Program .....	1
	2. Collider Detector at Fermilab .....	7
	a) Physics .....	7
	b) The CDF Operations .....	12
	3. The CDF Upgrade Project .....	14
	a) Run IIb Planning .....	14
	4. Non-Accelerator Physics at Soudan.....	16
	5. ZEUS Detector at HERA .....	23
	a) Physics Results.....	23
	b) HERA and ZEUS Operations .....	27
	<b>B. EXPERIMENTS IN PLANNING OR CONSTRUCTION</b> .....	28
	1. The Endcap Electromagnetic Calorimeter for STAR.....	28
	2. Neutrino Oscillation Experiments.....	29
	a) MINOS Main Injector Neutrino Oscillation Search .....	29
	b) Experiments to Measure the $\theta_{13}$ Neutrino Mass-mixing Parameter .....	34
	3. ATLAS Detector Research & Development.....	35
	a) Overview of ANL ATLAS Tile Calorimeter Activities .....	35
	<b>C. DETECTOR DEVELOPMENT</b> .....	36
	1. ATLAS Calorimeter Design and Construction.....	37
	a) Module Instrumentation and Testing .....	37
	b) Testbeam Program .....	37
	c) Engineering Design and Analysis.....	40
	d) Calorimeter Pre-Assembly.....	41
	e) Work in Collaboration with ATLAS Technical Coordination .....	43
	2. ATLAS Computing.....	44
	3. Linear Collider .....	46
	4. Electronics Support Group.....	49
<b>II.</b>	<b>THEORETICAL PHYSICS PROGRAM</b> .....	53
	<b>A. THEORY</b> .....	53
	1. Higgs Boson Production Including All-Orders Soft Gluon Resummation .....	53
	2. Squark Mixing in Electron-Positron Reactions .....	54
	3. $e^+e^-$ Annihilation into $J/\psi + J/\psi$ at $B$ Factories .....	56
	4. Relativistic Corrections to Gluon Fragmentation to $J/\psi$ .....	56
	5. Lattice Gauge Theory .....	57
	6. Precision Electroweak Data and Unification of Couplings in Warped Extra Dimensions .....	58
	7. Membrane Quantization Via Nambu Brackets .....	60

<b>III.</b>	<b>ACCELERATOR RESEARCH AND DEVELOPMENT</b>	62
<b>A.</b>	<b>ARGONNE WAKEFIELD ACCELERATOR PROGRAM</b>	62
1.	The Argonne Wakefield Accelerator Status	62
2.	The New Type of Dielectric Accelerator Developments	63
3.	Other Significant Beam Physics Related Studies	64
<b>B.</b>	<b>MUON COLLABORATION AND R&amp;D</b>	65
a)	Muon Ionization Cooling Experiment	65
b)	Understanding and Extending the Limits of RF Cavities	66
<b>IV.</b>	<b>PUBLICATIONS</b>	67
<b>A.</b>	Books, Journals, and Conference Proceedings	67
<b>B.</b>	Major Articles Submitted for Publication	73
<b>C.</b>	Papers or Abstracts Submitted to Conference Proceedings	76
<b>D.</b>	Technical Reports and Notes	78
<b>V.</b>	<b>COLLOQUIA AND CONFERENCE TALKS</b>	82
<b>VI.</b>	<b>HIGH ENERGY PHYSICS COMMUNITY ACTIVITIES</b>	87
<b>VII.</b>	<b>HIGH ENERGY PHYSICS DIVISION RESEARCH PERSONNEL</b>	91

# I. EXPERIMENTAL RESEARCH PROGRAM

## I.A. EXPERIMENTS WITH DATA

### I.A.1. Medium Energy Polarization Program

During the period January - June, 2003, data were collected with STAR for d + Au and polarized p + p collisions. Argonne physicists participated in STAR data collection shifts, as well as measurements with AGS and RHIC polarimeters. Construction and testing of shower maximum detector modules continued for the STAR endcap electromagnetic calorimeter, as described in another section of this report.

Several papers on STAR physics results were published and a number of others were submitted for publication. In addition, 18 instrumentation articles describing the STAR apparatus were published in Nucl. Instrum. and Meth. A499 (2003) in this period. Argonne authors were on the overview, the barrel electromagnetic calorimeter (EMC), and the endcap EMC papers (pages 624, 725, and 740, respectively).

One of the physics articles (“Azimuthal Anisotropy and Correlations in the Hard Scattering Regime at RHIC,” Phys. Rev. Lett. 90, 032301 (2003)) describes an analysis of Au + Au collisions at  $\sqrt{s_{NN}} = 130$  GeV. The azimuthal anisotropy of charged particles with transverse momenta  $2 < p_T < 6$  GeV/c relative to the reaction plane defined by low  $p_T$  particles was measured for three collision centralities, as shown in Fig. 1. The elliptic flow parameter,  $v_2$ , was obtained from fits to these azimuthal distributions, and the results as a function of  $p_T$  are plotted in Fig. 2. A saturation of  $v_2$  above about  $p_T = 3$  GeV/c is observed, which contradicts the predictions of nondissipative hydrodynamics models. Also, a comparison of the two-particle azimuthal correlation functions for particles with  $|\Delta\eta| < 0.5$  and  $|\Delta\eta| > 0.5$  suggests the existence of a short-ranged correlated component at high  $p_T$  in addition to underlying global elliptic flow. This may be the first direct evidence at RHIC for hard scattering and parton fragmentation in heavy ion collisions.

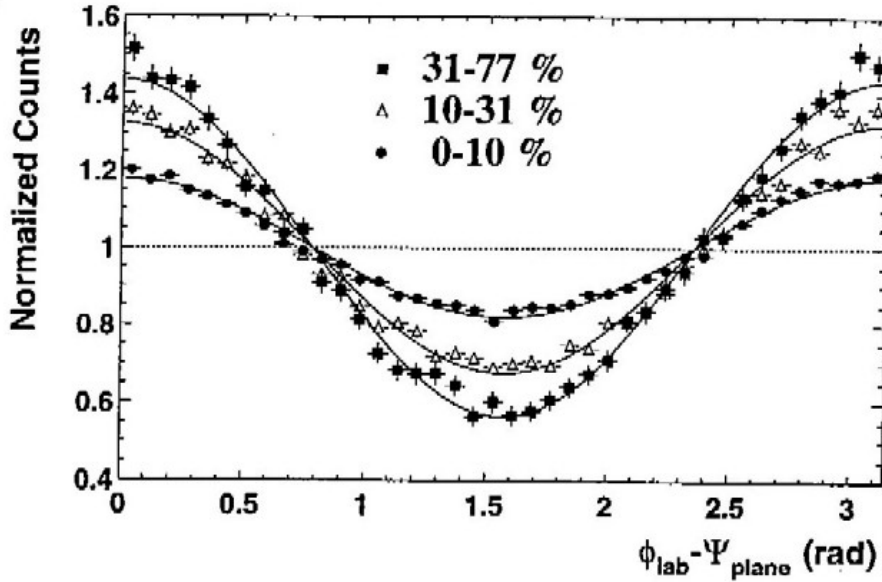


**Figure 1.** Azimuthal distributions with respect to the reaction plane of charged particles with  $2 < p_T < 6$  GeV/c for three collision centralities. The percentages are given with respect to the geometrical cross section. Solid lines show fits to the form  $1 + 2 v_2 \cos[2(\phi_{\text{lab}} - \Psi_{\text{plane}})]$ .

Another paper (“Narrowing of the Balance Function with Centrality in Au + Au Collisions at  $\sqrt{s_{\text{NN}}} = 130$  GeV,” Phys. Rev. Lett. **90**, 172301 (2003)) describes a new observable for heavy ion collisions based on the principle that charge is locally conserved when particles are pair-produced; it is similar in form to what was used over 20 years ago in the study of charge balance in  $p + p$  and  $e^+ + e^-$  interactions. Balance functions for charged particle pairs or identified charged pion pairs for peripheral collisions have widths consistent with model predictions based on a superposition of nucleon-nucleon scatterings. Widths in central collisions are smaller, consistent with trends predicted by models incorporating late hadronization. Further study of sensitivity to flow, resonance particle production, and diffusion is required before definitive statements can be made, however.

Yields of  $K^-$ ,  $\Lambda^0$ ,  $\Xi^-$ , and  $\Omega^-$  and their antiparticles are reported in “Strange Antiparticle-to-Particle Ratios at Mid-Rapidity in  $\sqrt{s_{\text{NN}}} = 130$  GeV Au + Au Collisions” (Phys. Lett. **B567**, 167 (2003)). The antiparticle-to-particle ratios appear to be independent of  $p_T$  and

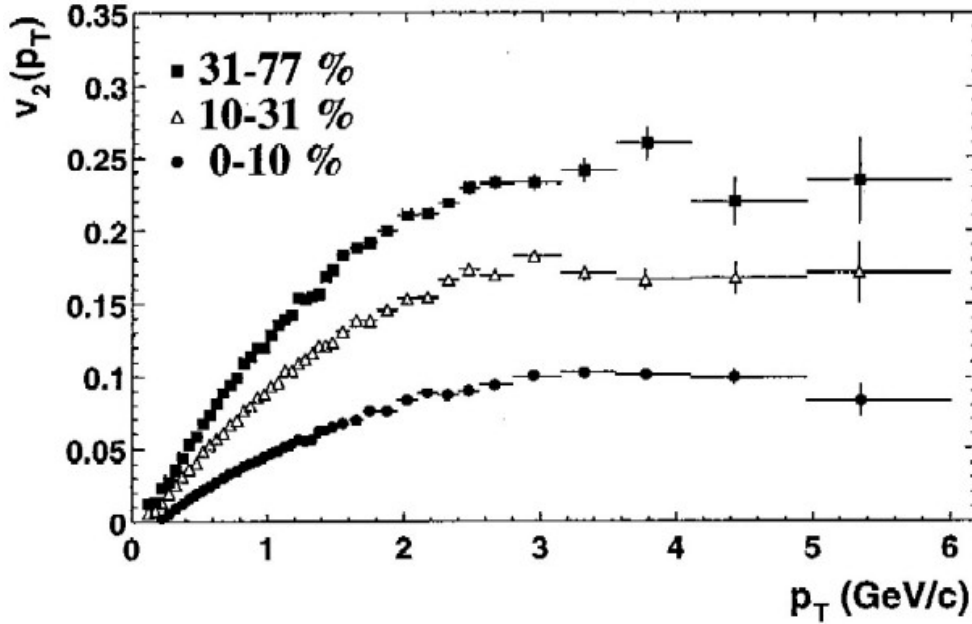


**Figure 2.** The elliptic flow parameter,  $v_2$ , as a function of  $p_T$  for different collision centralities. The errors shown are statistical only. The systematic uncertainties, which are highly correlated point-to-point, are +5% and -20%. The approximately linear rise of  $v_2$  up to  $p_T = 2$  GeV/c is followed by a saturation above 3 GeV/c.

there is an excess of hyperons over anti-hyperons. These results are consistent with simple quark counting models and with a statistical description of particle production, which is governed by a common baryon chemical potential and chemical freeze-out temperature.

A fourth STAR paper was “Disappearance of Back-to-Back Hadron Correlations in Central Au + Au Collisions at  $\sqrt{s_{NN}} = 200$  GeV” (Phys. Rev. Lett. **90**, 082302 (2003)). Azimuthal correlations for relatively high transverse momentum charged hadrons were measured over a wide pseudorapidity range and full azimuth in Au + Au and p + p collisions at  $\sqrt{s_{NN}} = 200$  GeV. The correlation functions required a trigger particle with  $4 < p_T^{\text{trig}} < 6$  GeV/c and associated particles with  $2 \text{ GeV/c} < p_T < p_T^{\text{trig}}$ . The small angle correlations observed in p + p and at all centralities in Au + Au collisions (see Fig. 3) are characteristic of hard-scattering

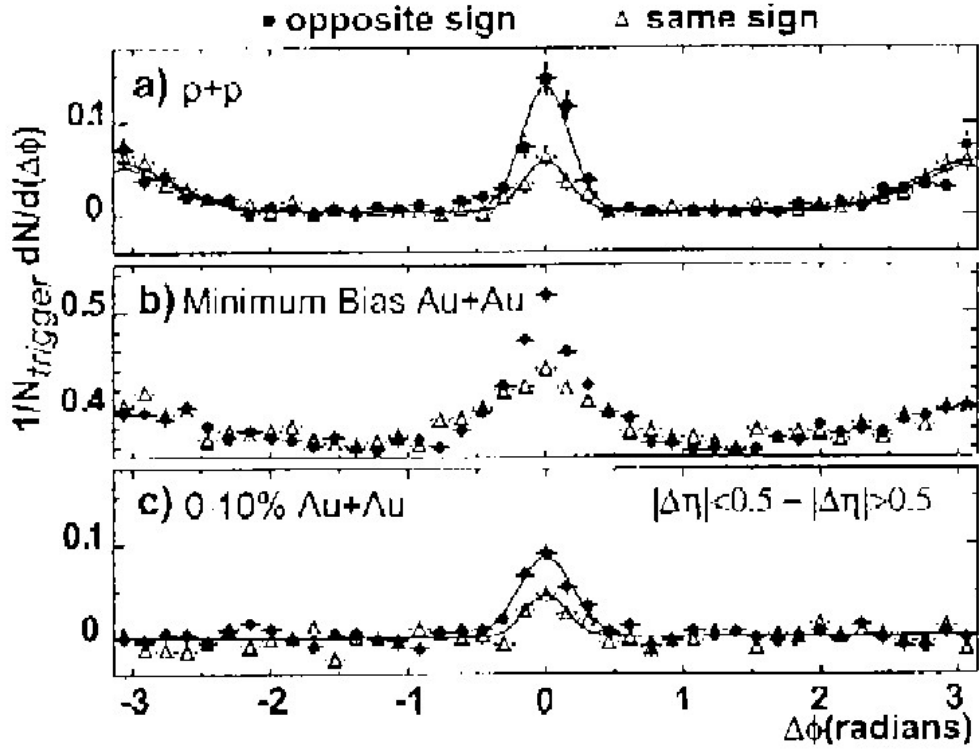


**Figure 3.** Azimuthal distributions of same sign and opposite sign pairs for (a)  $p + p$ , (b) minimum bias  $Au + Au$ , and (c) the difference between azimuthal distributions for  $|\Delta\eta| < 0.5$  and for  $0.5 < |\Delta\eta| < 1.4$  for central  $Au + Au$  collisions. The curves are one or two Gaussian fits. Near  $\Delta\phi = 0$ , the distributions have similar shapes.

processes, namely jets, previously observed in high energy interactions. A strong back-to-back correlation is observed for  $p + p$  and peripheral  $Au + Au$  collisions. In contrast, the back-to-back correlations are reduced considerably in the most central  $Au + Au$  collisions shown in Fig. 4, indicating substantial interaction of hard scattered partons or their fragmentation products in the medium, and suggesting a strong dependence on the geometry and distance of traversal.

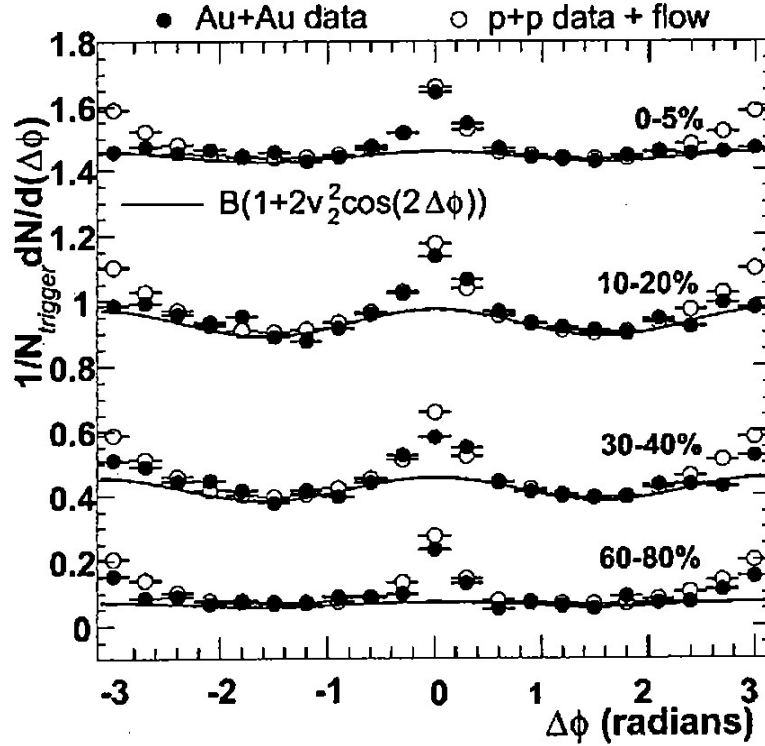


**Figure 4.** Azimuthal distributions for  $0 < |\Delta\eta| < 1.4$  and  $4 < p_T^{\text{trig}} < 6$  GeV/c for four centrality classes of Au + Au collisions (solid circles). The solid curves are the elliptic flow contributions. The open circles are from a simple model with elliptic flow plus hard scattering processes in common with p + p interactions. Note the increasing suppression below the model of the back-to-back correlations for more central collisions.

Preliminary STAR data from the d + Au running at  $\sqrt{s_{\text{NN}}} = 200$  GeV, which ended in March 2003, suggested final state suppression of high  $p_T$  hadrons in Au + Au central collisions compared to p + p and d + Au interactions. The data are shown in Fig. 5, comparing d + Au central collisions and minimum bias events, p + p minimum bias, and Au + Au central events; a paper describing these data was submitted for publication. These results and others from the RHIC heavy ion detectors prompted a meeting called by Brookhaven management to see if there was sufficient evidence to claim the discovery of a quark-gluon plasma. At the meeting, it was decided that additional measurements were required to truly establish or refute the presence of this new state of matter.

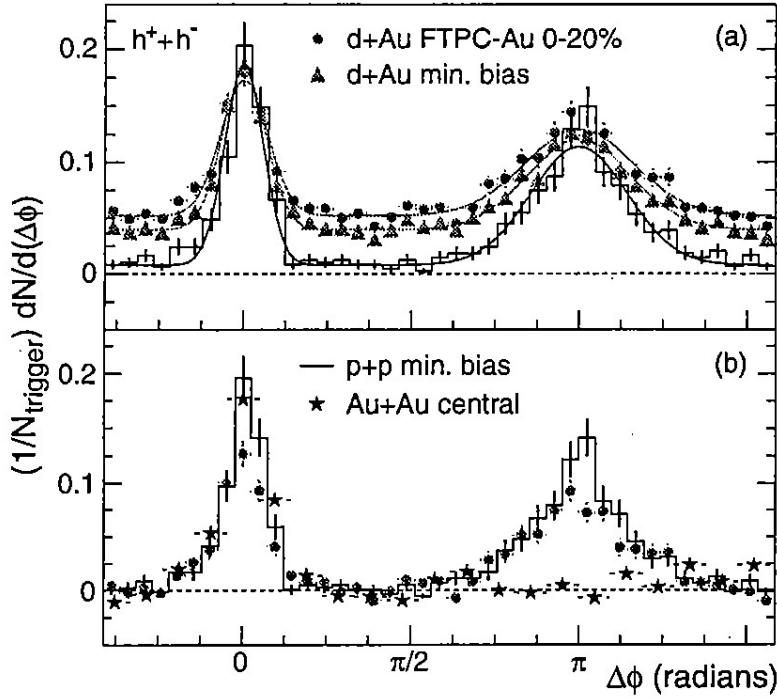


**Figure 5.** Efficiency corrected two-particle azimuthal distributions for minimum bias  $d + \text{Au}$  and  $p + p$  and for central  $d + \text{Au}$  and  $\text{Au} + \text{Au}$  collisions at  $\sqrt{s_{\text{NN}}} = 200$  GeV. The particles are required to satisfy  $0 < |\eta| < 0.7$ ,  $4 < p_{\text{T}}^{\text{trig}} < 6$  GeV/c, and  $2 < p_{\text{T}} < p_{\text{T}}^{\text{trig}}$ . The contrast between  $d + \text{Au}$  and central  $\text{Au} + \text{Au}$  collisions indicates that the cause of the strong high  $p_{\text{T}}$  suppression is associated with the medium produced in  $\text{Au} + \text{Au}$  but not in  $d + \text{Au}$  events.

A paper was also published from results with the Crystal Ball detector at Brookhaven. “Measurement of the  $\pi^- p \rightarrow 3 \pi^0 n$  Total Cross Section from Threshold to 0.75 GeV/c” (Phys. Rev. **C67**, 068201 (2003)) reports the cross sections from 0.47 to 0.75 GeV/c. Backgrounds from  $\eta \rightarrow 3 \pi^0$  decays are substantial above 0.68 GeV/c, and have been subtracted. A simple analysis of the data results in the estimated branching fraction  $B[N^*(1535) \rightarrow \pi N^*(1440)] = (8 \pm 2)\%$ , which is the first such estimate obtained with a three-pion production reaction.

Analysis of RHIC polarimeter data from the 2001/2002 run by a number of physicists, including some from Argonne, indicated systematic errors were present at a level comparable to statistical uncertainties per run ( $\delta P_B \sim 0.03$  for the beam polarization). In early 2003, an explanation for these systematic errors in terms of rate effects was developed by an Argonne scientist. Numerical estimates were consistent with the magnitude of the observed systematic errors, and this explanation was discussed with physicists working on the AGS and RHIC polarimeters. Subsequently, plans to improve the polarimeter performance are being considered.

(H. Spinka)

## I.A.2. Collider Detector at Fermilab

### a) Physics

The quality of the vast majority of the new data continues to be good enough for physics. Samples of about  $72 \text{ pb}^{-1}$  were created for analyses aimed at the winter conferences. Samples of about  $126 \text{ pb}^{-1}$  were available for summer conferences so that statistics of run II have caught up with run I, and systematic understanding of the data is getting there.

Some analyses, such as the W and Z boson cross sections and the Z charge asymmetry have opted to go for publication on the initial sample and are going through publication preparation. Most analyses are updating as data comes in.

The silicon is only rarely excluded from data taking, and the coverage which is actually working for the trigger is over 90%. The silicon impact parameter trigger (SVT) efficiency has been substantially increased by implementing a 4/5 hit stub strategy in the silicon. Bill Ashmanskas, who joined us as a Compton Fellow, was a key contributor to making that happen. Large hadronic heavy flavor samples have become available, although  $B_s$  mixing samples are growing slowly and the overall tracking alignment needed to make sense of the innermost silicon layer is ongoing. The  $B_s$  signal in  $D_s\pi$  is shown in Fig. 1 and agrees with the simulation shown in Fig. 2. Unfortunately we need flavor tagging.

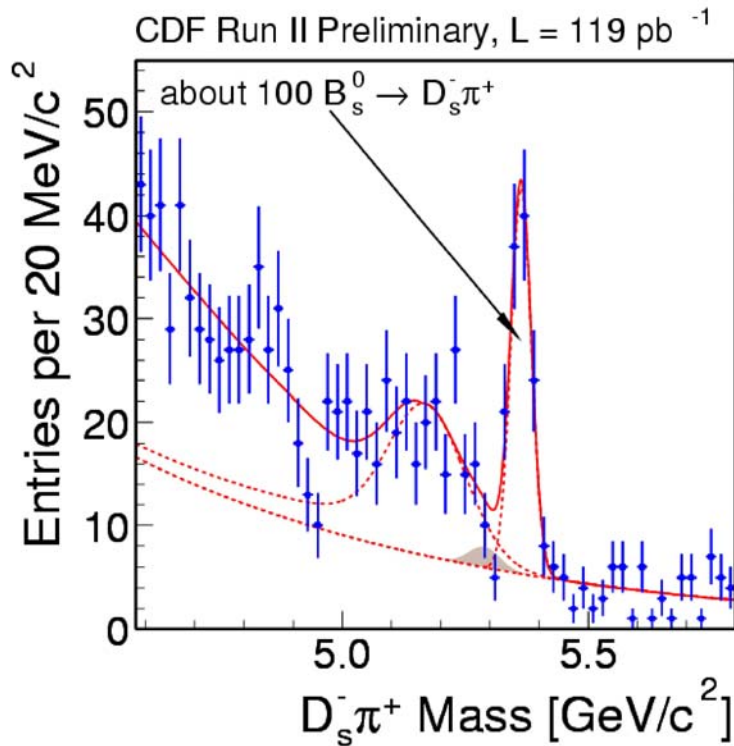
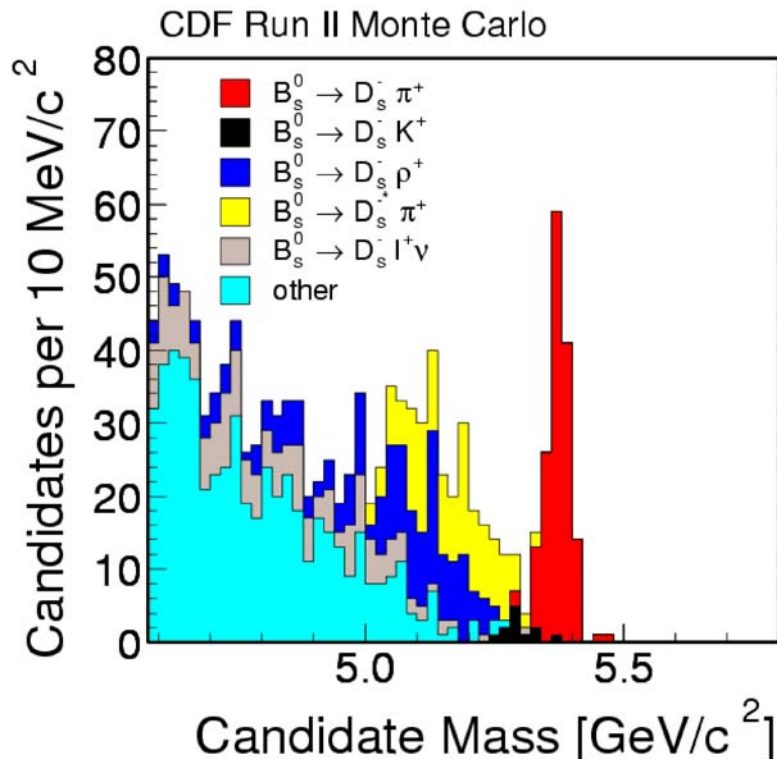


Figure 1.  $B_s$  signal in CDF run II data in  $D_s\pi$ .

While Bob Blair and Steve Kuhlmann work on QCD and searches involving photons, and Larry Nodulman works on electroweak physics, the rest of the group is working on b



**Figure 2.** Predicted sources of Bs signal in Dsπ for CDF run II data.

physics. Much of the early physics productivity of CDF run II is actually charm. Tom LeCompte has been pushing the low transverse momentum muon measurement for J/Ψ production and a result was released for the winter conferences, shown in Fig. 3. In 40 pb<sup>-1</sup> of data, the cross section time branching ratio for J/Ψ to μμ with absolute pseudorapidity less than 0.6 was found to be 240 +35 -28 nb where the uncertainties are essentially systematic. This program will eventually disentangle b production over the full transverse momentum range as well.

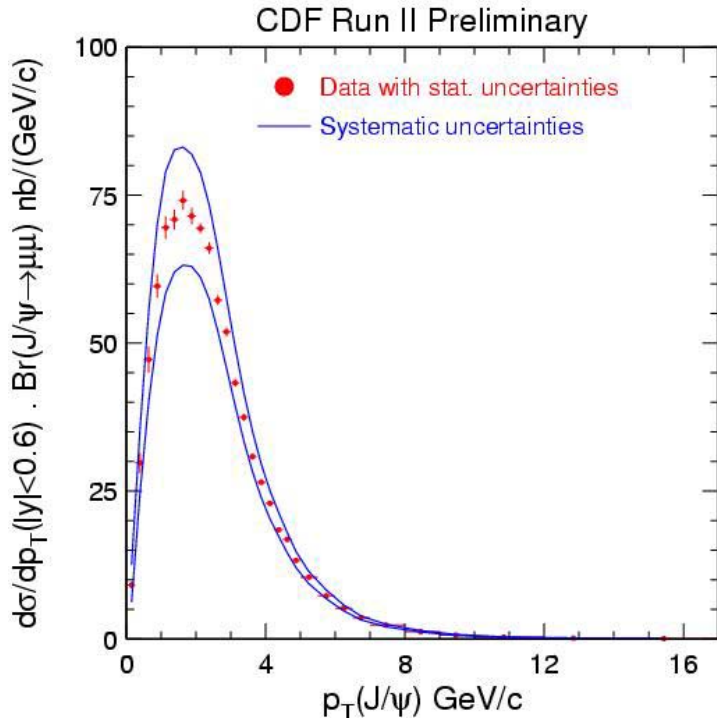


**Figure 3.** Dimuon  $J/\Psi$  transverse momentum distribution.

Another early result involves Bill Ashmanskas; hadronic impact parameter triggers are used to set a limit on the branching ratio for  $D^0$  to  $\mu\mu$ .  $D^*$  decays with  $D$  to  $\pi\pi$  are used for normalization, shown in Fig. 4. The search for muon pairs in the relevant mass window is shown in Fig. 5, and limits of  $2.4 \times 10^{-6}$  (90%) and  $3.1 \times 10^{-6}$  substantially improve on previous results from BEATRICE and E771.

## CDF Run II Preliminary

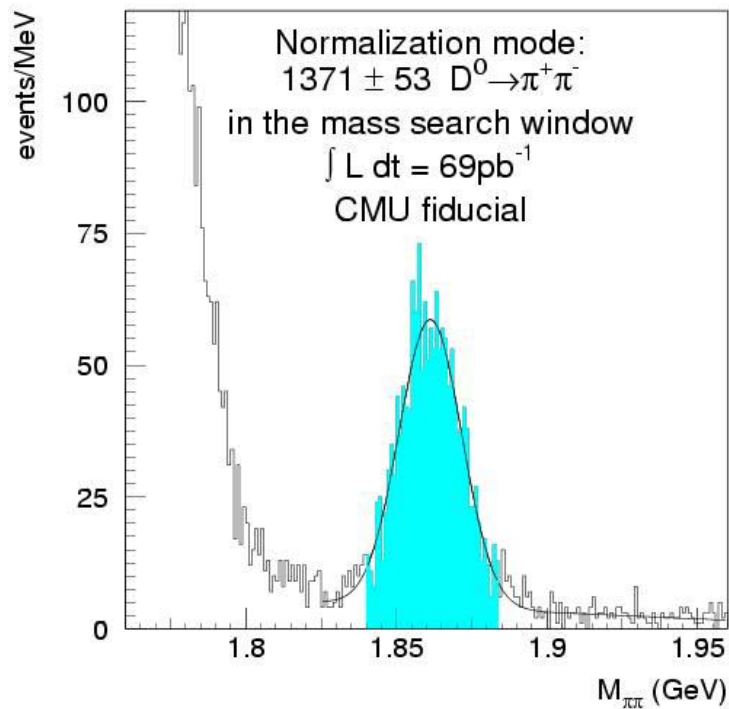


**Figure 4.** Two pion normalization mode for  $D^0$  decay; the pions are required to be pointed at muon chambers (CMU).

Masa Tanaka has become involved in studying various systematic effects which could contribute to an apparent discrepancy between lifetimes as measured in fully reconstructed inclusive B decays and silicon triggered semileptonic decays. So far his studies show that the trigger bias is accounted correctly.

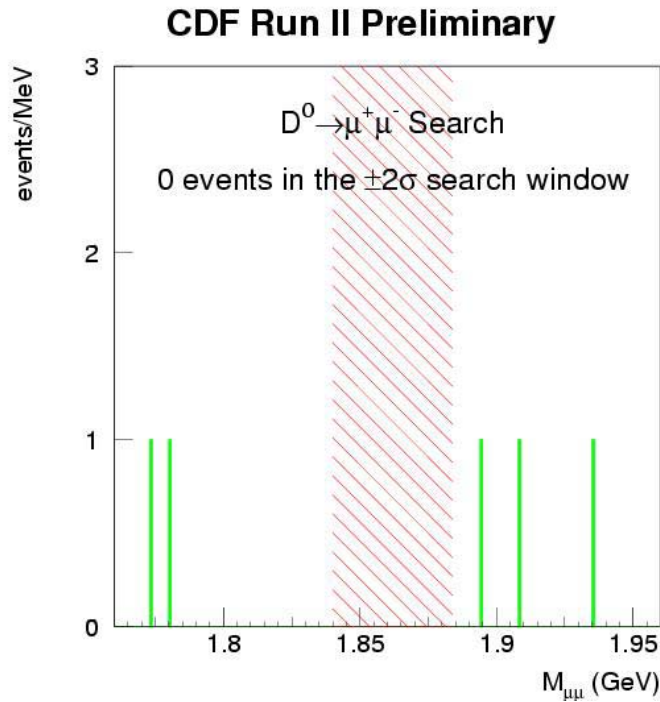


**Figure 5.**  $D^0$  muon pair search window.

In photon physics, the basic run 1 techniques for distinguishing signal and background have been reestablished with the substantial material changes of run II and physics results will follow soon.

The top mass has many devotees and despite the lack of physics impact of a result at this stage, having some result was felt to be needed as a sign of rebirth of the CDF physics program, and a result was released for winter conferences, shown in Fig. 6. Work continues on refining the understanding the systematics of the measurement which will eventually allow improvement on our run I results. For the W mass, a small group has begun to work on both muons and electrons.

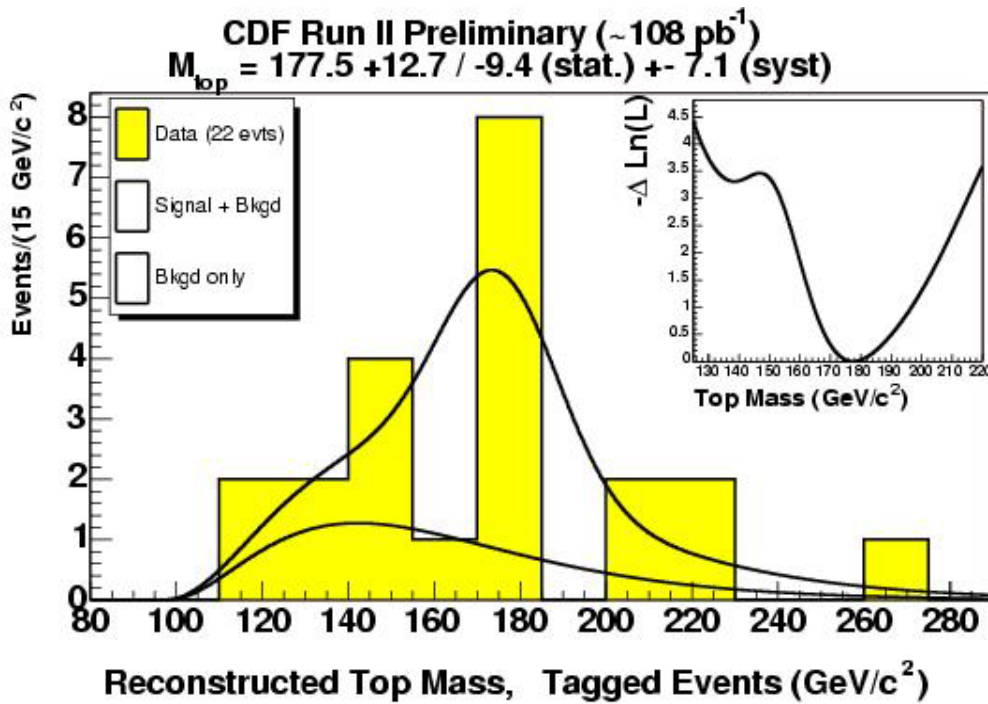


**Figure 6.** Run II top mass reconstruction from the lepton plus jets with vertex tag sample. Good thing it was prettier in run I.

**b) The CDF Operations**

Steady data taking of physics quality continued. Jimmy Proudfoot’s operational concerns as Deputy Head of CDF Operations included monitoring data quality, increasing operational efficiency, and developing of the trigger and DAQ bandwidth. There has been considerable progress in all those areas. The progress is illustrated in Fig. 7. Larry Nodulman

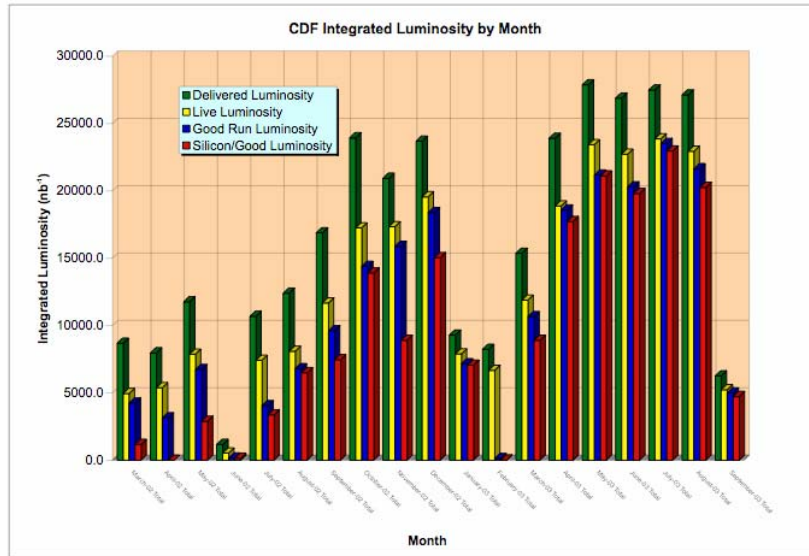


**Figure 7.** Luminosity delivered, written, good for physics, and including silicon by month for the 19 months run of run II through September 2003.

continued as co leader (“SPL”) for calorimeter operations. Masa Tanaka started his term as one of the three operations managers. The efficiency of data taking is shown in Fig. 8.

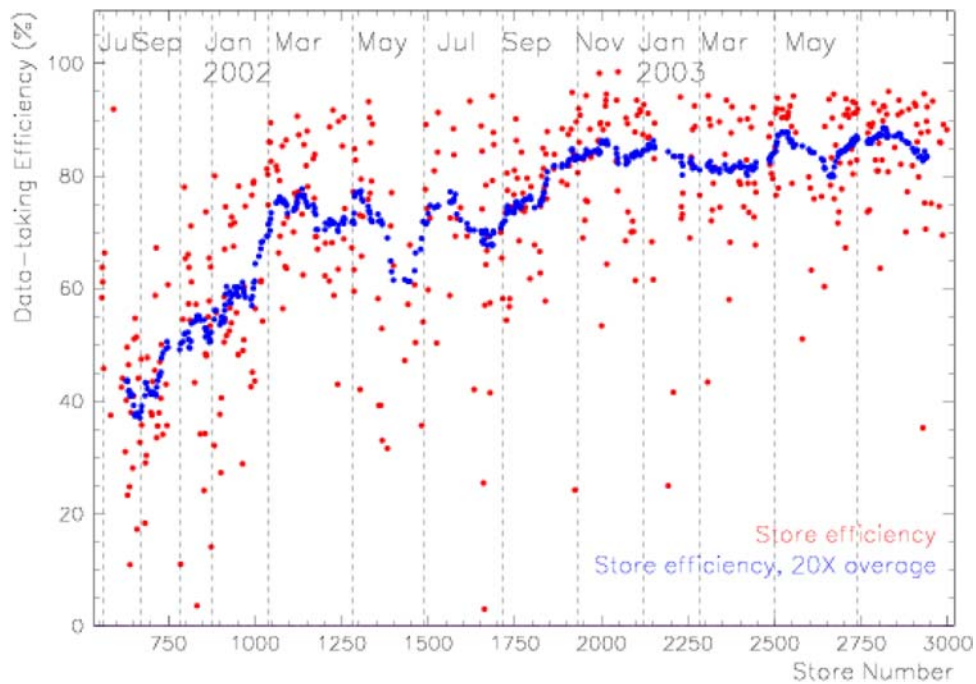


**Figure 8.** Efficiency of CDF data taking in run II.

Karen Byrum, with help from Steve Kuhlmann, Jimmy Proudfoot and Larry Nodulman and Gary Drake and company, as well as Mike Lindgren from UCLA, continued support the shower max readout operations; this continues to be a reasonably stable operational equilibrium.

Our electronics in the Level 2 trigger, the shower max trigger and the isolation trigger, continued operations supported by Masa Tanaka, Karen Byrum, Steve Kuhlmann and Bob Blair. Bill Ashmanskas gradually detached himself from supporting the silicon track trigger.

Larry Nodulman worked to monitor the performance of the central EM calorimeter. The overall scale continued to fall slowly during the period and online scale factor was again increased by 3% to keep trigger gain close to being correct. The gains for individual towers began to show dispersion as time went on since the pmt gains were downloaded. Detailed run dependence and tower corrections from inclusive electrons are provided for use offline. .

Bob Wagner continued to head the offline electron and photon software effort. He also, along with Barry Wicklund and Larry Nodulman, worked with the Electron Task Force to define electrons correctly and provide convenient access to the relevant numbers derived from the data. Most of the emphasis of the Electron Task Force continues to be on developing the plug region..

Barry Wicklund was also a leader of the B physics trigger strategy group. Improvements of the capabilities and strategy for triggering on tracks with impact parameter are continuing.

We are planning for a long shutdown in the fall, motivated by recycler work. We plan to do calorimeter source runs, drift chamber wire plane replacements, silicon repairs and some initial installation of the EM timing calorimeter upgrade.

### **I.A.3. The CDF Upgrade Project**

#### **a) Run IIb Preparation**

While the silicon upgrade appeared to be increasingly vulnerable in light of decreasing projected luminosity achievement for the Tevatron (all of run II has become run IIa), the preradiator project remained possible. Steve Kuhlmann is the Level 2 manager for calorimeters, which also includes the EM timing upgrade, as well as taking a leading role in the preradiator project. The preradiator upgrade, with considerable support from Japan, Italy and Russia, continues to pass hurdles and prototypes were built and tested. The MINOS test stand at Argonne has been modified to do development and production quality control. A scan of a prototype preradiator, corrected for pmt and fiber bundle variation, is shown in Fig. 9. The

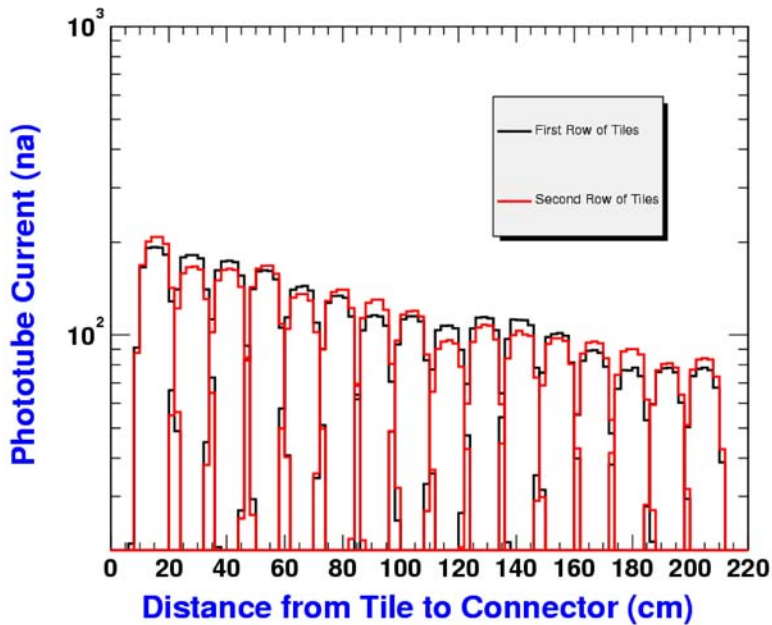


**Figure 9.** Scan results from the prototype preradiator on the MINOS test stand, corrected for pmt and fiber bundle gain/transmission variation. Attenuation is disappointing but the light yield and scintillator uniformity is good.

prototype is shown in Fig. 10. Design work and planning for production at Argonne are essentially complete and installation issues have become most important as we may not be hiding behind a silicon installation.

Jimmy Proudfoot and Bob Blair have a plan to use ATLAS ROI builder technology as part of the DAQ upgrade; this fits in well with the new Level 2 trigger scheme.

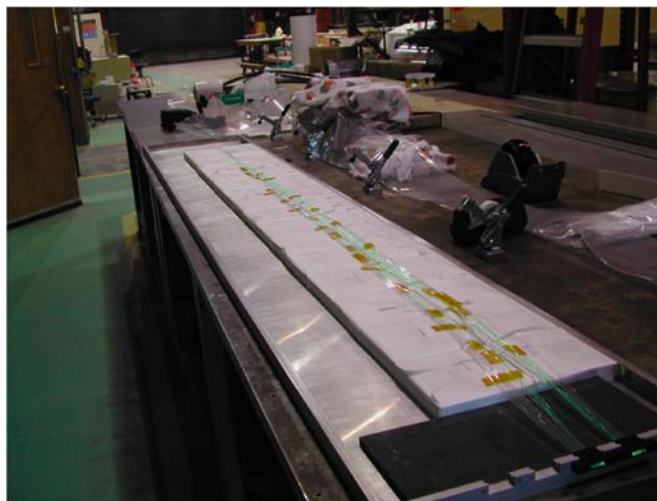


**Figure 10.** CPR tiles and fibers being assembled for the preradiator prototype.

**(L. Nodulman)**

#### I.A.4. Non-Accelerator Physics at Soudan

In July 2001, the Soudan-2 experiment completed the taking of data using its fine-grained iron tracking calorimeter of total mass 963 tons. Results on atmospheric neutrinos presented here are based upon the total exposure, which is 5.91 fiducial kiloton-years (kTy). Soudan-2 was originally designed to study proton decay and thus has excellent resolution and pattern recognition properties in the visible energy region around 1 GeV where the peak in the atmospheric neutrino event rate occurs. Although the exposure of the experiment is less than that of Super-K, the full event reconstruction, and thus good energy and direction resolution for the incident neutrino, compensates to some extent for the smaller number of events.

The Soudan 2 data are variously classified according to containment, veto shield activity, topology and resolution. There are two containment classes.

1. Fully Contained Events (FCE): Containment is defined by the requirement that no portion of the event approaches closer than 20 cm to the exterior of the detector and that no particle in the event could enter or escape the detector through the space between modules. The containment criterion limits high energy  $\nu_\mu$  events to those with a muon of energy less than  $\sim 1$  GeV.
2. Partially Contained Events (PCE): These events recover a fraction of the high energy  $\nu_\mu$  events rejected by the containment criterion. As the muon does not stop in the detector, its energy from range cannot be measured. Instead an estimate of the energy was obtained from the observed range, with a small added correction based on the amount of multiple scattering on the track.

Two classes of events are defined on the basis of the presence or absence of hits in the veto shield.

1. Quiet shield events: These events have no in-time hits in the veto shield except for those associated with the leaving lepton in PCEs. They are neutrino candidates but contain background. They will be called “*qs-data*” events.
2. Shield tagged “*ck*” events: Events initiated by the passage of a cosmic ray muon generally have in-time hits in the veto shield. Secondary neutral particles can enter the detector and interact, mimicking neutrino interactions.

The average shield efficiency for detection of a minimum ionizing particle was measured to be 94%. Study of events with a single shield hit showed that the contamination of *qs-data* events by cosmic ray muons which pass through the shield and enter the detector is negligible. It was however possible for neutrons and gamma rays to enter the detector with no identifying shield hit when all of the charged particles associated with the production event in the

rock passed outside the shield or were not detected due to shield inefficiency. These quiet shield rock events (called “*qs-rock*”) are a background to the neutrino sample. They may be statistically distinguished from neutrino events by the depth distribution of the interaction vertices.

The background from *qs-rock* events is significantly different in low and high multiplicity events and in low multiplicity electron and muon samples. The FCE data are thus further divided into topology classes.

1. Events with a single track-like particle with or without a recoil proton, called “tracks”. These are mostly quasi-elastic  $\nu_\mu$  interactions and are assigned  $\mu$ -flavor.
2. Events with a single showering particle with or without a recoil proton called “showers”. These are mostly quasi-elastic  $\nu_e$  interactions and are assigned e-flavor.
3. Events with multiple outgoing tracks and/or showers called “multiprongs”. These can be of either flavor. The flavor is assigned according to whether the highest energy secondary is a track ( $\mu$ -flavor) or shower (e-flavor). A small fraction of multiprongs have no muon or electron candidate and are defined as neutral current (NC). A further small sample had no obvious flavor and are defined as ambiguous. The NC events are too few to provide constraints on the oscillation analysis but they and the ambiguous events are added into the event total, contributing to the flux normalization.

At low neutrino energies the correlation between the direction of the outgoing lepton and the incoming neutrino is poor. Using the ability of Soudan~2 to reconstruct the recoil proton from quasi-elastic interactions and the low energy particles from inelastic reactions gives a major improvement in the neutrino pointing and energy resolution. Utilizing this improved reconstruction, the events are finally divided into two samples depending on the L/E resolution.

1. A high resolution “HiRes” sample:
  - A. events with a single lepton of kinetic energy  $>600$  MeV,
  - B. events with a single lepton of kinetic energy  $>150$  MeV with a reconstructed recoil proton,
  - C. multiprong events with lepton kinetic energy  $>250$  MeV, total visible momentum  $>450$  MeV/c and total visible energy  $>700$  MeV,
  - D. partially contained events. The mean neutrino pointing error for events in this sample is  $33^\circ$  for  $\nu_\mu$  FCE,  $21^\circ$  for  $\nu_e$  FCE and  $14^\circ$  for  $\nu_\mu$  PCE. This yields a mean error in  $\log_{10}(L/E)$  approximately 0.2.
2. A low resolution “LoRes” sample, comprising all other events.

The numbers of events analyzed are shown in Table 1. The oscillation analysis described in this paper imposed a minimum 300 MeV/c cut on the lepton momentum for LoRes track and shower events and the total visible momentum for LoRes multiprong events. The numbers headed “Raw” in the table are those for the total event sample without this cut, the other numbers include the cut. The table shows that the rock background is concentrated in low energy events which are removed by the cut. The value of the cut was chosen to optimize the analysis sensitivity by reducing the background component while retaining the neutrino signal. The final two columns are the fitted number of *qs-rock* events and the number of neutrino events after subtraction of the *qs-rock* background.

Class	Flavor	<i>qs-data</i>	MC	rock	<i>qs-data</i>	MC	rock	<i>qs-rock</i>	neutrino
		←---	Raw	-->	←---	-----	300 MeV cut	-----	-->
FCE HiRes	$\mu$	114	1149	73	114	1115.1	73	12.1±6.9	101.9±12.7
FCE HiRes	e	152	1070	69	152	1047.4	69	5.3±	±
FCE LoRes	$\mu$	148	900	406	61	457.5	77	11.5±6.2	49.5±9.9
FCE LoRes	e	177	850	704	71	402.5	176	14.0±4.6	57.0±9.6
PCE	$\mu$	53	373	11	53	384.3	11	0.3±0.9	52.7±7.3
PCE	e	5	51	0	5	51.5	0	0.0±0.1	5.0±2.2
NC		46	246	190	32	165.7	110	7.6±6.7	24.4±8.8
Total		695	4639	1453	488	3624.0	516	50.8	437.2

**Table 1:** Event samples in the 5.90 fiducial kiloton-year exposure. The columns for raw events are the total numbers of events reconstructed in this experiment. The columns headed “300 MeV/c cut” give the event numbers used in the oscillation analysis described in this paper. The MC numbers in these columns have been weighted to convert from the Bartol 89 flux prediction to the Bartol 96 values. The *qs-rock* column gives the fitted number of background *qs-rock* events and the neutrino column is the number of neutrino *qs-data* events after subtraction of the *qs-rock* background.

An extended maximum likelihood analysis assuming two-flavor  $\nu_\mu \rightarrow \nu_\tau$  oscillations has been used to obtain estimates of the neutrino oscillation parameters. The significance of the result and the confidence intervals on the oscillation parameters are determined using the unified method advocated by Feldman and Cousins. The likelihood function used to describe the *qs-data* assumes that the sample is composed of neutrino interactions, represented by the Monte Carlo events, and *qs-rock* background events, represented by the rock sample. Each sample is divided into  $\mu$ -flavor, e-flavor and NC plus ambiguous events. Since neither  $\nu_e$  nor “NC” events are assumed to oscillate they can be considered as a single category. For shorthand in the following they are combined under the heading of e-flavor.

The L/E distribution of the  $\mu$ -flavor events is examined for evidence of oscillations. The total number of events,  $\mu$ -flavor plus e-flavor, provides the normalization of the Monte

Carlo exposure. Monte Carlo events with misidentified flavor are included in the  $\mu$ -flavor or e-flavor samples with the oscillation probabilities appropriate to their true parameters.

The two oscillation parameters to be determined are  $\sin^2 2\theta$  and  $\Delta m^2$ . Seven other unknown quantities, the normalization of the MC, A, the five rock fractions for the different  $\mu$ -flavor samples and the rock fraction for the e-flavor sample are nuisance parameters. In general their fitted values will be correlated with the values of the oscillation parameters. The amount of qs-rock background in the e-flavor sample is estimated by a fit to the e-flavor depth distributions and is assumed independent of the oscillation parameters.

The negative log likelihood is calculated on a 15 x 80 grid of  $\sin^2 2\theta$ - $\log_{10} \Delta m^2$  with  $\sin^2 2\theta$  between 0.0 and 1.0 and  $\Delta m^2$  between  $10^{-5}$  and  $10^0$  eV<sup>2</sup>. The oscillation probability, P, is averaged over the area of each grid point. The range of  $\Delta m^2$  was chosen such that outside this range the predictions for  $\log_{10}(L/E)$  are constant. Below the lower limit the oscillation probability is close to one for the whole  $\log_{10}(L/E)$  range, above the upper limit the probability averages to 0.5.

At each grid point the likelihood is minimized as a function of each of the remaining four  $\mu$ -flavor rock fractions. The value of A is calculated by requiring that the predicted number of Monte Carlo plus qs-rock events equals the number of qs-data events. For simple likelihood functions this is a mathematical condition for the minimum. It was tested and found to be a very good approximation for this likelihood function. The lowest negative log likelihood on the grid is found and the difference between that and the value at each  $\sin^2 2\theta$ - $\Delta m^2$  point ( $\Delta L$ ) is plotted in Figure 1.

Fig.1 exhibits a broad valley which curves from a mean value of  $\sin^2 2\theta$  of  $\sim 0.5$  at high  $\Delta m^2$  to  $\Delta m^2$  between  $10^{-4}$  and  $10^{-2}$  eV<sup>2</sup> at high  $\sin^2 2\theta$ . This is the locus of constant  $R_v$ . The shape information in the L/E distribution favors the high  $\sin^2 2\theta$  region. The best likelihood occurs for the grid point centered at  $\Delta m^2 = 0.0052$  eV<sup>2</sup>,  $\sin^2 2\theta = 0.97$ . The value of A is 91% of the Bartol 96 prediction and the total number of  $\mu$ -flavor *qs-rock* events is 16.8, 9.6% of the fully contained  $\mu$ -flavor sample.

Since the likelihood at each grid point is an average over the area of the point, there is no true no oscillation point in the analysis. The grid point with the lowest values of  $\sin^2 2\theta$  and  $\Delta m^2$  is taken as a good approximation to no oscillations. The likelihood rise from the minimum at this grid point is 11.3 and therefore the hypothesis of no oscillations is strongly disfavored.

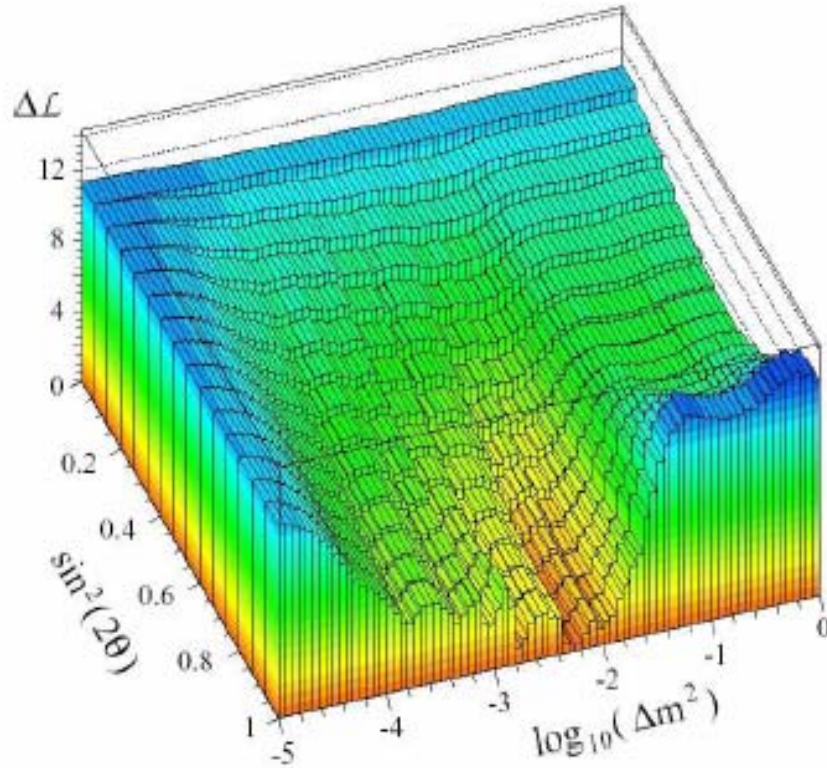


**Figure 1:** The data likelihood difference,  $\Delta\mathcal{L}$ , plotted as a function of  $\sin^2 2\theta$  and  $\log_{10}(\Delta m^2)$ .

Fig.1 shows that the likelihood surface is non-Gaussian. Errors on the parameters cannot be accurately defined using a simple likelihood rise. Confidence level contours have been determined using the method of Feldman and Cousins. If all errors were Gaussian, if there were no systematic effects and if there were no physical boundaries on the parameters, a 90% confidence contour in  $\sin^2 2\theta - \Delta\mu^2$  would be obtained from the data likelihood plot shown in Fig.1 by taking those points where the likelihood rose by 2.3 above the minimum value. However this is far from the case in this analysis. The values of  $\sin^2 2\theta$  are bounded by 0.0 and 1.0 and the best fit is close to the upper bound.

The procedure proposed by Feldman and Cousins is a frequentist approach which uses a Monte Carlo method of allowing for these effects. In their method MC experiments are generated and analyzed at each grid point on the  $\sin^2 2\theta - \Delta m^2$  plane. These experiments have the statistical fluctuations appropriate to the data exposure and can have systematic effects incorporated.

In this analysis each MC experiment was generated by selecting a random sample of the MC and rock events from the total sample of these events. The normalization of the MC neutrino events was based on the number of background subtracted e-flavor events and allowed to fluctuate within its statistical errors. A random amount of *qs-rock* background was added

according to the value and error of the background estimated from the *qs-data* at the given  $\sin^2 2\theta - \Delta\mu^2$  grid point.

The following systematic effects were incorporated into the analysis:

1. The energy calibration of the detector has estimated errors of  $\pm 7\%$  on electron showers and  $\pm 3\%$  on muon range. In each MC experiment the calibration was varied within these errors.
2. To allow for the uncertainty in the neutrino flux as a function of energy, the predicted flux was weighted by a factor  $1.0 + b E_\nu$  where  $b$  was randomly varied from 0.0 for each MC experiment with a Gaussian width of 0.005 ( $E_\nu$  in GeV).
3. The predicted ratio of  $\nu_e$  to  $\nu_\mu$  events was randomly varied with a Gaussian width of 5%.
4. To allow for the uncertainties in the neutrino cross-sections, the ratio of quasi-elastic events to inelastic and deep-inelastic events was randomly varied with a Gaussian width of 20%.

In addition the method automatically included the boundary on  $\sin^2 2\theta$  and the effects of resolution and event misidentification. The normalization of the MC flux ( $A$  parameter) was determined independently for each MC experiment and the fraction of *qs-rock* background in each data category was fitted for each MC experiment. One thousand MC experiments were generated at each  $\sin^2 2\theta - \Delta m^2$  grid point. The best fit grid point in  $\sin^2 2\theta - \Delta m^2$  was obtained for each experiment, not in general the same as that at which it was generated. The likelihood difference between the generated and best fit  $\sin^2 2\theta - \Delta m^2$  grid point ( $\Delta L_{MC}$ ) was calculated.

Combining the likelihood analysis of the data and ( $\Delta L_{MC}$ ), a 90% confidence level contour is obtained and plotted in Figure 2. At the 68% ( $1\sigma$ ) level there are two regions. One corresponds to the lower part of the Super-K 90% confidence region. The other, larger region is at higher  $\Delta m^2$  and contains the best fit point of this analysis. The data likelihood is relatively flat in the region immediately below  $\Delta m^2 = 10^{-3} \text{ eV}^2$ , which is reflected in the relatively large increase in area going between 90% and 95% confidence.

The probability of the no oscillation hypothesis is given by that fraction of the MC experiments at the no oscillation grid point having  $\Delta L_{MC} > 11.3$ , the value of  $\Delta L$  for this grid point. Fifty-eight of the 100,000 experiments exceeded 11.3, giving a probability for the no oscillation hypothesis of  $5.8 \times 10^{-4}$ . This probability takes account of the statistical precision of the experiment and all the systematic effects included in the Feldman-Cousins analysis.

The dotted line in Figure 2 is the 90% confidence sensitivity, defined by Feldman and Cousins as the Monte Carlo expectation for the 90% confidence contour, given this data

exposure and  $\sin^2 2\theta = 0.97$ ,  $\Delta m^2 = 0.0052$ , the best fit point of this analysis. The data 90% limit is in reasonable agreement with the expected sensitivity but lies inside the sensitivity curve, which corresponds closer to the 95% limit from the *qs-data*. This arises because the flavor ratio for the *qs-data* is lower than that expected by the MC at the best fit point.

In Figure 2 the Soudan 2 result is in good agreement with both Super-K and MACRO. From our analysis the probability of the hypothesis of no oscillations is  $5.8 \times 10^{-4}$ . There is no evidence of any departure from the predicted L/E distribution of the electron events confirming that the oscillation is predominantly  $\nu_\mu$  to  $\nu_\tau$  or  $\nu_\sigma$ . The zenith angle distribution of the  $\mu$ -flavor events shows the same features as those observed by Super-K.

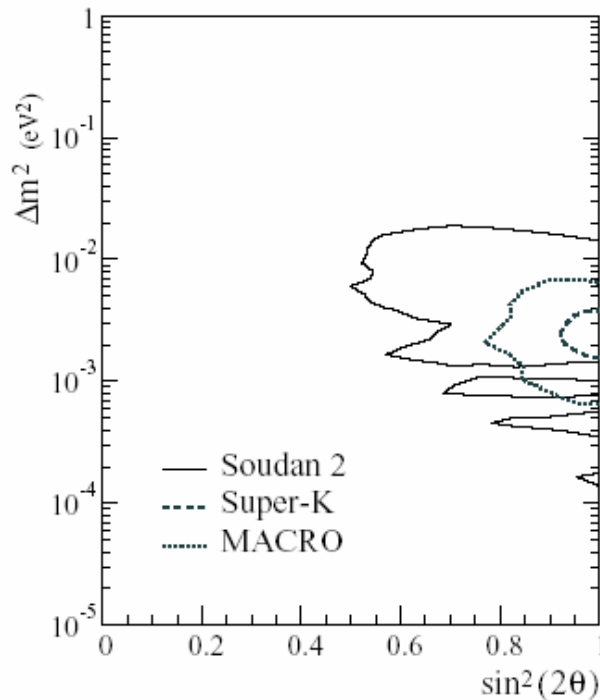


**Figure 2:** The Soudan 2 90% confidence allowed region in  $\sin^2 2\theta$ – $\Delta m^2$  (solid line) compared with the most recent allowed regions of Super-K (dashed line) and MACRO (dotted line).

This is the first detailed study of contained and partially contained atmospheric neutrino interactions in an experiment using a detection technique, an iron calorimeter, which is very different from that of Super-K and previous water Cherenkov detectors. The event detection and reconstruction properties of Soudan-2 are different, and in many cases superior, to those of Super-K but the exposure is much smaller. The geographical locations and backgrounds of the two experiments are different. Therefore any detector systematic effect which might simulate neutrino oscillations or bias the determination of oscillation parameters is highly unlikely to be present in both experiments. The excellent agreement between the experiments is a strong confirmation of the discovery of neutrino oscillations in the atmospheric neutrino flux.

**(M. C. Goodman)**

## I.A.5. ZEUS Detector at HERA

### a) Physics Results

Ten papers were published in this period and four more manuscripts were submitted for publication. In the following, we shall summarize some of the published papers.

i) *A ZEUS Next-to-Leading-Order QCD Analysis of Data on Deep Inelastic Scattering*

Next-to-leading-order QCD analyses of the ZEUS data on deep inelastic scattering together with fixed-target data have been performed, from which the gluon and quark densities of the proton and the value of the strong coupling constant,  $\alpha_s(M_Z)$ , were extracted. The study presents a full treatment of the experimental systematic uncertainties including the point-to-point correlations. The resulting uncertainties in the extracted parton density functions are presented. A combined fit for  $\alpha_s(M_Z)$  and the gluon and quark densities yields a value for  $\alpha_s(M_Z)$  in agreement with the world average. The parton density functions derived from ZEUS data alone indicate the importance of HERA data in determining the sea quark and gluon distributions at low  $x$ , see Figure 1. The limits of applicability of the theoretical formalism have been explored by comparing the fit predictions to ZEUS data at very low  $Q^2$ . At  $Q^2 \sim 1 \text{ GeV}^2$ , the fit predicts that the sea distribution is still rising at small  $x$ , whereas the gluon density is suppressed. The fit is unable to describe the precise ZEUS data for  $Q^2 \leq 1 \text{ GeV}^2$  and also predicts unphysical negative values for  $F_L$  in this  $Q^2$  region. Hence the use of the NLO QCD DGLAP formalism at  $Q^2 \leq 1 \text{ GeV}^2$  is questionable.

ii) *Measurement of High  $Q^2$   $e^-p$  Neutral Current Cross-Sections at HERA and the Extraction of  $xF_3$*

Cross sections for  $e^-p$  neutral current deep inelastic scattering have been measured at a centre-of-mass energy of 318 GeV using an integrated luminosity of  $15.9 \text{ pb}^{-1}$ . Results on the double-differential cross-section  $d^2\sigma/dx/dQ^2$  in the range  $185 < Q^2 < 50,000 \text{ GeV}^2$  and  $0.0037 < x < 0.75$ , as well as the single-differential cross-sections  $d\sigma/dQ^2$ ,  $d\sigma/dx$ , and  $d\sigma/dy$  for  $Q^2 > 200 \text{ GeV}^2$ , are presented. To study the effect of Z-boson exchange,  $d\sigma/dx$  has been measured for  $Q^2 > 10,000 \text{ GeV}^2$ . The structure function  $xF_3$  has been extracted by combining the  $e^-p$  results with the recent ZEUS measurements of  $e^+p$  neutral current deep inelastic scattering. All results agree well with the predictions of the Standard Model. To compare the measurement of  $xF_3$  to that obtained at lower  $Q^2$  in fixed-target experiments, it is convenient to use two structure functions  $xG_3(x, Q^2)$  and  $xH_3(x, Q^2)$ , where  $xG_3$  contains the  $\gamma - Z$  interference term, while the  $xH_3$  term arises purely from Z exchange and is negligible in comparison with  $xG_3$ . The results of the extraction of  $xG_3$  are shown in Figure 2, together with measurements obtained by the BCDMS collaboration. The ZEUS data extend the measurement of  $xG_3$  down to lower values of  $x$ .

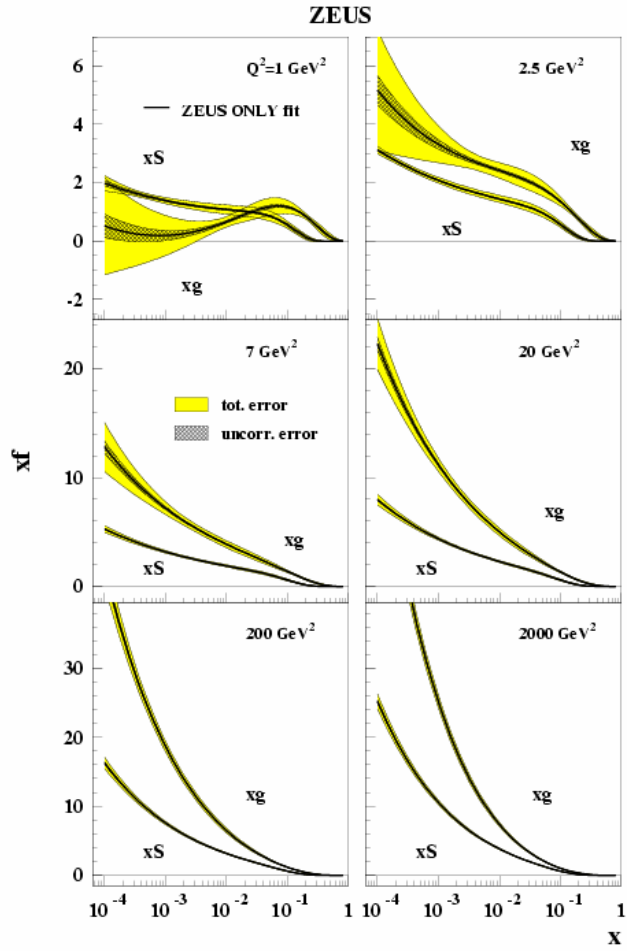


**Figure 1.** The gluon and sea distributions from the ZEUS – ONLY NLO QCD fit in various  $Q^2$  bins. The error bands show the uncertainty from the statistical and other uncorrelated sources separately from the total uncertainty including correlated systematic uncertainties. The value of  $\alpha_s(M_Z)=0.118$  is fixed.

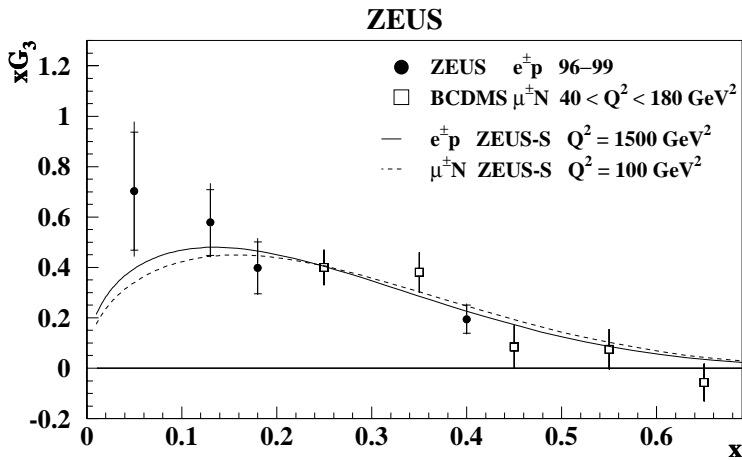


**Figure 2.** The structure function  $xG_3$  for  $e^+p$  scattering (solid points) compared to that from BCDMS (open squares, total errors only). The predictions based on the ZEUS QCD fits at  $Q^2 = 1500 \text{ GeV}^2$  ( $100 \text{ GeV}^2$ ) is shown as the solid (dashed) line.

iii) *Observation of the Strange Sea in the Proton via Inclusive  $\phi$  – Meson Production in Neutral Current Deep Inelastic Scattering at HERA*

Inclusive  $\phi(1020)$  – meson production in neutral current deep inelastic  $e^+p$  scattering has been measured with an integrated luminosity of  $45 \text{ pb}^{-1}$ . The  $\phi$  mesons were studied in the range  $10 < Q^2 < 100 \text{ GeV}^2$  and in restricted regions in the transverse momentum,  $p_T$ , pseudorapidity,  $\eta$ , and the scaled momentum in the Breit frame,  $x_p$ . Monte Carlo models with the strangeness-suppression factor  $\lambda_s$  as determined by analyses of  $e^+e^-$  annihilation events overestimates the cross sections. A smaller value of the strangeness-suppression factor reduces the predicted cross sections, but fails to reproduce the shapes of the measured differential cross sections. Figure 3 shows the cross sections for three bins of  $x_p$  in the current region of the Breit frame for the full  $Q^2$  range. The hatched bands represent uncertainties in the simulation of the  $\phi$  meson production by the MC models LEPTO, ARIADNE and HERWIG. The uncertainty due to  $\lambda_s$  values between 0.2 and 0.3 is also included. For  $x_p > 0.8$  the MC uncertainties are small and the measured cross section clearly requires a contribution from interactions with the strange sea. This constitutes the first direct evidence for the strange sea in the proton at low  $x$ .

iv) *Measurement of Subjet Multiplicities in Neutral Current Deep Inelastic Scattering at HERA and Determination of  $\alpha_s$*

The subjet multiplicity has been measured in neutral current  $e^+p$  interactions at  $Q^2 > 125 \text{ GeV}^2$  using an integrated luminosity of  $38.6 \text{ pb}^{-1}$ . Jets were identified in the laboratory frame using the longitudinally invariant  $k_t$  cluster algorithm. The number of jet-like sub-

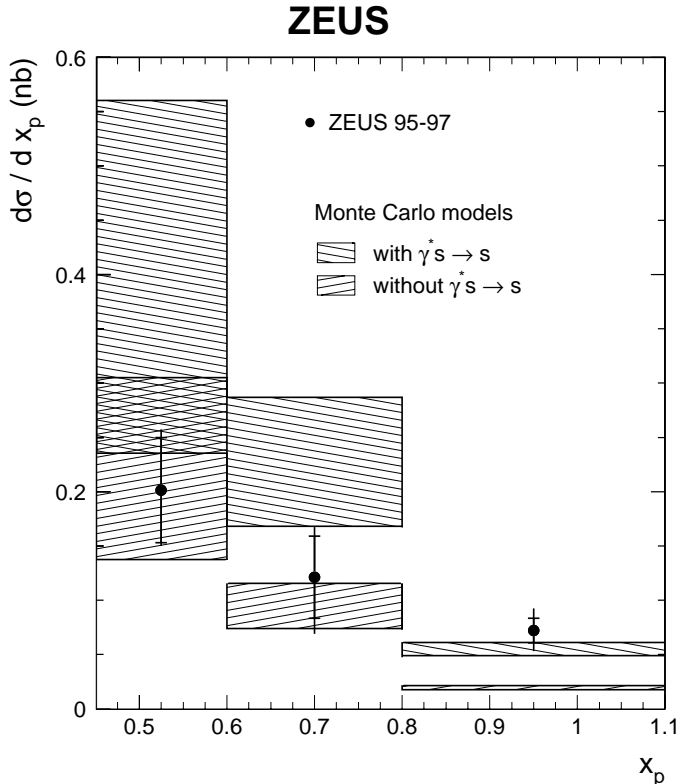


**Figure 3.** The cross section for leading  $\phi$  mesons as a function of  $x_p$  in the current region of the Breit frame. The hatched bands represent the uncertainties in the simulation of the  $\phi$  meson production by the Monte Carlo models and include LEPTO ( $\lambda_s = 0.2 - 0.3$ ), ARIADNE and HERWIG.

structures within jets, known as the subjet multiplicity, is defined as the number of clusters resolved in a jet by reapplying the jet algorithm at a smaller resolution scale  $y_{\text{cut}}$ . Measurements of the mean subjet multiplicity for jets with transverse energies  $25 < E_{T,\text{jet}} < 71$  GeV and with a resolution parameter  $y_{\text{cut}} = 0.01$  is shown in Figure 4. Next-to-leading order perturbative QCD calculations describe the measurements well. From these data a value of  $\alpha_s(M_Z) = 0.1187 \pm 0.0017$  (stat.)  $^{+0.0024}_{-0.0009}$  (syst.)  $^{+0.0093}_{-0.0076}$  (theo.) is obtained.

v) *Search for Single Top Production in ep Collisions at HERA*

A search for single-top production,  $ep \rightarrow e t X$ , has been performed using an integrated luminosity of  $130.1 \text{ pb}^{-1}$ . Events from both the leptonic and hadronic decay channels of the W boson resulting from the decay of the top quark were sought. For the leptonic mode, the search was made for events with isolated high – energy leptons and significant missing transverse momentum. For the hadronic mode, three – jet events in which two of the jets had an invariant mass consistent with that of the W were selected. No evidence for top production was found. The results are used to constrain single-top production via flavor-changing neutral current (FCNC) transitions. The ZEUS limit excludes a substantial region in the FCNC  $\kappa_{t\gamma}$  coupling not ruled out by other experiments, see Figure 5. The values for  $\kappa_{t\gamma}$ , the magnetic coupling, and for  $v_{t\gamma}$ , the vector coupling, are expected to be zero in the Standard Model.

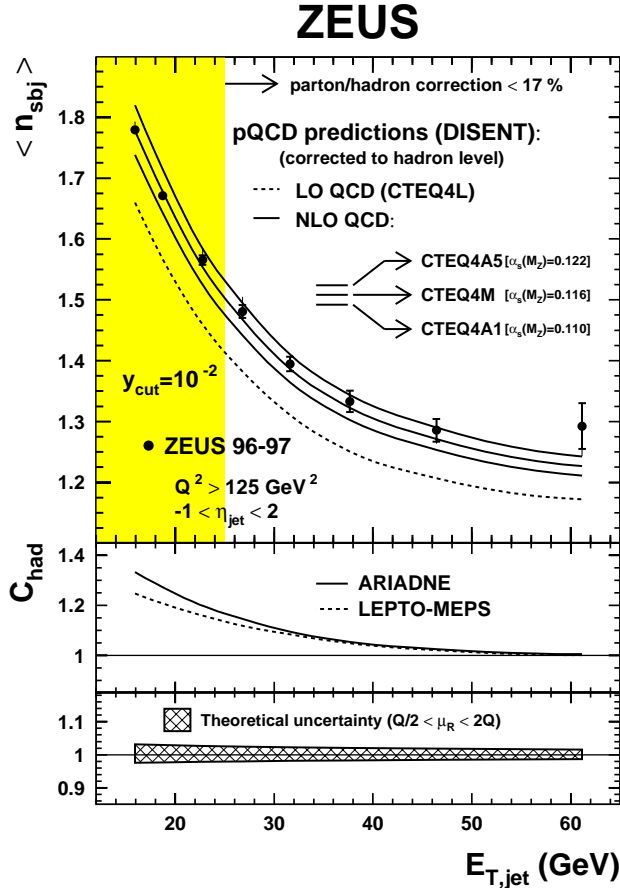


**Figure 4.** a) The mean subjet multiplicity corrected to the hadron level at  $y_{\text{cut}} = 0.01$  as a function of the transverse momentum of the jet for inclusive jet production in NC DIS with  $Q^2 > 125 \text{ GeV}^2$ . b) The parton-hadron correction used to correct the QCD predictions. c) The relative uncertainty on the NLO QCD calculations due to the variation of the renormalization scale.

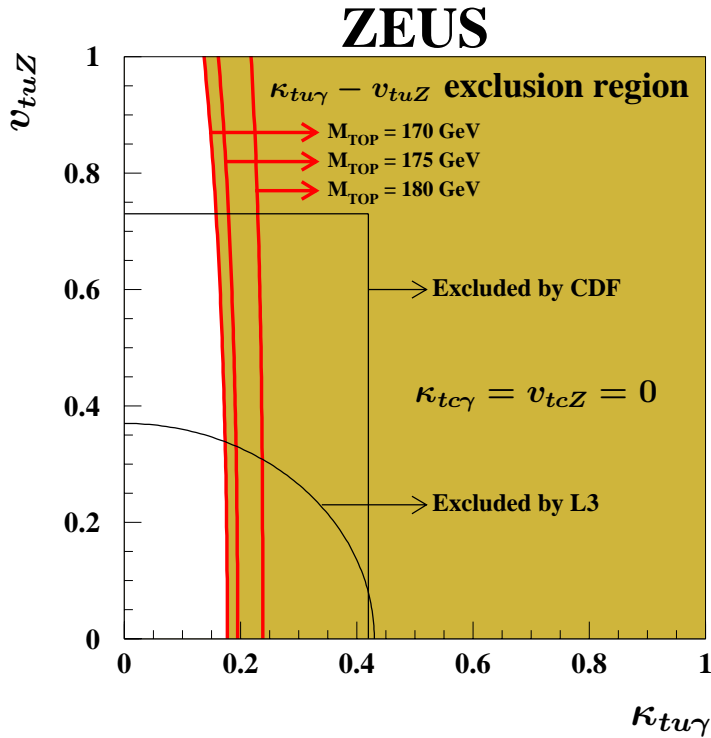


**Figure 5.** Exclusion regions at 95% CL in the  $\kappa_{tu\gamma} - \nu_{tuZ}$  plane for three values of the  $m_{top}$  assuming  $\kappa_{tc\gamma} = \nu_{tcZ} = 0$ . The CDF and L3 exclusion limits are also shown.

## b) HERA and ZEUS Operations

The first two months of 2003 were used to further investigate the reasons for the high machine backgrounds as observed by the colliding beam detectors and to provide some luminosity to the experiments. Three different backgrounds have been identified: positron-gas interactions, proton-gas interactions and synchrotron radiation. Currently these background rates are such that the tracking detectors can not be operated in the presence of larger positron or proton beam currents. The studies involved the tracking systems as well as the calorimeter. In addition, detailed Monte Carlo studies of the beam lines have been performed to redesign the set of collimators employed to reduce the rate of synchrotron radiation entering the detectors.

In March machine operation were halted to permit access to the beam line and the detectors. New collimators were installed and a section of the beam pipe replaced in the ZEUS interaction region. The shutdown was also utilized to repair the Straw Tube Tracker. In a labor-intensive operation the tracker was removed from the experiment, transported to an assembly hall, completely disassembled, repaired, reassembled and reinstalled in the detector. The repair effort included repairing four sectors which were not able to hold the high voltage and several repairs on the front-end electronic cards, such as the replacement of wrongly mounted capacitors and the addition of LVDS drivers between the main boards and the signal driving boards. The operation took about 18 weeks and was highly successful. First tests performed after re-installation indicated that all problems, i.e. randomly blowing fuses, cross talk between sectors etc., were solved.

**(J. Repond)**

## **I.B. EXPERIMENTS IN PLANNING OR CONSTRUCTION**

### **I.B.1. The Endcap Electromagnetic Calorimeter for STAR**

Previous reports have described the extensive involvement of the Argonne group in the construction of the Endcap Electromagnetic Calorimeter (EEMC) for the STAR experiment at the Relativistic Heavy-Ion Collider (RHIC). The Argonne group is responsible for construction of a shower maximum detector (SMD) for the EEMC, which will allow discrimination between direct photons and neutral pions. The goal is to extract the spin asymmetry for direct photon production in polarized proton-proton collisions, which is sensitive to the polarization of the gluons within the proton.

Construction was nearly completed during the first half of 2003. As of June 30, 25 SMD modules have been glued at Argonne. Twenty-three of these have been machined to the proper dimensions and testing of the twenty-first module with cosmic rays is underway. Eight modules were installed in the calorimeter at STAR in September of 2002. Another four were delivered to STAR in May 2003, and we plan to deliver another ten in July 2003. Our goal is to produce and test 27 modules, which will include 3 spares, and to install the 24 modules needed to fill the detector before the run which begins late in 2003.

During a RHIC run which lasted through May 2003, STAR took data on deuteron-gold and proton-proton collisions. Commissioning work began on the EEMC towers, but due to delays in the production of electronics by a collaborating institution, we were unable to acquire data from the SMD in the EEMC. A Forward Pion Calorimeter which included SMD arrays assembled at Argonne was also installed at STAR prior to the FY2003 run, and those SMD arrays were instrumented and read out during the run.

A master's degree student at Ball State University joined our group after his spring term was completed. It is expected that he will work on simulations of the SMD response to study effects such as attenuation of light in the SMD strips, crosstalk between pixels on the multi-anode phototubes, and the production of light by electrons passing through wavelength-shifting fibers in the SMD.

We expect that by the end of 2003, construction work at Argonne will be completed and the group will be heavily involved in commissioning of the detector and analysis of the data.

**(R. V. Cadman)**

## I.B.2. Neutrino Oscillation Experiments

### a) MINOS - Main Injector Neutrino Oscillation Search

The phenomenon of neutrino oscillations allows the three flavors of neutrinos to mix as they travel through space or matter. The MINOS experiment will use a Fermilab muon neutrino beam to study neutrino oscillations with higher sensitivity than any previous experiment. MINOS is optimized to explore the region of neutrino oscillation parameter space (values of the  $\Delta m^2$  and  $\sin^2(2\theta)$  parameters) suggested by atmospheric neutrino experiments: IMB, Kamiokande, MACRO, Soudan 2 and Super-Kamiokande. The study of oscillations in this region with an accelerator-produced neutrino beam requires measurements of the beam after a very long flight path. This in turn requires a very intense neutrino beam (produced for the MINOS experiment by the Fermilab Main Injector accelerator) and massive detectors. MINOS compares the rates and characteristics of neutrino interactions in a 980-ton “near” detector, close to the source of neutrinos at Fermilab, and a 5400-ton “far” detector, 735 km away in the underground laboratory at Soudan, Minnesota. The MINOS detectors are steel-scintillator sandwich calorimeters with toroidally magnetized 1-inch thick steel planes. The detectors use extruded plastic scintillator with fine transverse granularity (4-cm wide strips) to provide both calorimetry (energy deposition) and tracking (topology) information. The neutrino beam and MINOS detectors are being constructed as part of the NuMI (Neutrinos at the Main Injector) Project at Fermilab.

Results from the Super-Kamiokande, Soudan 2 and MACRO experiments provide evidence that neutrino oscillations are taking place within the region of parameter space that MINOS was designed to explore. The best value of  $\Delta m^2$ , around  $3 \times 10^{-3} eV^2$ , has motivated the use of a lower energy beam for MINOS than was initially planned in order to improve sensitivity at low  $\Delta m^2$ . Argonne physicists and engineers have been involved in several aspects of MINOS construction: scintillator-module factory engineering, near-detector scintillator-module fabrication, near-detector front-end electronics, near- and far-detector installation and the construction and installation of neutrino beamline components.

MINOS detector work was highlighted by several important achievements during the first half of 2003. The first half of the far detector, Supermodule 1, recorded cosmic-ray muon and atmospheric-neutrino data throughout the period with the magnetic field turned on. Despite ongoing installation work on Supermodule 2, data taking achieved a duty cycle of about 50% over the six-month period. At the April meeting of the APS Division of Particles and Fields in Philadelphia, the MINOS Collaboration reported the observation of the first twelve atmospheric neutrino events in the far detector. In June, the installation of all 486 far-detector planes was completed and the magnet coil was installed in the second half of the detector, Supermodule 2. Figure 1 shows the coil conductors emerging from the last detector plane. The Argonne group continued to manage the production manufacturing of near-detector electronics throughout the

reporting period. Mass-production assembly of Master, Minder and Keeper/Trigger boards began in late winter and early spring. Finally, the MINOS Collaboration submitted its proposed 5-year run plan to the Fermilab Directorate at the end of May.



**Figure 1.** The last plane of the MINOS far detector. The photograph shows the last plane of the MINOS far detector at Soudan and the magnet coil conductors of Supermodule 2.

The magnetization of the steel planes of the MINOS far detector enables us to perform a unique atmospheric-neutrino measurement. The bending of charged particles in the magnetic field distinguishes positive from negative muons up to about 70 GeV/c, which allows the detector to measure charged-current muon-neutrino and antineutrino interactions separately. A difference in the oscillation parameters of neutrinos and antineutrinos would constitute a violation of CPT symmetry, which could not have been observed in earlier experiments. However, the study of atmospheric neutrino events in MINOS data (unlike beam neutrino events) requires a veto shield to suppress backgrounds from downward going cosmic-ray muon interactions. A prototype shield was installed in 2002, using far-detector scintillator modules covering the top and sides of the detector to flag the presence of cosmic-ray muons in candidate neutrino events. An optimized shield covering Supermodule 1 was completed in January 2003, allowing the search for CPT violation in atmospheric neutrino events to begin. The shield over

the first half of Supermodule 2 was commissioned in early June and the remainder of the shield is scheduled for completion during the summer.

One major focus of work by the Argonne MINOS group has been scintillator module construction. ("Modules" are subassemblies of 20 or 28 extruded plastic scintillator strips.) Scintillator module assembly for MINOS was performed at assembly facilities at Argonne, Caltech and the University of Minnesota in Minneapolis. The Argonne group designed and built the assembly machines and tooling for all three module factories. Argonne physicists and engineers served as NuMI Project WBS Level 3 Managers for the design and construction of the machines needed to construct scintillator modules and for the operation of the three factories. This work was successfully completed in early 2003 with the decommissioning of the Minnesota factory in February (after a total production of 2032 far-detector and veto-shield modules) and the Caltech factory in April (total production of 2115 modules for the far detector and calibration detector). As previously reported, the Argonne factory completed the assembly of all 573 near-detector modules in November 2002. The Argonne factory was set up in Building 369 in late 2001 with substantial financial assistance from the Laboratory administration. All near-detector planes had been assembled at Fermilab by the end of the 2002 and are ready to be mounted on the detector when the underground laboratory is completed in 2004.

The second major focus of the Argonne MINOS group is electronics and data acquisition for the experiment. The near detector must have fast front-end electronics with no dead time because of the high instantaneous rate of neutrino events at Fermilab. This is accomplished using a special MINOS modification of the Fermilab QIE ASIC chip. Most components of the near-detector front-end electronics, along with protocols for communication among the various boards, are the responsibility of the Argonne electronics group. The group also developed software to operate and study the performance of the readout electronics chain and performed simulations of electronics response. An Argonne engineer continued to serve as the Level 3 manager for the near-detector front-end electronics in 2003. The Argonne physicist who was previously the Level 2 manager for all detector electronics completed his term at the end of 2002 and became Level 2 co-manager for near detector installation.

During the first half of 2003 physicists and engineers from Argonne and Fermilab completed certification of the final pre-production versions of all near-detector electronics boards, crates, power supplies and cables. The mass production of boards for all 9500 channels of near detector electronics was under way by late spring. The first 1600 channels of electronics is being shipped to CERN, immediately after checkout, for the September 2003 Calibration Detector (CalDet) test-beam run. The very successful 2002 CalDet run compared the responses of near and far detector front-end electronics that were used to read out opposite ends of the same scintillator strips in the calorimeter. The 2003 run will use near-detector electronics to read out all CalDet strips to perform the final energy calibration of the near detector. The 2002 CalDet run had only enough near-detector front-end channels to read out the 128 pixels of two M64 near-detector photomultiplier tubes. The data showed the expected correlation of near and far detector responses for test-beam particles, as illustrated in Figure 2.

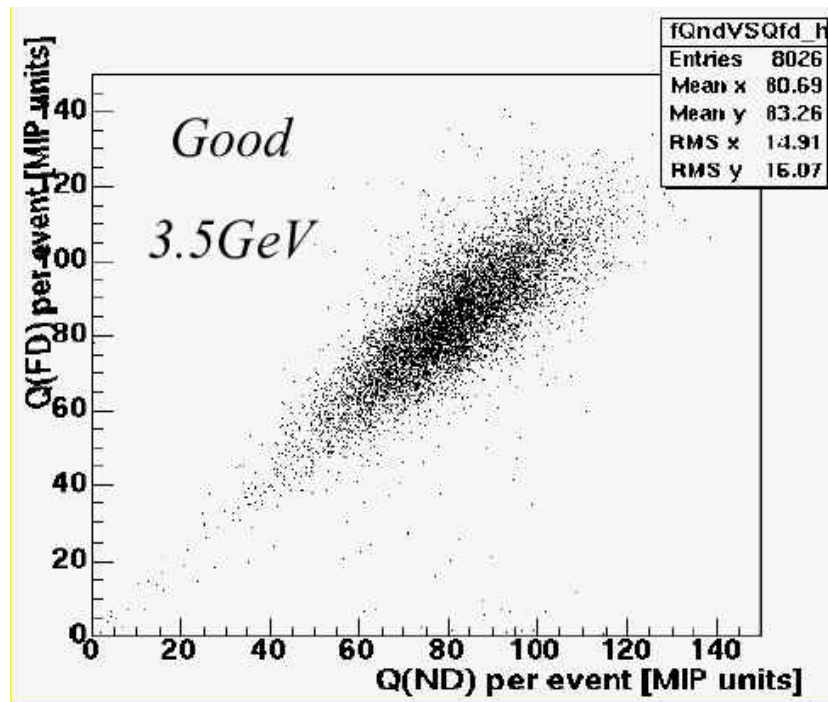


**Figure 2.** Far- versus near-detector electronics response from the MINOS CalDet run. The scatter plot shows the correlation of pulse heights recorded from opposite ends of the same scintillator strips by far-detector (FD) and near-detector (ND) electronics. The data shown are for 3.5 GeV test-beam electron events recorded during the 2002 run of the MINOS Calibration Detector at CERN.

As work on MINOS electronics, scintillator module fabrication and far detector installation ramps down, Argonne physicists have started to shift their effort to more urgent tasks for MINOS and to studies of possible next-generation neutrino oscillation experiments. An Argonne physicist is now co-manager for MINOS near detector installation and three others have been devoted increasing effort to construction and testing of NuMI neutrino beam components at Fermilab. Argonne involvement in planning for future neutrino oscillation experiments, to measure the  $\theta_{13}$  mass mixing parameter, is described in the next section.

The work of the Argonne MINOS group on NuMI neutrino beam devices at Fermilab spans a wide range of activities. One physicist is the Deputy Level 3 Manager for Neutrino Beam Devices and is also responsible for preparation of the “Hot Cell” facility to repair highly radioactive beam components. Another physicist is conducting vibration measurements of the production target and magnetic focusing horns and is also performing horn magnetic field measurements. In addition, Argonne physicists and engineers are responsible for the readout and integration of all target hall instrumentation. Achievements in these areas during the first half of 2003 are summarized in the paragraphs below.

Vibration measurements of the NuMI production target, which will be positioned inside the neck of the first focusing horn during low-energy beam running, showed no significant motion induced by horn pulsing. Similarly, the flow of cooling air around the target in the low-

energy configuration induced only small amplitude vibrations. However, the flow of cooling air did induce enough target motion in the medium-energy location, outside of the Horn 1 neck, that additional mechanical support may be needed. Figure 3 shows the setup for vibration measurements of the final Horn 1 stripline, which showed no significant change in the oscillations induced by horn pulsing after the installation of the final “remote clamp” section. The first three production “Bdot” coils, which monitor horn magnetic fields during operation, were assembled and installed in Horn 2 in June. The final Horn 2 alignment “crosshair” assemblies, which are used to check the relative locations of the horn and the proton beam, were also installed in June. Argonne physicists worked on the design and prototyping of both the Bdot coils and the crosshairs and will study their behavior during the test pulsing of Horn 2 in July.

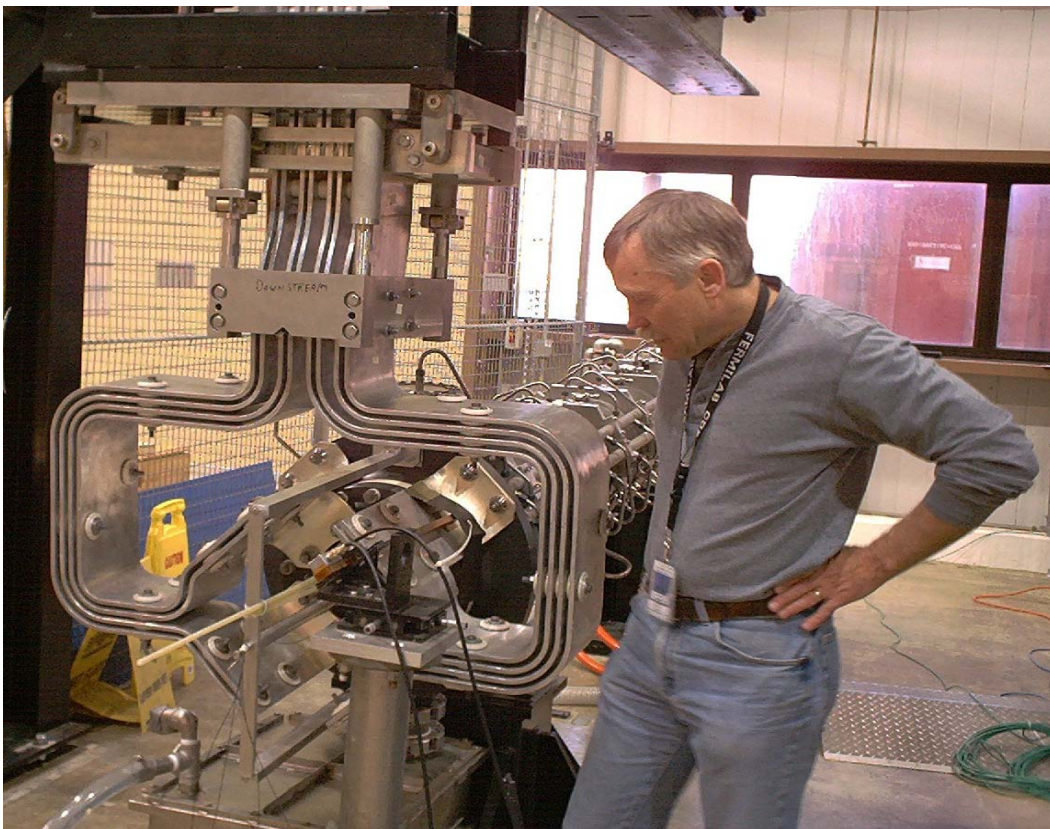


**Figure 3.** NuMI magnetic horn vibration measurements. Argonne physicist Bob Wagner is shown with the setup for measuring the amplitudes and frequencies of vibrations of the stripline of the prototype magnetic focusing horn. The stripline is the folded aluminum structure in the foreground, which delivers a 200 kA current pulse to the horn (the dark structure with cooling water pipes behind the stripline) during the 10  $\mu$ sec beam spill. This final configuration of the stripline includes the “remote clamp” (top section of the stripline structure). The remote clamp allows the stripline to be connected or disconnected under remote control after it has become radioactive during beamline operation. The vibration characteristics were found to be similar to those measured before remote clamp installation.

During the first half of 2003, Argonne physicists and engineers continued work on the preparation of the electronics used to read out target hall instrumentation. Argonne’s

instrumentation readout responsibilities include the thermocouples that measure temperatures at many locations, the beam-loss monitors used for horn crosshair alignment measurements, the readout of the precise positions of remotely movable devices, and the specification of radiation-hard instrumentation cabling. Argonne work on the design of signal conditioning electronics used to interface instrumentation signals to the ACNET data acquisition system also began during this period. Work on the “Hot Cell” facility, used to repair or replace highly radioactive horns and targets, included the preassembly of the remotely controllable lift-table system, which was still in progress at the end of June. Other Hot Cell work involved the specification of machining tolerances and fabrication procedures for several steel shielding components built during May and June and planning for the preassembly of the Hot Cell structure prior to underground installation.

### **b) Experiments to Measure the $\theta_{13}$ Neutrino Mass-mixing Parameter**

During the past two years Argonne physicists and engineers have devoted increasing levels of effort to the design of a next-generation experiment, the so-called off-axis experiment, in the NuMI neutrino beam. They were co-authors on the Letter of Intent, submitted to the Fermilab PAC in June 2002, to build a massive new detector to search for  $\nu_{\mu} \rightarrow \nu_e$  oscillations several degrees off the axis of the NuMI beamline in Minnesota or Canada. The observation of such events would allow a measurement of the  $\theta_{13}$  mass-mixing parameter, which could eventually lead to the construction of an even larger detector to search for CP violation effects in the NuMI beam. Recent Argonne work, in collaboration with Fermilab, has focused on the design and prototyping of resistive plate counter (RPC) detectors and the associated calorimeter structure. In April, Argonne hosted the second in a series of workshops on the design of a 50 kiloton detector for the NuMI off-axis experiment.

In an independent effort, Argonne physicists have begun a study of a possible reactor experiment to measure  $\theta_{13}$ . This experiment would measure the survival probability for electron antineutrinos at a distance of about 1 kilometer from a reactor. During the past twelve months Argonne physicists have worked on the design of detectors for the experiment and have performed simulations to find the optimum distance between the detector and the reactor. Figure 4 shows how “atmospheric” and “solar” neutrino oscillations are expected to affect electron antineutrino survival probability as a function of distance from a reactor. Since previous experiments have already shown that any disappearance effect is quite small,  $\sin^2(2\theta_{13}) < 0.1$ , the systematic errors in an improved experiment would be carefully controlled by the use of a second detector to measure the unoscillated antineutrino flux close to the reactor. Argonne co-hosted a workshop on this topic at the University of Alabama in April.

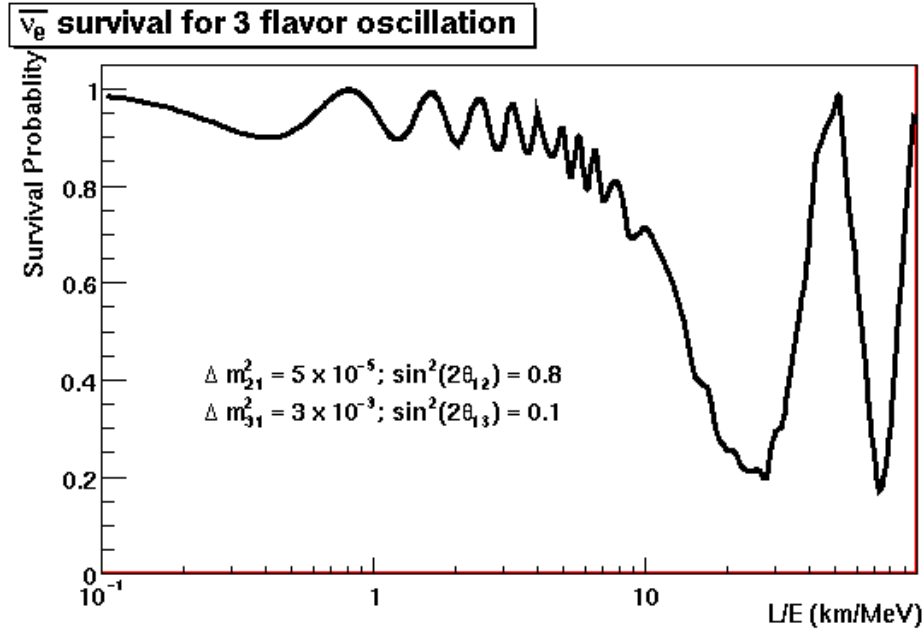


**Figure 4.** Sensitivity of a reactor experiment to the neutrino mass-mixing parameter  $\theta_{13}$ . The graph shows the electron antineutrino survival probability as a function of  $L/E$ , where  $L$  is the distance from the reactor and  $E$  is the antineutrino energy. The effects of both “atmospheric” (around  $L/E = 1$  km/MeV) and “solar” (above 10 km/MeV) neutrino oscillations are included. The optimum sensitivity to  $\theta_{13}$  is obtained at a distance of about 1 km. The earlier CHOOZ experiment, which was limited by knowledge of the reactor power and other systematic effects, did not observe any deficit at this distance and set a limit of  $\sin^2(2\theta_{13}) < 0.1$ . The goal of the future experiment would be to improve this sensitivity by about an order of magnitude by using two detectors at different distances to reduce systematic errors.

(D.S. Ayres)

### I.B.3. ATLAS Detector Research & Development

#### a) Overview of ANL ATLAS Tile Calorimeter Activities

The TileCal subsystem continued making good progress in the first half of 2003. All module construction activities were completed at Argonne and the final module was shipped to CERN in April 2003, along with tooling that was to be returned to collaborators at CERN. Argonne technical staff made significant contribution to the pre-assembly of the EBC cylinder, which was successfully completed in April and is shown in Fig. 1. The geometrical data taken during this work is being analyzed to determine on how to improve the shape of the cylinder when it is constructed in the cavern. Argonne technical staff also made significant contributions to the initial work to prepare EBA modules for pre-assembly (even though this task has now been rescheduled for the middle of 2004.) Finally, Argonne engineers continue to collaborate with Atlas Technical coordination on areas associated with the calorimeter and shielding movement systems.



**Figure 1.** Surface pre-assembly of the first Tile Calorimeter cylinder (EBC).

**(J. Proudfoot)**

## **I.C. DETECTOR DEVELOPMENT**

### **I.C.1. Atlas Calorimeter Design and Construction**

Module instrumentation of the remaining Tile Calorimeter modules at Argonne was completed in this period. Module 65 was shipped to CERN in April along with all tooling that had been provided by Atlas collaborators in Europe. The construction area in Building 366 was cleared and the remaining materials and tooling consolidated to allow for the space to be utilized for other projects while still allowing us to re-start module construction in the event of a disaster (for example the destruction of several modules during shipping and handling). The areas of ongoing work comprise: testbeam measurement of detector performance; engineering and technical support of the pre-assembly efforts at CERN (EBC, Barrel and EBA); continued engineering evaluation of the detector design as changes are requested from other subsystems; work in collaboration with Atlas Technical Coordination on components associated with the movement systems on the Atlas main rails (guide brackets, the hydraulic system and controls).

### a) Module Instrumentation and Testing

During this period, Argonne technical staff completed repairs on one remaining module from MSU (Module 56). In addition, with the new repair techniques that are now available to us (having been developed through the construction experience), Argonne technical staff went to CERN to complete minor repairs to 12 modules where the initial scan data taken during instrumentation had indicated that some fibers were damaged. These repairs did little to affect the overall uniformity, but significantly reduced the number of problematic tile fiber couplings. In addition, one module had been damaged during mounting in the testbeam and repairs were also completed on it. Fig. 2 shows the module uniformity for all modules instrumented in the U.S. that have been scanned using the cesium system at Argonne (including most of the 32 modules that were instrumented by our collaborators at Michigan State University). All modules comfortably meet our design goal of having non-uniformity less than 10% rms.

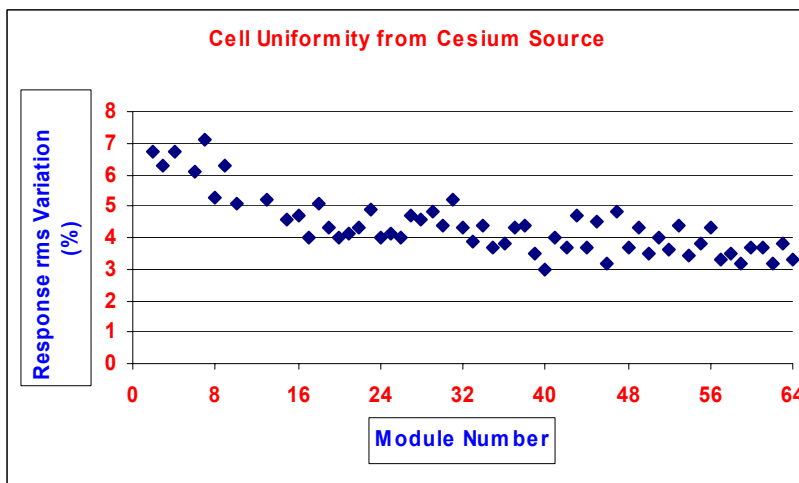


Figure 2. Module instrumentation non-uniformity as a function of module number.

(J. Proudfoot)

### b) Testbeam Program

R. Stanek from Argonne continues to be the testbeam coordinator for the Tile Calorimeter testbeam program. 2003 is the final year of testbeam calibration of tile calorimeter production modules. At the end of the September 2002 testbeam run, we summarized the non-working, or not understood, sticking points of the run. The major issues to be resolved were some of the following:

- No readout through CANbus with long cables
- Modification of DCS system to incorporate additional power supplies

- Test the electronics having modified TTCrx circuitry
- Re-program the ADC flash memory in the field

In January, we organized a group of experts to come and address these issues. This so-called “experts week” was a great success. ANL provided 300m of good quality CANbus cable for some of these tests. It is expected that the cable lengths in ATLAS will be ~145m at the most, so we checked operation with cables up to 200m without apparent errors. However, the CAN bit rate needed to be changed to 250kbs, down from 500kbs. This was expected. The other feature we discovered was that with 300ma flowing in the CANbus nodes, the voltage drop in the cable was significant to warrant that CAN V+ be raised to about 17 volts. This value can be the same both for the HV and the ADC CAN systems. In order to slow the speed of the CAN receivers, the microprocessors in the drawers needed modification. In the case of the HV, the speed is set with dip switches. The ADC board needed reprogramming of its flash memory. We were successfully able to reprogram these cards through CANbus. This was never done before. These tests were very important in terms of understanding the cabling and operation for the ATLAS configuration.

The TTCrx chips were found to have a glitch in the clock if some of the JTAG lines were left floating. These lines were easily corrected in the motherboard mezzanine cards with jumpers, but some complicated removal and re-balling of the chips in the digitizers. All mezzanine cards were corrected on the testbeam modules, and 1 module had corrected digitizers. No problems were found with the mezzanine cards, but the digitizers showed missing bits in the header words. This was later traced to a second batch of TTCrx chips that showed a slightly different timing. Once again, the collaboration found for the entire ATLAS collaboration possible disaster scenarios in the global electronics.

In May, we had a second of the 25nsec structured beam periods provided by the SPS. The previous was in October 2001. The goals for this run were fairly straightforward as there was no calibration to be done.

- Certify the new DAQ
- Certify the beamline and beam quality
- Certify correct operation of production drawers

Several weeks prior to this run, the DAQ and network were redone in the testbeam. The following modifications were included.

- Private Fast Ethernet control network
- Upgrade to online version 0.0.18 with data format changed
- Access to CERN network via a dedicated gateway with a firewall
- DHCP support
- Wireless support
- Private Gigabit Ethernet Dataflow network
- Dedicated server for:

- Network booting of the diskless SBCs
  - Software server for Online and Dataflow software
  - Analysis tools: PAW, CERNLIB, ROOT, CLHEP, JAS

The quality of the beam was actually better than expected. The beamline was extensively modified to produce a very low energy (VLE) beam later in the year. In November 2002, Monte Carlo simulations showed that the beam would be very broad. However, this run showed that, except for alignment, the size and spread of the beam were at least as good as in the previous years. We also made some studies of the beam structure for the machine people. In 2001, the satellites around the main bunches of beam were about 8%. This year, that contamination is <0.1%. Also seen in Fig. 3 below, is that the beam structure is what is promised: 48 bunches of beam every 23  $\mu$ sec. This data we recorded from the digitizers on the calorimeter.

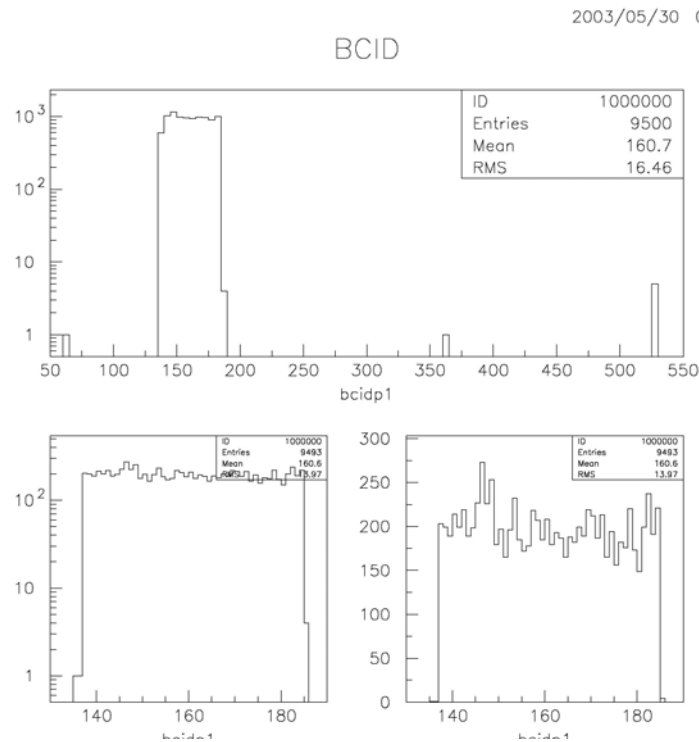


**Figure 3.** BCID response of digitizer in module P1.

The main goal of the 25nsec data taking was to determine the calorimeter global timing. Each digitizer board can be fine-tuned with the Deskew2 clock of the TTCrx chip to accommodate delays across the drawer. We took  $\eta$  scans and calculated what the deskew2 setting should be for each PMT. A typical scan looked as follows in Fig. 4 for both high and low gain channels.

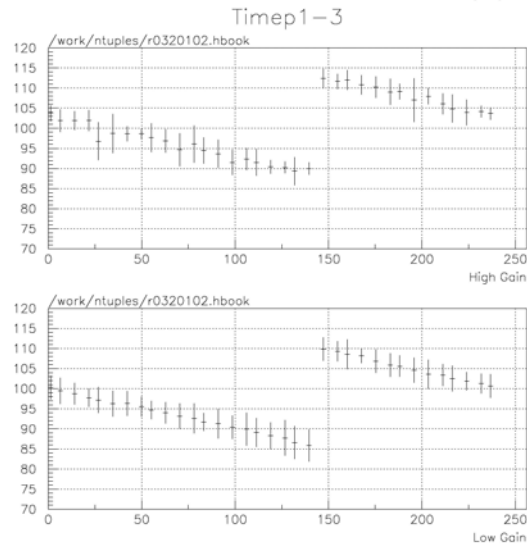


**Figure 4.** Reconstructed Time in nsec vs. DESKEW2 setting.

The discontinuity at  $\sim 150$  is the result of the clock edge changing. We tried to stay away from this edge and selected 95nsec as the required point for all channels. Then averaging the desired values in groups of 6 (per digitizer) we took a final  $\eta$  scan and found most channels behaved as expected. There were several however, that, although the deskew2 point was away from the discontinuity, the channels were shifted by 25nsec. Unfortunately, the beam went off and we could not iterate. But it is clear that we understand how timing should best be set in ATLAS.

**(R. Stanek)**

### c) Engineering Design and Analysis

Argonne engineering staff has the responsibility for several of the engineering tasks associated with the assembly of the calorimeter as a whole and with its support structure. These tasks include: evaluation of stresses in the cylinder connecting elements, deflections in the cylinder during pre-assembly (at each stage and including the cryostat dummy load when appropriate) and evaluation of the stability of the assembly as a whole (with special emphasis on the conditions during the initial mounting of the cryostats).

Several engineering calculations are in progress or have been completed in this period.

- FEA calculations were completed for the deflections and stresses in the EBC cylinder at several critical points during assembly. The deflections calculated in the model were in reasonable agreement to those observed during EBC.

- FEA models have been completed for the stresses in the connections in the barrel.
- There has been further work to check the impact of changes in the endcap cryostat supports, which were made in this period. This has continued as the design of the cryostat supports has continued to evolve. A key issue is to understand the stability of the structure at the point at which the cryostat load is applied and this study is ongoing.
- FEA calculations are in progress to estimate deflections and stresses in the barrel calorimeter structure at various stages during pre-assembly. This work is ongoing and a particular issue is the stability of the structure if the cryostat dummy load is applied after 32 modules are mounted (rather than after the cylinder is closed).

**d) Calorimeter Pre-Assembly**

Argonne Technical and scientific staff have had significant participation in the ongoing preassembly of the EBC cylinder at CERN. J. Proudfoot is one of the three leaders of the pre-assembly team and V. Guarino has the responsibility for the evaluation of the geometrical envelope and deformation of the cylinder under its static load.

The EBC saddles, which were procured by CERN, were delivered late and significantly out of specification. The tile calorimeter engineering group of Miralles, Guarino, and Topilin evaluated the impact of this and it was determined to modify the saddles rather than to accept a significant schedule delay. These modifications were executed almost entirely by Argonne technical staff under the leadership of V. Guarino. The modifications were quite extensive and included increasing the diameter of many clearance holes, as well as widening the slot in which the key on the double link plate sits. In addition, they required us to dismount the saddles entirely from the box beam as shown in Fig. 5. In total, this represented about 6 man-weeks of arduous work, but the result was that the EBC pre-assembly schedule could avoid a delay of as much as 6 months.



**Figure 5.** Some views of the EBC saddles during repair in Building 185 at CERN

Once the saddle repairs had been completed, the remainder of the EBC pre-assembly proceeded relatively smoothly towards its completion in April 2004 (Fig. 1). However, we encountered one additional problem along the way that was associated with the cylinder geometry and, Argonne staff was central to its understanding. The problem is shown in Fig. 6, where it can be seen that the cylinder was following a slightly smaller radius as it is built up from the 6 o'clock position. Argonne staff was the first to appreciate the significance of this and they developed a basic understanding, such that we were able to implement some corrective shims to largely re-establish the design envelope (This is, in part, the wiggle at around  $x \sim 0$  in Fig. 6. As a result of this and some subsequent corrective action, the cylinder was easily closed.) The final module was inserted with relatively little effort into a slot, which was approximately 7mm smaller than the module. The weight of the module itself was sufficient to push the two halves of the cylinder apart. In addition, we appreciated several interesting features of this construction and are in the process of developing a model to use for the prediction of the cylinder shape during the assembly sequence. This will see action soon as the barrel pre-assembly is scheduled to commence in July 2003.

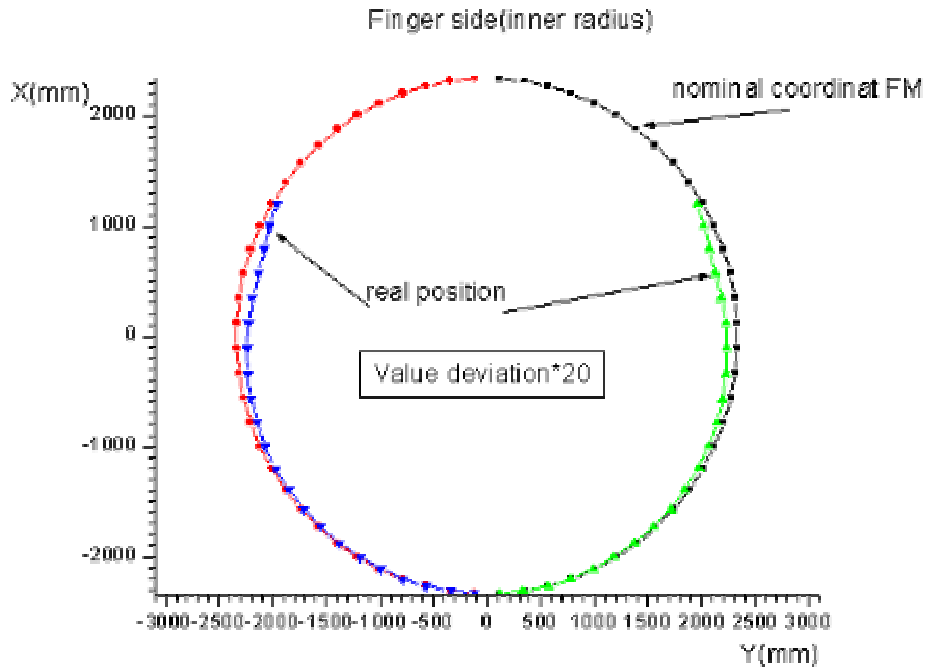


**Figure 6.** EBC cylinder envelope when approximately 44 modules have been mounted and the first adjustments were made for the deviation of the envelope from its nominal.

**(J. Proudfoot)**

**e) Work in Collaboration with ATLAS Technical Coordination**

Argonne technical staff has established a strong collaboration with ATLAS technical Coordination to design the guide and movement systems for the several components, which must be moved on the main rails to access the detector. In this period, several significant steps forward were made. The design of the calorimeter Z bracket has been completed. The design and fabrication drawings have been completed for the Toroid X and Z brackets. An initial layout of the components needed for the support and movement of the JD disk was completed.

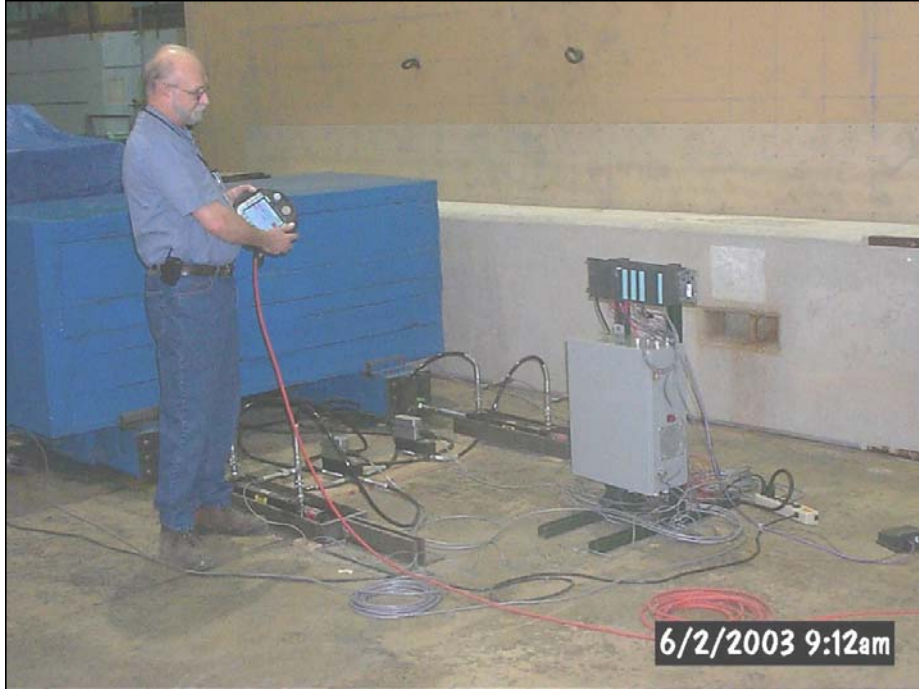


**Figure 7.** The prototype hydraulic control system under test at Argonne.

A specification for the hydraulic control system to be used to move each of these massive systems was completed in this period and an initial prototype system assembled and tested at Argonne (Fig. 7). This system has now been shipped to CERN where it will be used in a preliminary test of the HF Truck with a 220 Ton load.

**(J. Proudfoot and J. Grudzinski)**

## **I.C.2. ATLAS Computing**

Argonne (through David Malon) continued to lead the ATLAS-wide database effort in the 1st half of 2003. Three of the four LHC experiments have decided to develop and adopt a common persistency solution, called POOL, and efforts this year were directed towards this goal. ANL's direct contribution to POOL is in the realm of Collections and Metadata (essentially, data about the event store - "where can I find a sample of 20 GeV electrons" would be an example of a question answered by this work). To that end, a new developer, Kristo Karr was brought on board in April. His efforts have gone into incorporating previous ANL developed software into POOL as well as implementing a suite of functionality and performance (particularly scalability) tests.

Alexandre Vaniachine contributed software development and support for the NOVA database. This database is now used as a primary source of the detector description parameters

in all ATLAS offline software subsystems, and has been shown to work for LAr calibration parameters. He also provided support for both ATLAS main relational database prototyping server at CERN and the database development server for the LCG project at CERN. The ATLAS server experienced considerable growth in user load due to the increased adoption of relational database services in ATLAS Data Challenge 1 and core ATLAS software development efforts during the reporting period.

US ATLAS has established a prototype subset of its grid test bed in order to evaluate emerging middleware and coordinate interoperability tests. Work was done at ANL by Ed May and Jerry Gieraltowski to assess the availability of the EDG test bed compute queues by creating a script to submit and monitor simple jobs. The results showed that, on average only 60% of the published resources are really available. Work is being done to evaluate details of RLS (Replica Location Service - the grid component that identifies the best place to find data needed by a job) on one of the EDG development test beds. Chimera is a major Virtual Data service that is being evaluated by US ATLAS, especially ANL and the University of Chicago. The interfaces to RLS and ATLAS software have been established. In particular, Chimera has been deployed on a number of US ATLAS grid test bed sites via the standard installation procedures. Chimera and RLS have been used to successfully execute simple event simulation programs in order to understand its behavior. In the next quarter, we intend to continue to test Chimera/RLS with increasing challenges in terms of CPU and data requirements.

ANL is also participating in the design and development of the Grid2003 project. Grid2003 is a coordinated project between iVDGL, GriPhyN, PPDG, and the physics experiments, principally being led by USCMS and USATLAS. The goal of the Grid2003 project is to develop, integrate, deploy and apply a functional grid across (at least) the LHC institutions, extending to non-LHC institutions and to international sites, working closely together with the existing efforts.

Tom LeCompte extended the a prototype Tile Calorimeter calibration structure that was installed in the TileCal reconstruction code last quarter. Previously only cable maps were supported; now a variety of calibrations and conditions data is supported: for example, electronics gains, pedestals and a dead channel list. The structure for applying time-varying conditions data is present, although Athena does not presently support this, so the program uses ASCII files to select between different calibration sets. Once Athena does support this (which is further awaiting LHC Computing Grid software development), the software will be adapted to do this using the appropriate Athena services. At the very end of this reporting period, Tom LeCompte was appointed the planning officer for ATLAS computing: responsible for scheduling, manpower estimates and general project management issues. This concludes his term as Tile Calorimeter database coordinator.

**(T. LeCompte)**

### I.C.3. Linear Collider

A group of physicist from the division has initiated an effort to develop the design of the hadron calorimeter (HCAL) for the Linear Collider. The aim is to develop a detector with a jet energy resolution of  $30\%/\sqrt{E}$  or better. This type of resolution is necessary to properly disentangle different Higgs mechanisms responsible for the generation of massive particles.

Up to date, the best jet energy resolution, of the order of  $50\%/\sqrt{E}$ , has been obtained by the ZEUS experiment. A novel approach, named Energy Flow Algorithms (EFAs), is being evaluated to improve this performance further and possibly reach  $30\%/\sqrt{E}$ . EFAs utilize both the tracking and the calorimeter information to measure the energy of hadronic jets. Their optimal performance requires a calorimeter with extremely fine segmentation, of the order of  $1\text{ cm}^2$  laterally and layer-by-layer longitudinally. This fine segmentation leads to the order of 50 million readout channels for the entire HCAL. A traditional analog readout of this large number of channels would be prohibitively expensive, leading us to consider a simple digital readout. The favored technology choice for the active medium for this type of calorimeter uses Resistive Plate Chambers (RPCs).

The group works on the Monte Carlo simulation of the response of various detector designs with the goal of developing a set of complete Energy Flow Algorithms. Studies of analog versus digital hadron calorimetry were completed with the release of a LC Note LC-DET-2003-009. In this study, it was shown (in simulation) that the energy deposits of neutral hadrons can be measured in a digital hadron calorimeter with better than or equal energy resolution to that in a traditional analog calorimeter. This note also included studies of the effects of different absorber materials and cell sizes on the digital measurement.

Progress was also made on E-flow algorithm development in two areas. A photon-finder was written and tested and the use of local density weighting in the digital hadron calorimeter was studied as a means to separate charged hadron showers from photons and neutral hadron showers.

On the hardware side, three RPCs have been built at Argonne and have been thoroughly tested with sources and cosmic rays. The chambers are  $20\times 20\text{ cm}^2$  in area and feature two gas gaps of 0.64 mm each. All three chambers were tested with a single pick-up pad of approximately  $100\text{ cm}^2$  and performed very well. After extensive measurements with a single readout pad, the chamber were read out with 25 pads of  $1\text{ cm}^2$  each, see Figure 1 for a sketch of the geometrical layout of the pads. The signals were fed into the RABBIT system, thus providing a precise measurement of the charges induced in each pad.

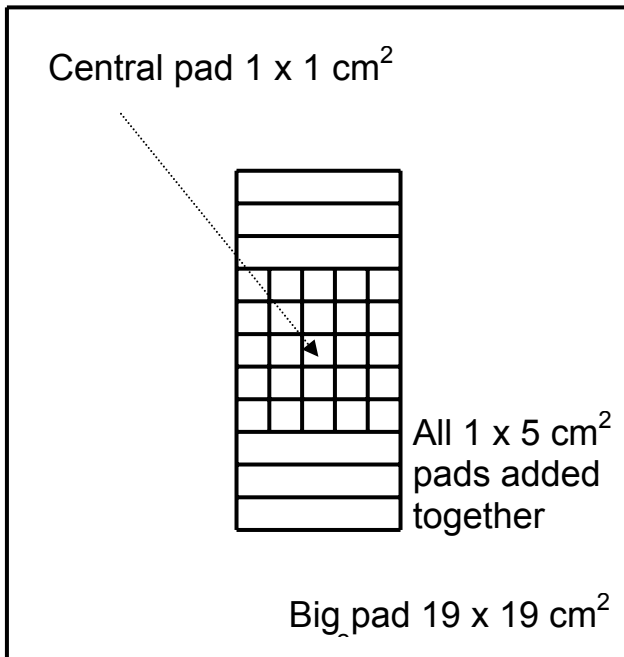


**Figure 1:** Layout of the readout pads.

Events in which the central pad registered the maximum charge were identified as events in which the cosmic ray traversed this pad. These events are of particular interest, since they permit to measure the induced charge distribution as a function of distance from the initial avalanche. Figure 2 shows the charge distribution for the central pad, the sum over the 8 surrounding pads, the sum over the 16 pads surrounding the 8 pads adjoining the central pad, and the sum over the 1x5 cm<sup>2</sup> pads and the big pad. The charge distribution in the central pad is quite broad, as expected for operation in avalanche mode, and peaks at about 400 fC. The sum of the charges in the first ring surrounding the central pad is significantly smaller. For the second ring and the big pads the recorded charges often go negative. This can also be seen in Figure 3, which shows the mean charges in the different regions, plotted as a function of the distance from the central pad.

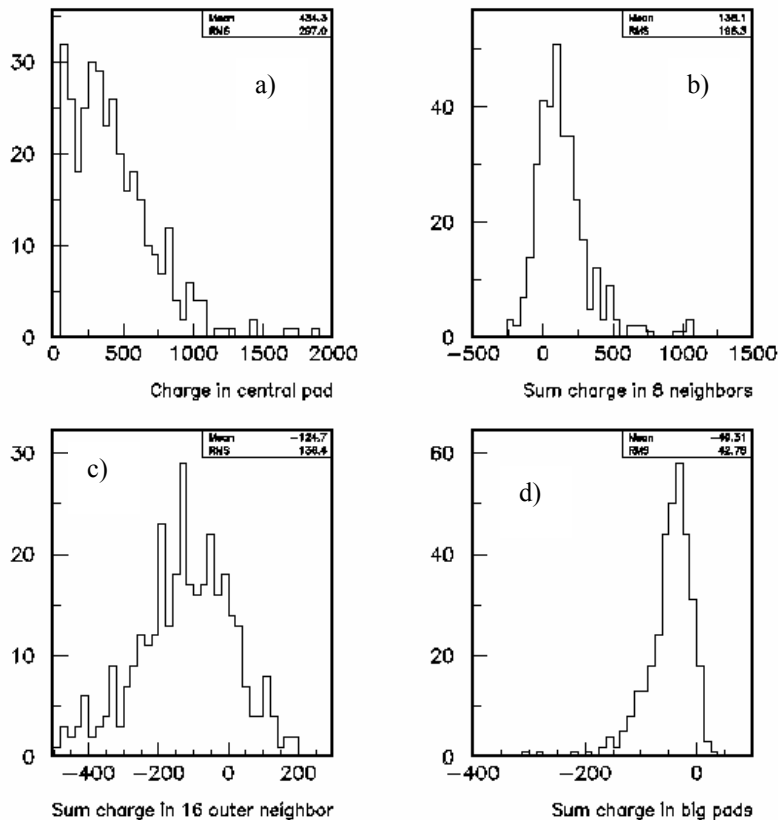


**Figure 2:** a) charge distribution in central pad, b) sum of charges in first ring of pads surrounding the central pad, c) sum of charges in the second ring, d) sum of charges in the remaining pads. The units of the x-axis are approximately fC.

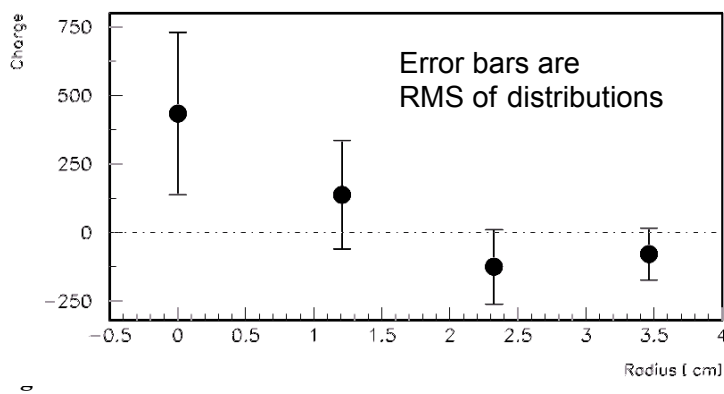


**Figure 3.** Mean charge recorded in the pads as a function of distance from the central pad. The point at  $R=0$  cm contains the central pad only, the point at  $R=1.25$  cm contains the sum over the 8 pads in the first ring surrounding the central pad, and so on...

Figure 4 shows the fraction of charge recorded individually in the surrounding pads compared to the charge induced in the central pad. As can be seen, the average charge per pad for pads located more than a 1 cm<sup>2</sup> from the pad hit is quite small. These results indicate that the induced charge is confined to about an area of 1 cm<sup>2</sup> and, therefore, pad sizes of approximately this size can be used for reading out resistive plate chambers, without incurring too much ‘cross-talk’ between the individual pads.

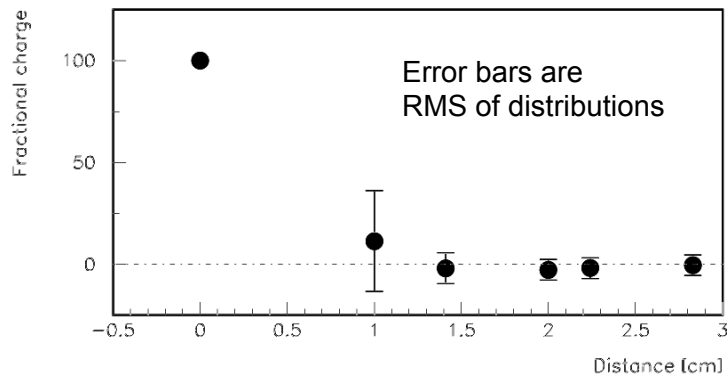


**Figure 4.** Fraction of charge measured individually in the surrounding pads as a function of distance from the central pad.

**(J. Repond)**

#### I.C.4. Electronics Support Group

CDF: We had major responsibilities for electronics for the CDF Detector at Fermilab, as part of the upgrade for Run IIA. These included the building of the front-end electronics and read-out system for the Shower Max Detector, and two sets of boards for the Level 2 Trigger called RECES and Isolated Photon Trigger. These were major projects for our group. For the Shower Max Detector, the work involved the coordination of the design engineering and system integration for the entire system, overseeing the production of all components, and ensuring that the overall system meets performance requirements. The system has 20,000 channels of low-noise electronics, and services two detector subsystems. The development work was a collaborative effort between Argonne and Fermilab.

The production work for the electronics was completed in the spring of 2001. All electronics were installed on the detector and commissioned for operation. We were successful in meeting the schedule goals in getting ready for Fermilab Run II, which is now in progress. To date, the system has performed well, with no major problems. In this period, we continued our participation with the experiment by providing technical support for the maintenance and repair of all of the electronics for this subsystem. This includes those projects that were designed and produced by Fermilab personnel. We anticipate providing this support through the life of the experiment. The system includes 100 VME read-out boards called SMXR Modules, 600 front-end boards called SMD Modules, 6000 front-end daughter cards called SQUIDS, 100 front-end crate controllers called SMC Modules, 600 preamp boards, 15,000 preamp SIPS (Single In-line Package), and 60 crate monitor boards. We also support the two sets of boards that we built for the trigger system.

There are several upgrades being planned for the detector for the second part of Run II. One of these is the replacement of the Central Preradiator Chambers (CPR). They currently are

wire chambers, similar in construction and performance to the Shower Max detector. The plan is to replace them with scintillator and phototubes. Another is the replacement of several components of the trigger system. We are working with division physicists who are involved with these projects, and expect to provide support for building these new components.

ATLAS: We have major responsibilities in the development of electronics for the Level 2 Trigger of the ATLAS Detector at CERN. Working with colleagues from Michigan State University, we are responsible for the development of two parts of this system: the Level 2 Trigger Supervisor, and the Region of Interest (ROI) Builder.

The ROI Builder is the interface between the first level trigger and the second level trigger. When an event occurs in the detector, signals are sent from the front-end electronics to the Level 1 Trigger. The Level 1 Trigger collects event fragments from the front-end electronics over the entire detector, and stores them in a Readout Buffer. It evaluates the data, and identifies regions of the detector that could have an interesting event. The Level 1 Trigger boards then sends a list of addresses called pointers to the ROI Builder, identifying where the event data from the “Region of Interest,” can be found. The ROI Builder collects the pointers for the event, and “builds” the event using the pointer list. It then sends the result to the Trigger Supervisor for distribution to Level 2 processors. The selected Level 2 Processor then executes algorithms using the pointers, and can request information to be sent from the Readout Buffers as needed. The ROI Builder is highly complex, using high-speed, highly complex Field programmable Gate Arrays (FPGAs) to implement the functionality.

In early 2001, we built the first ROI Builder prototype, and sent it to CERN for testing in a system there called the ATLAS Test Bed. The tests were largely successful, and helped refine the system requirements and specifications. In the fall of 2001, we built a card called the Gigabit Ethernet Link Source card. This card receives information from the front-end electronics, buffers it, and then sends it to the ROI Builder using Gigabit Ethernet protocol. The cards make extensive use of large programmable logic arrays. They also have a large, fast synchronous memory that might allow their use as an intermediate data storage element. Testing of the prototype occurred at Argonne and at CERN in the winter of 2001-2002. The system worked very well. In February 2002, the ROI Builder was reviewed by an internal ATLAS review committee. The merits of using the Link Source card as a front end to the ROI Builder were discussed. While the general features were deemed acceptable, there were certain issues identified associated with error reporting and data slow control. In this period, we worked on refining the design to address these issues and concerns. We have created a new design document, which describes how the new features will be implemented. We expect to have the new design approved by the review committee around mid-2003. We will then initiate a new design cycle that incorporates these features. We expect to build and test the next version by the end of 2003 or early 2004

MINOS: We have major responsibilities for the development of electronics for MINOS, the Neutrino Oscillation Experiment at Fermilab and the Soudan Mine. We are responsible for the design, development, and production of electronics Near Detector, one of the two major detectors for this experiment. One member of our group is the Level 3 Manager for the Near Detector Electronics.

The heart of the front-end electronics for the Near Detector is a custom integrated circuit designed at Fermilab, called the QIE. The QIE digitizes continuously at 53 MHz. The operations are pipelined so that there is no deadtime due to digitization. The digitized data will be stored in a local memory during the entire period of the beam spill. The data will be sent from the local memory to a read-out board after the spill is over. In between spills, the electronics will record data from cosmic rays.

The QIEs and associated circuitry will be built on small daughter boards called MENU Modules, which resemble memory SIMMs. The boards contain a high density of surface mount parts. The MENU Modules plug in to a motherboard called the MINDER Module. The MINDERS reside in front end crates called MINDER Crates, which are a semi-custom design. There is a crate controller in the MINDER Crates called the KEEPER, which controls all activity in the crate. When data is acquired, it is stored on the MENU Modules. After data is acquired, the MINDER then initiates a readout operation, where the data is sent from the MENUs to a VME readout board, called the MASTER Module. The MASTER resides in a 9U VME crate located some distance away from the MINDER Crates. All of the board designs contain a high level of programmable logic to do the complex processing of data and control of operations.

The chip design, and the development of the QIE daughter board, are responsibilities of Fermilab. Argonne is responsible for the design the MASTER Module, the MINDER Module, the KEEPER, the MINDER Crate, signal and data cables, and AUX cards for receiving signals in through the back of the VME Crates. We also have overall responsibility for the design of the rest of the system for the Near Detector, including the specifications for the QIE performance. This is a major design and production project for our group.

In 2002, we completed the development stage of this project, including the building and testing of 200 channels of the read-out system. The system was sent to CERN for use in a test beam, which was set up to calibrate the detector. The system performed very well. In early 2003, the final design changes were implemented on all parts of the system, and all sub-projects were signed off for production. Argonne is responsible for the production of 100 MASTERS, 600 MINDERS, and 60 KEEPERS. We have outside vendors do the printed circuit board fabrication and board assembly. We do the checkout work in-house with our staff technicians. To date, all boards have been fabricated, and assembly is in progress. To date, we have completed ~20% of the production work. These first units from the production line are being sent to CERN for another test beam run, scheduled to begin in September 2003. We will again send personnel over to CERN to help install, commission, and run the system during the run. We expect to complete the production work by the end of calendar year 2003.

ZEUS: We were involved with the development of front-end electronics for the new Straw Tube Tracker Detector of the ZEUS experiment at DESY. The front-end electronics is situated directly on the detector. It uses a custom integrated circuit designed at PENN, called the ASDQ. The device receives charge pulses from the detector, and sends a digital signal to the “back end” electronics located off the detector in a counting room, where a timestamp for the signal is recorded. The back end processors then use the timestamps to reconstruct the trajectory of the particle through the tracking detector. There are ~12,000 channels in the detector in total, although the front end electronics multiplexes 6 detector channels into each readout channel to reduce the number of signal wires between the front end and the back end.

The production and installation of 200 electronics boards was completed in the spring of 2001. In the time since, significant experience was obtained in operating the detector and electronics, and two problems have emerged. One problem is that the fuses on the front-end boards are blowing, despite the fact that they are sized with a factor of two above nominal operating conditions. The other problem is that the digital signals produced on the front-end boards are radiating noise into other detector components. In 2002, we studied the problems, and developed solutions for them. The solutions were reviewed by a committee appointed by the ZEUS management in November. In early 2003 we built small circuit boards that were part of the modifications to the system. There was a shutdown of the experiment in the spring of 2003, where we had an opportunity to work on the STT. We sent personnel to DESY in April, to assist with installing the boards and implementing other repairs to the detector. The detector has now been reassembled, and is in the process of being commissioned. Initial tests indicate that the repairs have been successful. Data taking is scheduled to resume in the fall of 2003.

**(G. Drake)**

## II. THEORETICAL PHYSICS PROGRAM

### II.A. THEORY

#### II.A.1. Higgs Boson Production Including All-Orders Soft Gluon Resummation

The search for the Higgs boson is a central motivation for the experimental programs at the Fermilab Tevatron and the CERN Large Hadron Collider (LHC), with detection techniques guided by theoretical expectations about its production dynamics and decay properties. Precise theoretical calculations of the expected differential cross sections for production of the signal and backgrounds are important for quantitative evaluation of the required measurement accuracies and detector performance. Good estimations of the expected transverse momentum distributions can suggest selections in this variable that should improve background rejection.

Working with Jianwei Qiu of Iowa State University, Ed Berger completed a calculation of the transverse momentum  $Q_T$  distribution for inclusive Higgs boson production at the energy of the Fermilab Tevatron. Predictions are provided in Argonne report ANL-HEP-PR-03-028 [hep-ph/0304267], accepted for publication in Physical Review Letters. Berger and Qiu concentrate on the behavior of the distribution in the region of small and intermediate values of  $Q_T$  where the cross section is large. Using an impact-parameter  $b$ -space formalism, they employ all-orders resummation to master the large logarithmic coefficients that appear in finite-order perturbative expansions of the cross section in the strong coupling strength  $\alpha_s$ . There are two major improvements in their work relative to prior investigations. Their resummed results merge smoothly at large  $Q_T$  with the fixed-order expectations in perturbative QCD, as they should, with no need for a matching procedure. Second, the  $Q_T$  distribution is insensitive to the functional form employed for the non-perturbative input at large  $b$ , so long as the form used for this extrapolation does not modify the perturbative  $b$ -space distribution at small  $b$ .

Berger and Qiu provide  $Q_T$  distributions for Higgs boson masses from  $M_Z$  to 200 GeV, as well as analogous results for  $Z$  boson production. Two points are evident in the comparison of  $Z$  boson and Higgs boson production. The peak in the  $Q_T$  distribution occurs at a smaller value of  $Q_T$  for  $Z$  production, and the distribution is narrower for  $Z$  production. The larger QCD color factors produce more gluonic showering in the glue-gluon scattering subprocess that dominates inclusive Higgs boson production than in the fermionic subprocesses relevant for  $Z$  production. After all-orders resummation, the enhanced showering suppresses the large- $b$  (small  $Q_T$ ) region more effectively for Higgs boson production. The harder  $Q_T$  spectrum for Higgs boson production suggests that the signal to background ratio can be enhanced if Higgs bosons are selected with large  $Q_T$ . Examples of results are shown in Fig. 1.

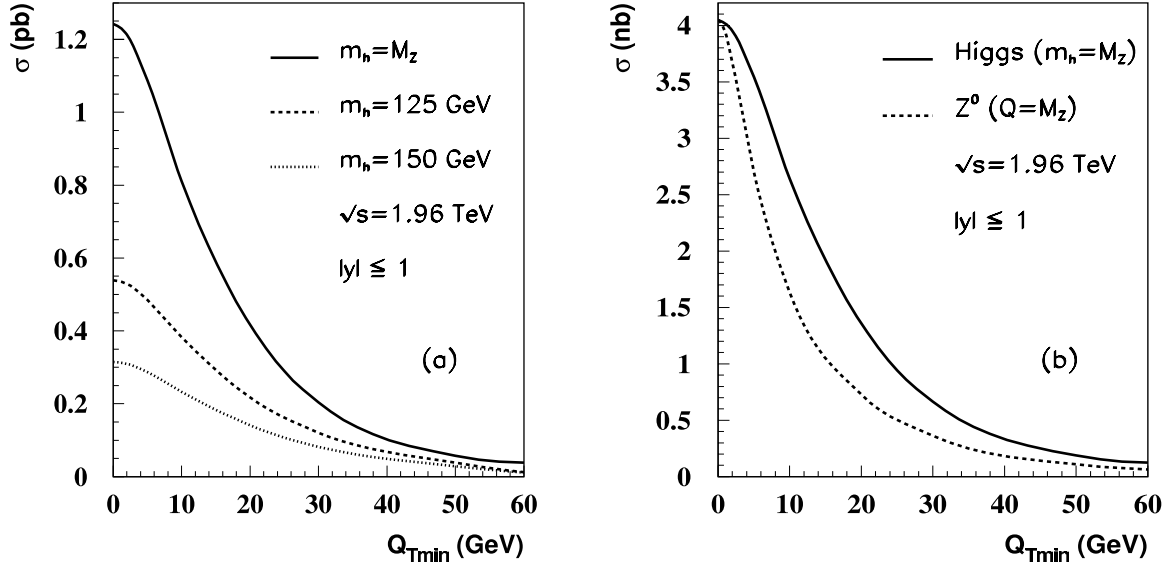


**Figure 1.** (a) Cross sections for Higgs boson production at  $\sqrt{S} = 1.96$  TeV integrated over the ranges  $Q_T > Q_{T\min}$  and rapidity  $|y| < 1.0$  for three values of the mass of the Higgs boson:  $m_h = 125$  GeV, 150 GeV, and  $m_h = M_Z$ . In (b), analogous results are shown for Z boson production and, for ease of comparison, the curve for Higgs boson production at  $m_h = M_Z$  rescaled so that the cross-section at  $Q_{T\min} = 0$  is the same as that for the Z case.

(E. L. Berger)

## II.A.2. Squark Mixing in Electron-Positron Reactions

For each squark flavor there are two mass eigenstates, one heavier than the other. The mixing that results in these two states is characterized by a mixing angle  $\theta_q$ . Ed Berger, Tim Tait and Jungil Lee examined prospects for a direct measurement of the top- and bottom-squark mixing angles from data on associated production of a heavy and a light squark of the same flavor in electron-positron annihilation reactions at CERN's LEP-II and at a future linear collider. They provide predictions of cross sections top-squark pair production at linear collider energies and for bottom-squark pair production at LEP-II energies. Their results are presented in Argonne report ANL-HEP-PR-03-027, hep-ph/0306110, submitted for publication in Physical Review D.

At typical linear collider energies, the cross sections for associated production of a light- and a heavy-top-squark are typically of order a few femtobarns (fb) for masses within the range allowed by kinematics. At a linear collider with hundreds of inverse fb of data, the cross section and mixing angle could be measured at the few per cent level. In the context of the light bottom squark scenario, Berger, Lee, and Tait show that existing data from LEP-II should show definitive evidence for the heavier bottom squark provided that its mass is less than 120 GeV. Predicted numbers of events are shown in Fig. 1. For a mass above 130 GeV, too few events would have been produced at LEP-II to permit discovery or the establishment of a bound. These results are important, in part, because the viability of the light bottom squark scenario has been questioned for reasons having to do with the potential size of SUSY-QCD loop-contributions to observables measured at CERN's LEP-I. Berger was invited to speak about this work at the Cornell Linear Collider meeting in July 2003.

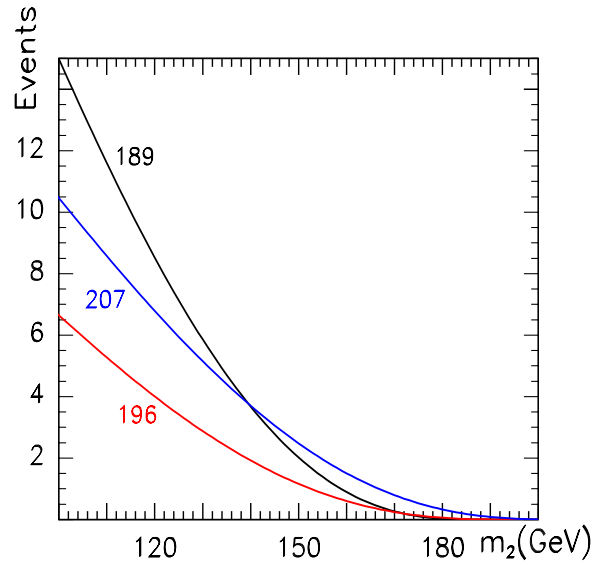


**Figure 1.** Predicted numbers of events from  $e^+ + e^- \rightarrow \tilde{b}_1 \tilde{b}_2^*$  at center-of-mass energies 189, 196, and 207 GeV as a function of the mass  $m_2$  of the heavier bottom squark. The mass of the lighter bottom squark is  $m_1 = 3.5$  GeV, and the mixing angle is fixed by  $\sin^2 \theta_b = 1/6$ .

**(E. L. Berger)**

### II.A.3. $e^+e^-$ Annihilation into $J/\psi + J/\psi$ at $B$ Factories

This research was presented in the report for July 1, 2002--December 31, 2002. Papers describing it, ANL-HEP-PR-02-110 (hep-ph/0212181) and ANL-HEP-PR-02-105 (hep-ph/0212352), have been published during the current reporting period in Phys. Rev. Lett. **90**, 162001 (2003) and Phys. Rev. D **67**, 054023 (2003), respectively.

(G. T. Bodwin)

### II.A.4 Relativistic Corrections to Gluon Fragmentation to $J/\psi$

Work on this subject by G. Bodwin and J. Lee was discussed previously in the report for July 1, 2002--December 31, 2002.

The computation has now been completed and checked through independent calculations by Bodwin and Lee and also through comparison with lower-order calculations of the fragmentation functions (Braaten and Lee) and the related  $^3S_1$  quarkonium decay rate (Keung and Muzinich). The final results are that the corrections are  $+2.45v^2$  for the short-distance coefficient of the color-singlet fragmentation function and  $-1.8v^2$  for the short-distance coefficient of the color-octet fragmentation function. In the case of  $J/\psi$  fragmentation, the Gremm-Kapustin relation, which is based on the NRQCD equations of motion and is accurate up to corrections of relative order  $v^2$ , was used to obtain an estimate for  $v^2$  from the  $J/\psi$  binding energy. The result is  $v^2 \approx 0.2$ . Therefore, the color-singlet correction is about +50%, and the color-octet correction is about -40%. The large change in the color-singlet short-distance coefficient has little effect on the predictions for  $J/\psi$  production at the Tevatron because the color-singlet contribution to the cross section is only about 5% of the total over a wide range of  $p_T$ . The large correction to the short-distance coefficient of the color-octet fragmentation function will not immediately change the predicted size of the color-octet contribution to  $J/\psi$  production at the Tevatron, since the unknown color-octet matrix element that multiplies the short-distance coefficient is determined, at present, by fitting to the Tevatron data. However, the large correction will ultimately be important in evaluating the consistency of the fitted matrix element with the NRQCD velocity-scaling rules and with determinations of the matrix element from other processes and, eventually, lattice computations.

A paper describing this work (ANL-HEP-PR-03-065, hep-ph/0308016) has been submitted to Phys. Rev. D.

(G. T. Bodwin)

### II.A.5. Lattice Gauge Theory

During this period we completed our studies of 2-colour QCD at finite quark-number densities, finishing the analysis of the Goldstone spectrum. We have completed the simulations of 2-flavour QCD at finite isospin density in the vicinity of the finite temperature transition in the low density domain. We have continued our simulations of 2-flavour QCD with massless quarks in the neighbourhood of the phase transition from hadronic matter to a quark-gluon plasma.

2-colour QCD at finite quark-number chemical potential  $\mu$  has a mean-field (second order) phase transition to a superfluid state where quark number is broken spontaneously by a diquark condensate at  $\mu = m_\pi/2$ . We have analysed the spectrum of (pseudo)-Goldstone bosons associated with chiral and quark-number symmetry breaking. For the 4-flavour theory we studied, the lattice theory has 3 such bosons (Fig. 1). We have calculated the masses of these excitations from our simulations on a  $12^3 \times 4$  lattice and find that these masses are in excellent agreement with the predictions of effective Lagrangians, chiral perturbation theory and more general arguments for  $\mu < m_\pi/2$ . Above this transition, although there are deviations from these predictions, the qualitative behaviour is as expected, indicating that we understand the physics of these symmetry breakings. This model is of interest because this superfluid state is the analogue of the colour superconducting state predicted for finite baryon number density.

We are simulating QCD at a finite chemical potential  $\mu_I$  for isospin ( $I_3$ ) and temperature. In particular we have observed the  $\mu_I$  dependence of the finite temperature crossover from hadronic matter to a quark-gluon plasma for one quark mass,  $m = 0.05$ , for  $\mu_I < m_\pi$ , and are extending this to larger masses. The transition temperature drops only slowly with increasing  $\mu_I$ . In this region the  $\mu_I$  and  $\mu_q$  (quark number chemical potential) dependence of this temperature are the same. Our calculations indicate that by  $\mu_q \sim 180$  MeV (more than 10 times that expected to be probed by RHIC) this transition temperature has only dropped by  $\sim 10$  MeV from its value at  $\mu_q = 0$ . Thus we get information about finite quark-/baryon-number density, which cannot be simulated directly, by simulation at finite isospin density, which can be simulated directly.

We are continuing our simulations of the finite temperature chiral phase transition for QCD with 2 massless quark flavours using our action, which differs from the standard Lattice QCD action by the addition of an irrelevant chiral 4-fermion interaction. It is this modification which permits simulations at zero quark mass. We are currently accumulating statistics on  $16^3 \times 8$  and  $24^3 \times 8$  lattices. The indications are that the transition is second order, as expected, and we will extract the critical exponents thus determining the universality class of this transition.

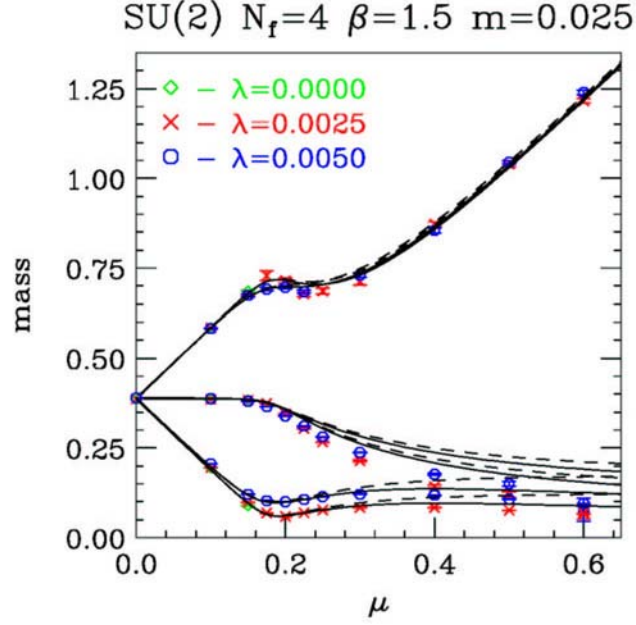


**Figure 1.** The pseudo-Goldstone spectrum for 2-colour QCD as a function of quark-number chemical potential.

(D. K. Sinclair)

## II.A.6. Precision Electroweak Data and Unification of Couplings in Warped Extra Dimensions

Warped extra dimensions allow a novel way of solving the hierarchy problem, with all fundamental mass parameters of the theory naturally of the order of the Planck scale. The observable value of the Higgs vacuum expectation value is red-shifted, due to the localization of the Higgs field in the extra dimension. It has been recently observed that, when the gauge fields propagate in the bulk, unification of the gauge couplings may be achieved. Moreover, the propagation of fermions in the bulk allows for a simple solution to potentially dangerous proton decay problems. However, bulk gauge fields and fermions pose a phenomenological challenge, since they tend to induce large corrections to the precision electroweak observables. In collaboration with M. Carena, A. Delgado, E. Ponton and T. Tait, we studied in detail the effect of gauge and fermion fields propagating in the bulk in the presence of gauge brane kinetic terms compatible with gauge coupling unification, and we present ways of obtaining a consistent description of experimental data, while allowing values of the first Kaluza Klein (KK) mode masses of the order of a few TeV (ANL-HEP-PR-03-29; hep-ph/0305188).

In Figs. 1 and 2, we present the results for the upper bound on the first weak gauge boson KK mass  $M_{KK}$  as a function of the Higgs mass. The fit to the data is significantly improved by

large values of the Higgs mass  $m_h \gtrsim 300$  GeV. However, the bound on the first weak gauge boson KK mode mass is still about 11 TeV and therefore difficult to detect at the LHC. In Phys. Rev. **D67**, 096006 (2003), we demonstrated that, in the case of light KK modes, the fit to the precision electroweak data is greatly improved by the presence of brane gauge kinetic terms [Acta Physica Polonica **B33**, 2355 (2002)]. For every gauge coupling  $g_i$ , we shall denote the size of the brane kinetic terms by the ratio  $r_{IR}^i$  of the dimensional gauge coupling to the local brane gauge coupling (ANL-HEP-PR-03-29; hep-ph/0305188). The main reason for this improvement is associated with the fact that for the same values of the warp factor  $k$  and the size of the extra dimension  $L$ , the mass of the first gauge boson KK mode becomes significantly lower for large values of  $r_{IR}^i$ , than in the case of vanishing brane kinetic terms. However, since we are interested in the question of unification of couplings, we cannot set  $r_{IR}^i$  to arbitrarily large values.

Even the addition of small kinetic terms in the infrared brane may have dramatic effects in the spectrum. In the case of  $kr'_{IR} = kr_{IR}^2 = 2(kr'_{IR} = kr_{IR}^2 = 1)$  a bound of about 4 TeV (5 TeV) may be obtained for values of the Higgs mass larger than 400 GeV. Given the above conclusions, it seems possible that the LHC can study the prospect of RS unification. For KK masses in the range of a few TeV, there is the hope that even the KK modes of the GUT sector could be produced and studied, providing clear experimental evidence of an RS unified theory (ANL-HEP-PR-03-29; hep-ph/0305188).

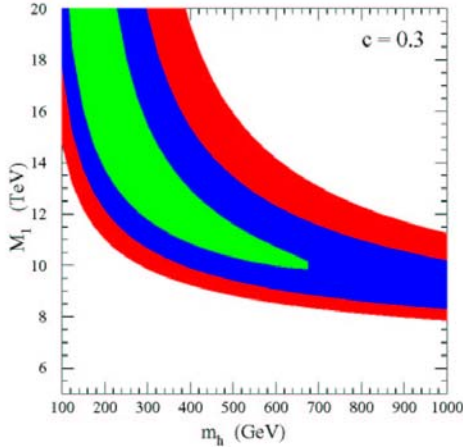


**Figure 1.** Allowed bands of the RS unified model in the parameter space of the Higgs mass and the first KK mode mass. The inner band represents  $1\sigma$  agreement with the fit to the precision electroweak data, whereas the surrounding middle and outer bands indicate  $2\sigma$  and  $3\sigma$  agreement, respectively.

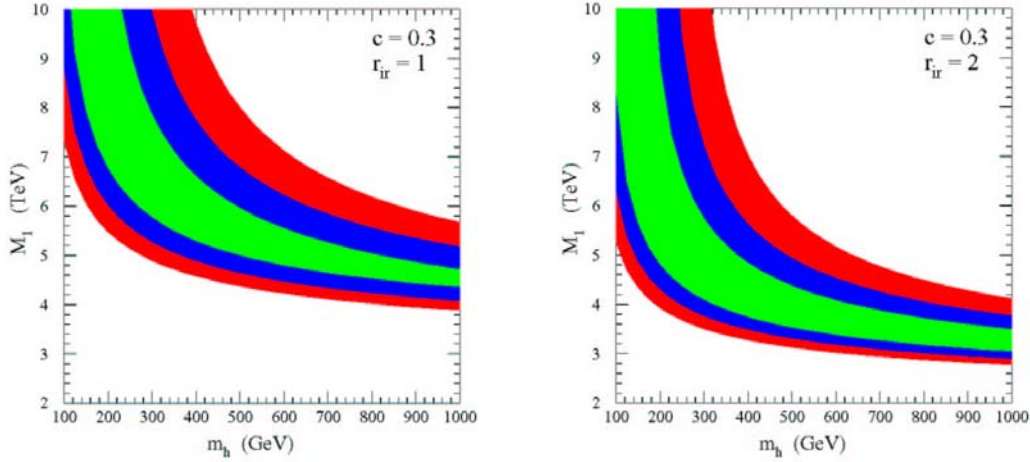


**Figure 2.** As Fig. 1, but with non-zero (unified) kinetic terms on the IR brane of  $kr_{IR} = 1,2$ .

(C.E.M. Wagner)

### II.A.7. Membrane Quantization Via Nambu Brackets

Classically, the evolution of topological  $p$ -branes is controlled by Nambu Brackets (NB). However, quantization of such membranes had been mooted by misperceived inconsistencies in quantizing these brackets. C. Zachos, in Phys. Lett. **B570** (2003) 82-88, demonstrates and illustrates explicitly how, in fact, quantization is achievable on the basis of prior results joint with T. Curtright (Miami) in an in-depth investigation of quantum ones (QNBs) [Phys Rev **D68**, 085001 (2003); AIP Conference Proceedings 672 (2003) pp. 183-196; AIP Conference Proceedings 672 (2003) pp. 165-182], which resolved consistency conundrums.

Specifically,  $(p-2)$ -branes embedded in  $p$ -space are evolved according to a  $(p-1)$ -form action arising on the boundary of an exact  $p$ -form, evocative of  $WZWN$  interactions, and pioneered by Estabrook. The equations of motion extremizing this action are Nambu's, rather than Hamilton's, equations. An inconsistency of quantization of the underlying NBs (identified by Nambu thirty years ago) is only operative for  $(p=\text{odd})$ -branes, but it was found to be plainly absent for  $(p=\text{even})$ -branes. Moreover, Zachos and Curtright appreciated that this odd-NB inconsistency has its origin in the improper classical limit of the odd QNBs; whereas the classical limit reached from even-QNBs (with one dynamical variable suitably saturated), reaches the proper odd classical NBs in one less dimension, as well. Thus, *both* even and odd (from even) QNBs are shown to be consistent.

Other misperceived inconsistencies stressed in the past decade merely resulted out of infelicitous and confused restrictions, which left the actual solutions provided by natural systems

outside the  $NBs$ ' domain of definition. A careful systematic consideration by the present authors of the mathematical structure of such brackets (such as the correct generalizations of the Jacobi Identity as an encoder of associativity), some discovered, some already known (but not widely so); and of the comparison with problems where the answer was already known (found by the authors in prior work) suffices to illustrate the validity and practicality of the method, as well as the proper avoidance of common pitfalls. Presently, wider applications to more diverse systems are sought, in which application of Hamiltonian techniques is not suitable.

**(C. Zachos)**

### III. ACCELERATOR RESEARCH AND DEVELOPMENT

#### III.A. ARGONNE WAKEFIELD ACCELERATOR PROGRAM

##### III.A.1. The Argonne Wakefield Accelerator Status

This new RF gun design was based on our experience with the original AWA drive gun --- which at present is the highest current photoinjector in existence. The gun was installed and RF conditioned to the designed gradient of 80 MV/m. Vacuum in the range of  $10^{-9}$  torr under full RF power (adequate for the use of high QE photocathodes). During this period, a numerous diagnostics such as emittance pepper pot plates, OTR screens, Cherenkov radiators were fabricated and installed in the beamline. Electron beam with charge of 1 nC ~ 25 nC were

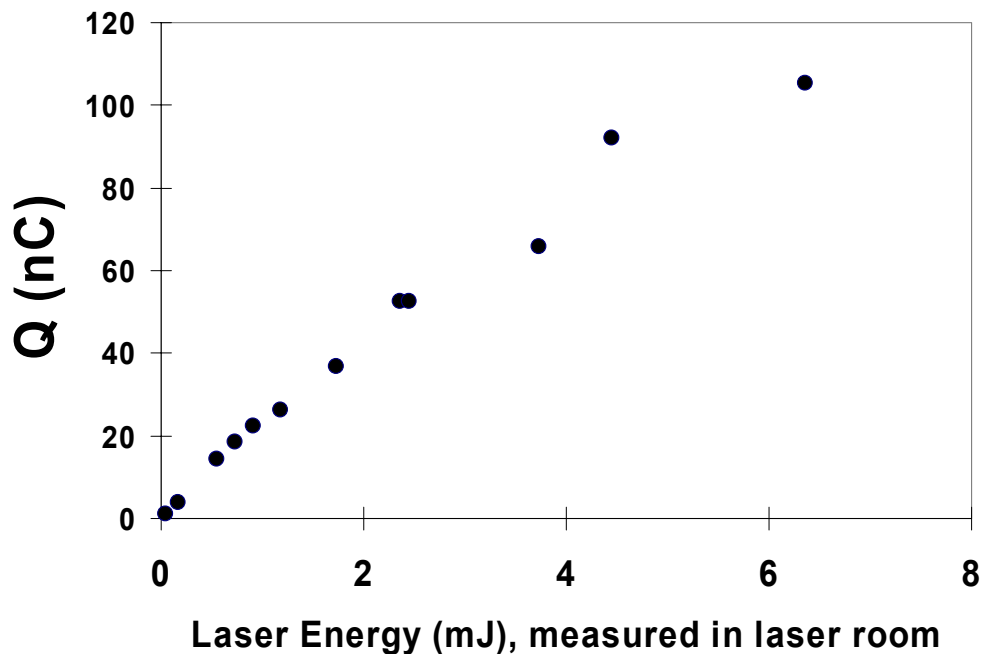


**Figure 1:** Measured electron Beam at exit of the RF gun vs the laser energy. More than 100 nC beam is generated and its bunch length are measured to be less than 10 ps FWHM.

generated using a copper cathode. The beam energy is 6 - 7 MeV. Initial beam characterization showed that beam has very low emittance as designed. However, using OTR did not obtain bunch length information because the OTR light for 6 – 7 MeV beam is to diffuse and dim. Thus, we have replaced the OTR with a quartz Cherenkov radiator. A Mg photocathode was also designed and fabricated. The electron beam with charge of a few nC to 100 nC was produced using the new laser beam and magnesium photocathode (figure 1). The electron bunch length was measured using Cherenkov light emitted from electron beam while passing through a

thin quartz plate. The measured rms bunch length is in a good agreement with the design and its FWHM < 10 ps for beam up to 70 nC.

### III. A. 2. The New Type of Dielectric Accelerator Developments

Due to the coupling problems developed during the high power tests for dielectric structures at NRL, we have re-examined the coupling schemes. We have found a new modular type coupling structures as shown in Figure 1. The scheme as a few advantages: The modular approach has several advantage: separate Coupling Problem from Acceleration; the coupling does not depend on location of taper with respect to the aperture; copper residue on outside of dielectric won't be harmful; larger coupling- aperture lowers the power density. We have fabricated and cold tested an Alumina based structure and the results are in good agreement with the theory and simulation. Upon completion of the new modular coupling and dielectric structures, a new round of experiments were performed at NRL. The dielectric structure used here was based on Alumina. The goals of this test were to confirm that the new RF coupling scheme would function at high power without breaking down and to test the high power response of the Alumina structure.

After two days of conditioning, the DLA structure could support an incident power of 5 MW at a 150 nsec pulse length with no signs of breakdown observed. Calculations show that this power level corresponds to a gradient of about 8 MV/m. One surprise uncovered during the test was an unexpected light emission from inner tubes of the structure. Our preliminary investigation into this phenomenon leads us to believe that we observed secondary electron emission (SEE) in the dielectric. We are now working on the interpretation of the data and investigating techniques (TiN coatings, etc.) to reduce the SEE.

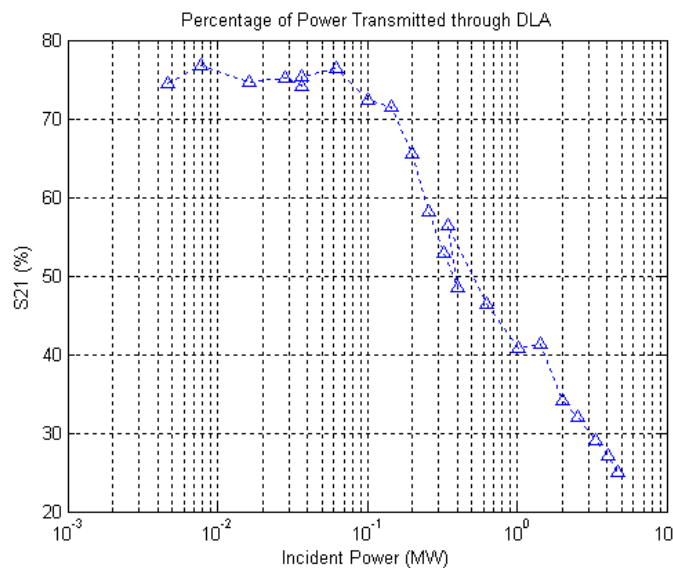
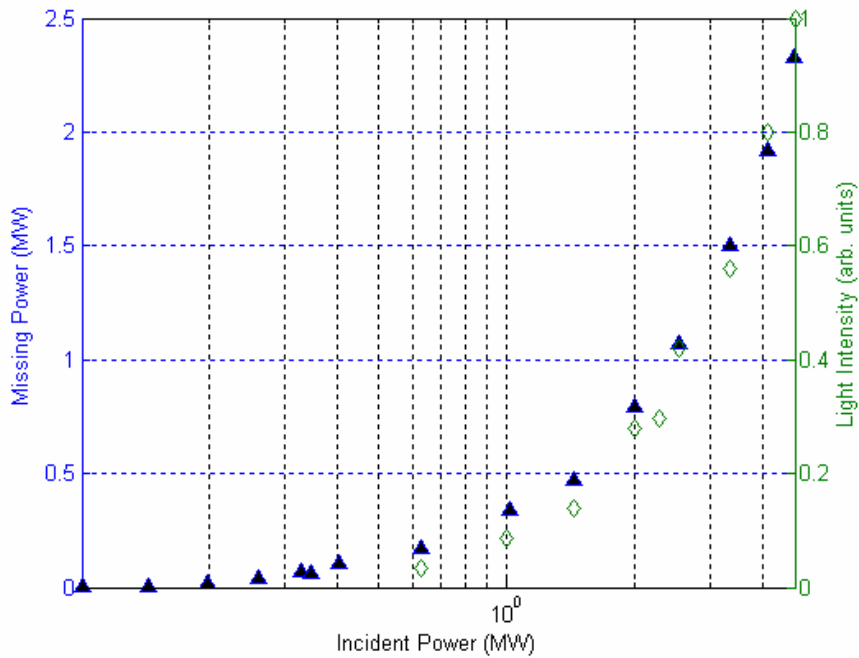


Figure 2. Measured transmitted power vs the input power during the high power test.



**Figure 3.** Observed light emission (diamond) and missing power (solid triangle) vs the incident power.

In summary, the winter 2003 run at NRL went very well. From this run we have drawn the following (preliminary) conclusions: (1) the redesigned DLA structure has eliminated the coupler-arcing problem; (2) no dielectric breakdown was observed; and (3) SEE appears to be absorbing RF power and producing light emission. Currently, a program has been setup to investigate TiN coating on inner radius of the dielectric tubes. Also, we are constructing a new set of modular structures with dielectric material MCT20 which may have a reduced sensitivity to SEE problems.

### III. A. 3. Other Significant Beam Physics Related Studies

During this period, we have conducted another round of coherent and incoherent RF signal generation using an intense electron beam passing through an air and some minerals. This study was for simulating the interaction between an ultra high energy cosmic ray and air and it is conducted by University of Hawaii and UCLA. Data were collected and is being analyzed.

We have investigated the high brightness electron beam generation at the ANL and its application to a precision wakefield measurement system. Through collaborative work with Fermilab and ANL-APS, it was apparent to us that a compact highness electron beam is needed for precision transverse wakefield measurements of linear collider structures. We have performed numerical simulations of a low charge 1 nC beam in the new AWA gun. Without any attempt at optimizing the hardware parameters (because the gun is already installed in place), we are able to achieve  $\sim 1$  mm mrad transverse emittance and pulse length of 5 ps. These parameters are close to or better all existing RF photocathode guns. Detailed experimental beam parameter characterizations will be done next year.

In addition to the efforts described above, there are a number of other research areas worth mentioning. Most involve collaborative efforts with outside institutions, and demonstrate the flexibility and vitality of the AWA program.

*Tunable dielectric based wakefield accelerator development.* Working with Dr. Kanareykin and Dr. Schoessow of Euclid Concepts, LLC, we have developed a practical method to tune the wakefield excitation frequency of a dielectric structure using a ferroelectric material and adjusting its dielectric constant using an externally applied DC electric field. Detailed analysis showed that we can vary the resonant frequency by a few per cent, sufficient to compensate for fabrication tolerances.

*Development of a modified Quad Scan to measure emittance.* In collaboration with SLAC, we are developing a modification to the usual Quad Scan routine so that includes both space-charge and emittance. The technique is based on numerical solutions to the 3D coupled, beam envelope equations.

*New Developments in the Enhanced Transformer Ratio Experiment.* This experiment requires that beams of vastly different charge, and therefore different space charge forces, be propagated through the same beam line. In the past this would not be possible since the beamline can only be optimized for a single charge. We have invented a new technique that makes propagation of differently charged beams possible by individually adjusting the radius of each beam so that each beam is matched.

*Field analysis of a partially filled dielectric rectangular waveguide.* We have investigated a new type of accelerating structures, a rectangular waveguide partially filled with dielectric. Not only can this new type of structure accelerate charged particle beams, it can also focus the beam at the same time. Detailed transverse wakefield calculations were performed and the results were submitted to Physical Review E.

(W. Gai)

### III. B. MUON COLLABORATION R & D

#### a) Muon Ionization Cooling Experiment

The primary effort during this period was devoted to measuring electrons and x-rays produced by field emission from the 805 MHz pillbox cavity in Lab G. This data was used to construct an argument that the backgrounds in the proposed Muon Ionization Cooling Experiment (MICE) would be at a level that was acceptable for the proposed silicon fiber and Gaseous Electron Multiplier (GEM) detectors. In fact, the MICE proposal seems to have had a quick passage through the Rutherford Appleton Laboratory experimental committee and has now been approved, subject to funding provided by the experimental group.

The principle goal of work in 2003 was to evaluate the behavior of Be in rf cavities. The single cell pillbox cavity was fitted with windows in which pre-stressed Be foils had been inserted and these windows were then subjected to normal cavity operation with and without 2.5 T magnetic fields for a period of 3 months before they were removed. The result of this test was very interesting. When the foils were removed and examined it was noted that they were covered with an uneven coating of copper dust which adhered to the foil. Under extensive analysis with an electron microscope at McCrone Associates, which had a device which would accept the entire window, we saw that there was no detectable damage to the Be surface. After the same treatment the copper cavities had large pits, most deeper than the thickness of the Be foil. We assume that the survival of the Be is due to its high tensile strength, in accordance with the new arguments developed which relate breakdown with tensile stress induced by the electric field and tensile strength of the metal surface.

In addition to the work in Lab G, we also worked with Laura Bandura of NIU on measurements of beam induced turbulence in liquid targets. This issue is relevant for the design of liquid hydrogen absorbers used in muon cooling. The experiment consisted of a Schlieren system looking at a small tank of water (or hexane) which was used as a target for 20 MeV electron beam. The experiment showed that deposited energies of 10 - 100 J gave a very clear image of the turbulence, which could be seen in both horizontal and vertical density gradients. This experiment earned Laura Bandura a Masters Degree from NIU.

An extension of this effort considered the problems caused by MW beams in liquid targets, where the targets were operated in a high magnetic field. The primary target for the muon based neutrino source or muon collider is a liquid mercury jet in a 20 T field, and when this jet is hit by the proton beam the mercury essentially explodes. The question is how efficiently the 20 T solenoidal field can damp this explosion. Laura Bandura and J. Norem proposed that this process could be studied very inexpensively using real explosives in Hg jet operated in an existing magnet at NHMFL in Florida.

#### **b) Understanding and Extending the Limits of RF Cavities.**

The initial stages of this work have identified fracture and fatigue of copper as one of the primary mechanisms causing breakdown. A paper was written and submitted to the 2003 Particle Accelerator Conference with Ahmed Hassanein and Isak Konkashbaev of ET which outlined the basic mechanisms involved with high voltage breakdown.

In addition to this mechanism, conversations with Dean Miller of ANL Material Science Division have made it possible to uncover a number of references on the conduction of electrons near grain boundaries and defects, that show that these points should have very high potentials and correspondingly high local ohmic heating powers which would be the cause of many of the failures seen at SLAC and KEK with NLC prototype cavities. We have begun to study these phenomena as a possible mechanism limiting the gradients that can be generated in the CLIC and NLC linac designs.

**(J. Norem)**

## IV. PUBLICATIONS

### IV. A. Books, Journals And Conference Proceedings

Azimuthal Anisotropy and Correlations in the Hard Scattering Regime at RHIC

R. V. Cadman, K. Krueger, H. M. Spinka, D. G. Underwood  
Phys. Rev. Lett. **90**, 032301, (January 2003).

Central Pseudorapidity Gaps in Events with a Leading Antiproton at the Fermilab Tevatron  
 $p\bar{p}$  Collider

R. E. Blair, K. L. Byrum, E. Kovacs, S. E. Kuhlmann, T. LeCompte, L. Nodulman, J. Proudfoot, R. Thurman-Keup, R. G. Wagner and A. B. Wicklund  
Phys. Rev. Lett. **91**, 011802 (2003).

Data Challenges in ATLAS Computing

A. Vaniachine  
Nucl. Instrum. & Meth. **A502**, 446 (April 2003).

Dark Current and X Ray Measurements of an 805 MHZ Pillbox Cavity

J. Norem, P. Gruber, *et al.*  
In: *Proceedings of the 2003 Particle Accelerator Conference (PAC2003)*,  
Portland, Oregon, May 12-16, 2003, edited by J. Chew, P. Lucas, and S. Webber,  
pp.1183-1185

Deformation Quantization of Nambu Mechanics

C. K. Zachos and T. L. Curtright  
In: *Short Distance Behavior of Fundamental Interactions: 31<sup>st</sup> Coral Gables Conference on High Energy Physics and Cosmology*, ed. by B. N. Kursunoglu, *et al.* (AIP Conference Proceedings 672, June 2003) pp. 183-196.

Differential Cross Section for Higgs Boson Production Including All-Orders Soft Gluon Resummation

E. L. Berger and J.-W. Qiu  
Phys. Rev. **D67**, 034026 (2003).

Disappearance of Back-to-Back High  $p_T$  Hadron Correlations in Central Au+Au Collisions at  $\sqrt{s_{NN}} = 200$  GeV

R. V. Cadman, K. Krueger, H. M. Spinka, D. G. Underwood  
Phys. Rev. Lett. **90**, 082302 (February 2003).

Dynamics of the  $\pi^-p \rightarrow \pi^0\pi^0n$  Reaction for  $p < 750$  MeV/c

C. E. Allgower and H. Spinka

Phys. Rev. Lett. **91**, 102301 (2003).

$e^+e^-$  Annihilation into  $J/\psi + J/\psi$

G. T. Bodwin, J. Lee, and E. Braaten

Phys. Rev. Letts. **90**, 162001 (April 2003).

Elastic Scattering and Direct Detection of Kaluza-Klein Dark Matter

G. Servant and T.M.P. Tait

New J. Phys. **4**, 99 (December 2002). *not previously cited*

Erratum: Next-to-Leading Order Supersymmetric QCD Predictions for Associated Production of Gauginos and Gluinos

E. L. Berger, M. Klasen, and T.M.P. Tait

Phys. Rev. **D67**, 099901 (May 2003).

Exclusive Double-Charmonium Production from  $e^+e^-$  Annihilation into a Virtual Photon

E. Braaten and J. Lee

Phys. Rev. **D67**, 054007 (March 2003).

Exclusive Double-Charmonium Production from  $e^+e^-$  Annihilation into Two Virtual Photons

G. T. Bodwin, J. Lee, and E. Braaten

Phys. Rev. **D67**, 054023 (March 2003).

Final State Phases in  $B \rightarrow D\pi$ ,  $D^*\pi$ , and  $D\rho$  Decays

C.-W. Chiang and J. L. Rosner

Phys. Rev. **D67**, 074013 (April 2003).

Higgs-Boson Production in Association with a Single Bottom Quark

J. M. Campbell, R. K. Ellis, F. Maltoni, and S. Willenbrock

Phys. Rev. **D67**, 095002 (May 2003).

Hunting for Glueballs in Electron-Positron Annihilation

S. J. Brodsky, A. S. Goldhaber and J. Lee

Phys. Rev. Letts. **91**, 112001 (2003).

Improved Results in Supersymmetric Electroweak Baryogenesis

M. Carena, M. Quiros, M. Seco, and C.E.M. Wagner

Nucl. Phys. **B650**, 24-42 (February 2003).

Is the Lightest Kaluza-Klein Particle a Viable Dark Matter Candidate?

G. Servant and T.M.P. Tait

Nucl. Phys. **B650**, 391-419 (2003).

Lattice QCD at Finite Isospin Chemical Potential and Temperature

J. B. Kogut and D. K. Sinclair

In: *Proceedings of the 20<sup>th</sup> International Symposium on Lattice Field Theory (LATTICE 2002)*, ed. by R. Edwards, *et al.* (North-Holland, Amsterdam, May 2003). Nucl. Phys. **B119** (Proc. Suppl.), 556-558 (May 2003).

Light Gluino and the Running of  $\alpha_s$

C.-W. Chiang, Z. Luo, and J. L. Rosner

Phys. Rev. **D67**, 035008 (February 2003).

Measurement of Event Shapes in Deep Inelastic Scattering at HERA

S. Chekanov, D. Krakauer, J. H. Loizides, S. Magill, B. Musgrave, J. Repond, R. Yoshida

Eur. J. Phys. **C27**, 531-545 (2003).

Measurement of the Mass Difference  $m(D_s^+) - m(D^+)$  at CDF II

R. E. Blair, K. L. Byrum, J. Dawson, G. Drake, V. Guarino, S. E. Kuhlmann, T. LeCompte, L. Nodulman, J. Proudfoot, R. Thurman-Keup, R. G. Wagner and A. B. Wicklund

Phys. Rev. **D68**, 072004 (March 2003).

Measurement of Proton-Dissociative Diffractive Photoproduction of Vector Mesons at Large Momentum Transfer at HERA

S. Chekanov, D. Krakauer, S. Magill, B. Musgrave, J. Repond, R. Yoshida

Eur. J. Phys. **C26**(3), 389-409 (January 2003)

Measurement of Subject Multiplicities in Neutral Current Deep Inelastic Scattering at HERA and Determination of  $a_s$

S. Chekanov, D. Krakauer, J. H. Loizides, S. Magill, B. Musgrave, J. Repond and R. Yoshida

Phys. Lett. **B558**, 41-58 (2003).

Measurement of the  $\pi^- p \rightarrow 3\pi^0 \eta$  Total Cross Section from Threshold to 0.75 GeV/c

C. E. Allgower and H. Spinka

Phys. Rev. **C67**, 068201 (June 2003).

Narrowing of the Balance Function with Centrality in Au+Au Collisions at  $\sqrt{s_{NN}} = 130$  GeV

R. V. Cadman, K. Krueger, H. M. Spinka and D. G. Underwood

Phys. Rev. Lett **90**, 172301 (May 2003).

Observation of the Strange Sea in the Proton via Inclusive  $\phi$ -Meson Production in Neutral Current Deep Inelastic Scattering at HERA

S.Chekanov, D. Krakauer, S. Magill, B. Musgrave, J. Repond, R. Yoshida  
Phys. Lett. **B553**, 141-158 (2003).

Opaque Branes in Warped Backgrounds

M. Carena, E. Ponton, T.M.P. Tait and C.E.M. Wagner  
Phys. Rev. **D67**, 096006 (May 2003).

Overview of  $\tan \beta$  Determination at a Linear  $e^+e^-$  Collider

J. Gunion, T. Han, J. Jiang, and A. Sopczak  
In: *Hamburg 2002: Proceedings of the 10<sup>th</sup> International Conference on Supersymmetry and Unification of Fundamental Interactions (SUSY02)*, Vol. 2, ed. by P. Nath *et al.* (Hamburg, 2003) pp. 680-685.

POOL File Catalog, Collection and Metadata Components

C. Cioffi, S. Eckmann, D. Malon, A. Vaniachine, M. Girone, H. Schmuecker, J. Wojcieszuk, J. Hrivnac, and Z. Xie  
In: *Conference for Computing in High-Energy and Nuclear Physics (CHEP 03)*, La Jolla, California, 24-28 Mar 2003; eConfC0303241:MOKT009 (June 2003) cs.db/0306065.

Primary Numbers Database for ATLAS Detector Description Parameters

A. Vaniachine, S. Eckmann, D. Malon, P. Nevski, and T. Wenaus  
In: *Conference for Computing in High-Energy and Nuclear Physics (CHEP 03)*, La Jolla, California, 24-28 Mar 2003; eConfC0303241:MOKT006 (June 2003) cs.db/0306103.

Prototyping Virtual Data Technologies in ATLAS Data Challenge 1 Production

A. Vaniachine, D. Malon, P. Nevski and K. De  
In: *Computing in High Energy and Nuclear Physics (CHEP03)*, La Jolla, CA, eConfC0303241 TUCP012, cs.dc/0306102 (June 2003).

Puzzles in Cabibbo-Suppressed Charm Decays

F. E. Close and H. J. Lipkin  
Phys. Letts. **B551**, 337-342 (January 2003).  
ANL-HEP-PR-02-070

Puzzles in Hyperon, Charm and Beauty Physics

H. J. Lipkin  
Nucl. Phys. **B115**, 117 (February 2003).

Quantizing Dirac and Nambu Brackets

T. L. Curtright and C. K. Zachos

In: *Short Distance Behavior of Fundamental Interactions: 31<sup>st</sup> Coral Gables Conference on High Energy Physics and Cosmology*, ed. by B. N. Kursunoglu, *et al.* (AIP, June 2003) pp. 165-182.

Radiative Decay of  $\Upsilon(nS)$  into  $S$ -wave Bottomonium

E. L. Berger, G. T. Bodwin, and J. Lee

Phys. Letts. **B552**, 223-228 (January 2003).

RHIC pC CNI Polarimeter: Experimental Setup and Physics Results

H. Spinka, D.G. Underwood R. Cadman

AIP **675**, 819 (2003).

RHIC pC CNI Polarimeter: Status and Performance from the First Collider Run

H. Spinka, D. Underwood and R. Cadman

AIP **675**, 817 (2003).

Scaling Violations and Determination of  $\alpha_s$  from Jet Production in  $\gamma p$  Interactions at HERA

S. Chekanov, D. Krakauer, J. H. Loizides, S. Magill, B. Musgrave, J. Repond and R. Yoshida.

Phys. Lett. **B560**, 7-23 (May 2003).

Search for Associated Production of  $\Upsilon$  and Vector Boson in  $p\bar{p}$  Collisions at  $\sqrt{s} = 1.8$  TeV

R. E. Blair, K. L. Byrum, E. Kovacs, S. E. Kuhlmann, T. LeCompte, L. Nodulman

J. Proudfoot, R. Thurman-Keup, R. G. Wagner, A. B. Wicklund

Phys. Rev. Letts. **90**, 221803 (June 2003).

Search for Long-Lived Charged Massive Particles in  $p\bar{p}$  Collisions at  $\sqrt{s} = 1.8$  TeV

R. E. Blair, K. L. Byrum, E. Kovacs, S. E. Kuhlmann, T. LeCompte, L. Nodulman,

J. P. Proudfoot, R. Thurman-Keup, R. G. Wagner, A. B. Wicklund

Phys. Rev. Lett. **90**, 131801 (April 2003).

Search for the Supersymmetric Partner of the Top Quark in Dilepton Events from  $p\bar{p}$  Collisions at  $\sqrt{s} = 1.8$  TeV

R. E. Blair, K. L. Byrum, E. Kovacs, S. E. Kuhlmann, T. LeCompte, L. Nodulman,

J. Proudfoot, R. Thurman-Keup, R. G. Wagner and A. B. Wicklund

Phys. Rev. Lett. **90**, 251801 (June 2003).

Search for W' Boson Decaying to a Top and Bottom Quark in 1.8 TeV  $p\bar{p}$  Collisions

R. E. Blair, K. L. Byrum, E. Kovacs, S. E. Kuhlmann, T. LeCompte, L. Nodulman,  
J. Proudfoot, R. Thurman-Keup, R. G. Wagner and A. B. Wicklund  
Phys. Rev. Letts. **90**, 081802 (February 2003).

STAR Detector Overview

M. Beddo, R. V. Cadman, D. Hill, H. M. Spinka and D. G. Underwood  
Nucl. Instrum. & Meth. **A499**, 725 (2003).  
ANL-HEP-PR-03-45

The STAR Barrel Electromagnetic Calorimeter

M. Beddo, E. Bielick, T. Fornek, V. Guarino, D. Hill, K. Krueger, T. LeCompte,  
D. Lopiano, H. Spinka, D. Underwood and A. Yokosawa  
Nucl. Instrum. & Meth. **A725**, 2003.  
ANL-HEP-PR-03-46

SU(2) Lattice Gauge Theory at Nonzero Chemical Potential and Temperature

J. B. Kogut, D. Toublan, and D. K. Sinclair  
In: *Proceedings of the 20<sup>th</sup> International Symposium on Lattice Field Theory*  
(LATTICE 2002), ed. by R. Edwards, *et al.* (North-Holland, Amsterdam, May  
2003). Nucl. Phys. **B119** (Proc. Suppl.), 559-561 (May 2003).

Suggestions for Benchmark Scenarios for MSSM Higgs Boson Searches at Hadron Colliders

M. Carena, S. Heinemeyer, C.E.M. Wagner, and G. Weiglein  
Eur. Phys. J. **C26**, 601-607 (February 2003).

Technical Compact Essay Encyclopaedic Entry Contributions (10)

C. Zachos  
In: *Concise Encyclopedia of Supersymmetry and Noncommutative Structures in*  
*Mathematics and Physics*, edited by S. Duplij, W. Siegel, and J. Bagger (Kluwer,  
Dordrecht, June 2003).

The Puzzle of the Bottom Quark Production Cross Section

E. L. Berger  
Int. J. Mod. Phys. **A18**, 1263 (March 2003).

Two-Body Cabibbo-Suppressed Charmed Meson Decays

C.-W. Chiang, Z. Luo, and J. L. Rosner  
Phys. Rev. **D67**, 014001 (January 2003).

#### IV.B. Major Articles Submitted For Publication

Abelian D Terms and the Superpartner Spectrum of Anomaly Mediated Supersymmetry Breaking

B. Murakami and J. D. Wells  
Phys. Rev. D  
ANL-HEP-PR-03-10

A Compact Wakefield Measurement Facility

J. G. Power, W. Gai, J. Lewellen, S. Milton, K.J. Kim, J. Simpson, H. Wang, D. Finley and H. Carter  
Presented at Particle Accelerator Conference 2003 (PAC 2003), Portland, Oregon, May 12-16, 2003.  
ANL-HEP-CP-03-44

A New High Intensity Electron Beam for Wakefield Acceleration Studies

M.E. Conde, W. Gai, C. Jing, R. Konecny, W. Liu, J. G. Power, H. Wang and Z. Yusof  
Presented at Particle Accelerator Conference 2003 (PAC 2003), Portland, Oregon, May 12-16, 2003.  
ANL-HEP-CP-03-30

Dark Current and X Ray Measurements of an 805 MHZ Pillbox Cavity

J. Norem, P. Gruber, *et al.*  
Presented at Particle Accelerator Conference 2003 (PAC 2003), Portland, Oregon, May 12-16, 2003.  
ANL-HEP-CP-03-40

Differential Cross Sections for Higgs Boson Production at Tevatron Collider Energies

E. L. Berger and J. Qiu  
Phys. Rev. Letts.  
ANL-HEP-PR-03-28

Dijet Angular Distributions in Photoproduction of Charm at HERA

S. Chekanov, M. Derrick, D. Krakauer, J. H. Loizides, S. Magill, B. Musgrave, J. Repond and R. Yoshida  
Phys. Lett. B  
ANL-HEP-PR-03-12

Dipole Mode Wakefields in Dielectric-Loaded Rectangular Waveguide Accelerating Structures

C. Jing, W. Liu, L. Xiao, W. Gai and P. Schoessow  
Phys. Rev. E.  
ANL-HEP-PR-03-33

Does the  $S(1580)_{3/2}$ - Resonance Exist?

C. E. Allgower and H. Spinka  
Phys. Rev. Lett.  
ANL-HEP-PR-03-14

Horizontal Muons and a Search for AGN Neutrinos in Soudan 2

D. S. Ayres, T. Fields, M. C. Goodman, T. Joffe-Minor and J. Thron, *et al.*  
Astroparticle Phys.  
ANL-HEP-PR-03-17

Hunting for Glueballs in Electron-Positron Annihilation

S. J. Brodsky, A. S. Goldhaber, and J. Lee  
Phys. Rev. Letts.  
ANL-HEP-PR-03-024

Hybrid Inflation and Brane-Antibrane System

D. Choudhury, D. Ghoshal, D. P. Jatkar, and S. Panda  
JHEP  
ANL-HEP-PR-03-036

Implications of a DK Molecule at 2.32 GeV

T. Barnes, F. E. Close and H. J. Lipkin  
Phys. Rev. D  
ANL-HEP-PR-03-34

Measurement of Beam Driven Hydrodynamic Turbulence

J. Norem  
Presented at Particle Accelerator Conference 2003 (PAC 2003), Portland, Oregon,  
May 12-16, 2003.  
ANL-HEP-CP-03-39

Mechanisms Limiting High Gradient RF Cavities

J. Norem  
Presented at Particle Accelerator Conference 2003 (PAC 2003), Portland, Oregon,  
May 12-16, 2003.  
ANL-HEP-CP-03-38

Membranes and Consistent Quantization of Nambu Dynamics

C. Zachos  
Phys. Lett. B  
ANL-HEP-PR-03-051

New Neutrino Experiments

M. Goodman

In: IX<sup>th</sup> International Symposium on Particles, Strings and Cosmology, Mumbai, India, Pramana, Journal of Physics, Indian Academy of Sciences (2002).  
ANL-HEP-CP-03-35

New Physics Contributions to the  $B \rightarrow \Phi K_S$  Decay

C.-W. Chiang and J. L. Rosner

Phys. Rev. D  
ANL-HEP-PR-03-005

New Predictions for Multiquark Hadron Masses

H. J. Lipkin

Phys. Letts.  
ANL-HEP-PR-03-052

New Projects in Underground Physics

M. C. Goodman

Presented in Tenth International Symposium on Neutrino Telescopes, Venice, Italy, March, 2003.  
ANL-HEP-CP-03-41

Precision Electroweak Data and Unification of Couplings in Warped Extra Dimensions

M. Carena, A. Delgado, E. Ponton, T.M.P. Tait, and C.E.M. Wagner

Phys. Rev. D  
ANL-HEP-PR-03-29

RF Induced Backgrounds in MICE

J. Norem, D. Li, A. Bross, A. Moretti, Y. Torum, E. McKigney

J. Phys. G  
ANL-HEP-PR-02-088

Search for Pair Production of Scalar Top Quarks in R-parity Violating Decay Modes in  $p\bar{p}$  Collisions at  $\sqrt{s} = 1.8$  TeV

W. Ashmanskas, R. E. Blair, K. L. Byrum, E. Kovacs, S. E. Kuhlmann, T. LeCompte, L. Nodulman, J. Proudfoot, M. Tanaka, R. Thurman-Keup, R. G. Wagner and A. B. Wicklund

Phys. Rev. Letts.  
ANL-HEP-PR-03-47

Squark Mixing in Electron-Positron Reactions

E. L. Berger, J. Lee and T. M. P. Tait

Phys. Rev. D  
ANL-HEP-PR-03-27

The Pseudo-Goldstone Spectrum of 2-Colour QCD at Finite Density

J. B. Kogut, D. Toublan, and D. K. Sinclair  
Phys. Rev. D  
ANL-HEP-PR-03-22

Two-Body Charmless  $B$  Decays Involving  $\eta$  and  $\eta'$

C.-W. Chiang, M. Gronau and J. L. Rosner  
Phys. Rev. D  
ANL-HEP-PR-03-37

What is Coherent in Neutrino Oscillations

H. J. Lipkin  
Phys. Lett.  
ANL-HEP-PR-03-32

#### **IV.C Papers Or Abstracts Submitted To Conference Proceedings**

A Compact Wakefield Measurement Facility

J. G. Power, W. Gai, J. Lewellen, S. Milton, K.J. Kim, J. Simpson, H. Wang, D. Finley  
and H. Carter  
Presented at Particle Accelerator Conference 2003 (PAC2003), Portland, Oregon,  
May 12-16, 2003.  
ANL-HEP-CP-03-44

A New High Intensity Electron Beam for Wakefield Acceleration Studies

M.E. Conde, W. Gai, C. Jing, R. Konecny, W. Liu, J. G. Power, H. Wang and Z. Yusof  
Presented at Particle Accelerator Conference 2003 (PAC 2003), Portland, Oregon,  
May 12-16, 2003.  
ANL-HEP-CP-03-30

Data Challenges in ATLAS Computing

A. Vaniachine  
Presented at VIII International Workshop on Advanced Computing and Analysis  
Techniques (ACAT 2002), Moscow, Russia, June 24-28, 2002.  
ANL-HEP-CP-03-8

Deformation Quantization of Nambu Mechanics

C. K. Zachos and T. L. Curtright  
Proceedings of the 2002 Coral Gable Conference on “Short-Distance Behavior of  
the Fundamental Interactions”, Ft. Lauderdale, FL, December 11-14, 2002.  
ANL-HEP-CP-03-9

### High Power Testing of X-Band Dielectric-Loaded Accelerating Structures

J. G. Power, W. Gai, R. Konecny, C. Jing, W. Liu, S.H. Gold and A.K. Kinkead  
Proceedings of the 2003 Particle Accelerator Conference (PAC2003), Portland,  
Oregon, May 12-16, 2003.  
ANL-HEP-CP-03-43

### Inclusive Heavy-Quarkonium Production in Hadronic Collisions

G. T. Bodwin, J. Lee, and R. Vogt  
CERN Yellow Book for the 2001-2002 CERN Workshop on Hard Probes in  
Heavy Ion Collisions at the LHC, Geneva, Switzerland.  
ANL-HEP-CP-03-031

### Mechanisms Limiting High Gradient RF Cavities

J. Norem  
Presented at Particle Accelerator Conference 2003 (PAC 2003), Portland, Oregon,  
May 12-16, 2003.  
ANL-HEP-CP-03-38

### Measurement of Beam Driven Hydrodynamic Turbulence

J. Norem  
Presented at Particle Accelerator Conference 2003 (PAC 2003), Portland, Oregon,  
May 12-16, 2003.  
ANL-HEP-CP-03-39

### New Projects in Underground Physics

M. C. Goodman  
Presentation at the Tenth International Symposium on Neutrino Telescopes,  
Venice, Italy, March 2003.  
ANL-HEP-CP-03-41

### New Neutrino Experiments

M. Goodman  
Presented at IX<sup>th</sup> International Symposium on Particles, Strings and Cosmology,  
Mumbai, India, Pramana, Journal of Physics, Indian Academy of Sciences (2002).  
*not previously cited*  
ANL-HEP-CP-03-35

### POOL File Catalog, Collection and Metadata Components

C. Cioffi, S. Eckmann, D. Malon, A. Vaniachine, M. Girone, H. Schmuecker, J.  
Wojcieszuk, H. Hrivnac, and Z. Xie  
Proceedings of the 2003 Conference on "Computing in High Energy and Nuclear  
Physics" (CHEP03), La Jolla, CA, March 24-28, 2003.  
ANL-HEP-CP-03-096

Primary Numbers Database for ATLAS Detector Description Parameters

A. Vaniachine, S. Eckmann, D. Malon, P. Nevski, and T. Wenaus

Proceedings of the 2003 Conference on “Computing in High Energy and Nuclear Physics” (CHEP03), La Jolla, CA, March 24-28, 2003.

ANL-HEP-CP-03-050

Prototyping Virtual Data Technologies in ATLAS Data Challenge 1 Production

A. Vaniachine, D. Malon, P. Nevski, and K. De

Proceedings of the 2003 Conference on “Computing in High Energy and Nuclear Physics” (CHEP03), La Jolla, CA, March 24-28, 2003.

ANL-HEP-CP-03-049

Quantizing Dirac and Nambu Mechanics

T. Curtright and C. Zachos

Proceedings of the 2002 Coral Gable Conference on “Short-Distance Behavior of the Fundamental Interactions”, Ft. Lauderdale, FL, December 11-14, 2002.

ANL-HEP-CP-03-016

Slit Scattering Effects in a Well Aligned Pepper Pot

J. G. Power

Presented at Particle Accelerator Conference 2003 (PAC 2003), Portland, Oregon, May 12-16, 2003.

ANL-HEP-CP-03-42

#### **IV. D. Technical Reports And Notes**

##### **Technical Reports**

Analysis of AGS Polarimeter Data at  $G\gamma = 7.5$

R. V. Cadman, H.M. Spinka, D.G. Underwood

ANL-HEP-TR-03-7

High Energy Physics Division, Semiannual Report of Research Activities

H.M. Spinka, L.J. Nodulman, M.C. Goodman, J. Repond, D.S. Ayres, J. Proudfoot, R.

Stanek, T. LeCompte, G. Drake, E.L. Berger, G.T. Bodwin, D.K. Sinclair, C. Zachos, W.

Gai, J. Norem, C.E.M. Wagner

ANL-HEP-TR-03-48

## Neutrino Technical Reports

Proposal for a Five Year Run Plan for MINOS

D. Ayres et al

Internal for MINOS distribution

ANL-HEP-TR-03-62

### CDF Notes:

- CDF-6249** Understanding and Using Lshr  
Robert G. Wagner  
CDF/DOC/ELECTRON/CDFR/6249
- CDF-6259** Run IIb Upgrade for CDF L2 Decision Crate  
Ashmanskas, Blair, Bogdan, Dawson, Demaat, Frisch, Hahn, Keener,  
Kroll, Kwang, Lewis, Lin, Liu, Meyer, Patrick, Pitkanen, Proudfoot,  
Reisert, Sanders, Shochet, Spinella, van Berg, Wilson, Wittich  
CDF/DOC/TRIGGER/CDFR/6259
- CDF-6267** COT Central Outer Tracker  
COT Group (incl. V. Guarino, L. Nodulman, R Thurman-Keup)  
CDF/PUB/TRACKING/PUBLIC/6267  
Subm. NIMPR
- CDF-6288** Measurement of the Run II Inclusive J/psi Cross-section  
Tomohiro Yamashita, Slawomir Tkaczyk, Ting Miao, Dmitri Litvintsev,  
Jonathan Lewis, Thomas LeCompte, James Kraus, Yuri Gotra, Mary  
Bishai  
CDF/PHYS/BOTTOM/CDFR/6288
- CDF-6312** Diphoton central-central cross-section measurement at CDF RunII  
Yanwen Liu, Xin Wu, Raymond Culbertson, Robert Blair, Steve  
Kuhlmann,  
Joey Huston  
CDF/PHYS/CDF/PUBLIC/6312
- CDF-6364** A minbias calorimeter ntuple  
L. Nodulman  
CDF/DOC/CALORIMETRY/CDFR/6364
- CDF-6379** A Technique To Measure the Total b Quark Cross-Section  
Thomas J. LeCompte  
CDF/PHYS/BOTTOM/PUBLIC/6379

- CDF-6409** Godparent Committee Report on CDF5833  
A. Beretvas, B. Wicklund, C. Gay  
CDF/PHYS/BOTTOM/CDFR/6409
- CDF-6418** Initial Identification of Low Energy Photons in the Run II J/Psi  $\rightarrow$   $\mu^+$   $\mu^-$  Data  
Robert G. Wagner  
CDF/PHYS/BOTTOM/CDFR/6418
- CDF-6483** B Flavor Identification Using Opposite Side Muons  
Denys Usynin, Matthew Jones, Joseph Kroll, Barry Wicklund  
CDF/ANAL/BOTTOM/CDFR/6483
- CDF-6502** The CDF Silicon Vertex Trigger  
Ashmanskas, Barchiesi, Bardi, Bari, Baumgart, Belforte, Berryhill, Bogdan, Carosi, Cerri, Chlachidze, Culbertson, Dellorso, Donati, Fiori, Frisch, Galeotti, Giannetti, Glagolev, Leger, Liu, Maruyama, Meschi, Moneta, Morsani, Nakaya, Punzi, Rescigno, Ristori, Sanders, Sarkar, Semenov, Shochet, Speer, Spinella, Vataga, Wu, Yang, Zanello, Zanetti  
CDF/PUB/TRIGGER/PUBLIC/6502  
Pub. Proceedings 9th Pisa Meeting on Advanced Detectors, La Biodola, Isola d'Elba, Italy, May 25-31, 2003. FERMILAB-CONF-03/168-E
- CDF-6653** Proposal to install the new CPR2 inside the B0 collision hall  
J. Huston, S. Kuhlmann, S. Lami, M. Lindgren, P. Lukens, L. Nodulman, R. Roser  
CDF/DOC/CALORIMETRY/CDFR/6653
- CDF-6745** Stntuple modules for central jet four-momentum recalculation using tracks  
Fabrizio Margaroli Steve Kuhlmann  
CDF/ANAL/JET/CDFR/6745

**PDK Notes:**

- PDK-802** Horizontal Muons & A Search for AGN Neutrinos In Soudan 2  
D.S. Ayres, J. H. Cobb, T.H. Fields, M.C. Goodman, T. Joffe-Minor, J. L. Thron et al  
June 27, 2003

**WF-Notes:**

- WF-211** The Effects of Machine Errors in Dielectric Loaded Accelerating Structure  
W. Liu, C. Jing, R. Konecny, W. Gai, January 3, 2003.

- WF-212**      PARMELA Simulations of Electron Beam from the AWA Gun with 1 nC Charge  
                  H. Wang, W. Gai, January 2003.
- WF-213**      A Method to Propagate Beams of Unequal Charges through the same Lattice  
                  J. Power, February 5, 2003.
- WF-214**      A Matlab Solution of the 1D, 2D, and 3D Beam Envelope Equations  
                  J. Power, January 17, 2003.
- WF-215**      Multisplitter Calculator  
                  J. Power, April 16, 2003.
- WF-216**      Wakefield Measurements Using Low Energy Beams  
                  J. Simpson, April 29, 2003.
- WF-217**      On the Relation between Image Resolution and the estimated s of a Gaussian like  
                  Spot  
                  W. Liu and J. Power, May 30, 2003.

## V. COLLOQUIA AND CONFERENCE TALKS

### **Edmond L. Berger**

Light Bottom Squark Phenomenology

Department of Physics, University of Oregon, Eugene, April 21, 2003.

Light Bottom Squark Phenomenology

Department of Physics, Michigan State University, East Lansing, February 25, 2003.

Light Bottom Squark Phenomenology

Aspen Winter Conference on Particle Physics, CO, January 23, 2003.

Higgs Boson Decay into Hadronic Jets

Arlington Linear Collider Workshop, University of Texas, Arlington, January 10, 2003.

Light Bottom Squarks

Arlington Linear Collider Workshop, University of Texas, Arlington, January 9, 2003.

### **Geoffrey Bodwin**

Resummation of Large QCD Corrections to Heavy-Quarkonium Decay Rates

Department of Physics, University of Maryland, College Park, March 19, 2003.

### **Robert V. Cadman**

Spin (and Nuclear) Dependence of Parton Densities with STAR at RHIC

PHENO 2003, Madison, WI, May 5, 2003

### **John Campbell**

Vector Boson + Jet Production and the Monte Carlo MCFM

SLAC, Stanford, CA, May 7, 2003.

Vector Boson + Jet Production and the Monte Carlo MCFM

EFI, University of Chicago, IL, April 21, 2003.

Vector Boson + Jet Production and the Monte Carlo MCFM

Department of Physics, University of Wisconsin, Madison, March 7-8, 2003.

Overview of the Monte Carlo Program MCFM

Phenomenology Monte Carlo at Hadron Colliders Workshop, U Durham, UK, January 14-17, 2003.

### **Chengwei Chiang**

Extracting New Physics Information in the  $B \rightarrow \phi K_S$  Decay

PHENO 2003, Madison, WI, May 5-7, 2003.

Strong Phase Information in Heavy Meson Decays

Department of Physics, University of Wisconsin, Madison, April 11, 2003.

Phenomenology of Light Bottom Squark in MSSM

Department of Physics, University of Minnesota, Minneapolis, April 10, 2003.

Final State Phases in B and D Meson Decays

TRIUMF, Vancouver, Canada, February 16-18, 2003.

### **Jing Jiang**

NLO Charged Higgs production at the LHC

LoopFest, BNL, Upton, NY, May 14-16, 2003.

NLO  $bg \rightarrow tH$  at the LHC

PHENO 2003, Madison, WI, May 5-7, 2003.

Higgs Mechanism and Phenomenology

Physics Department, Southern Methodist University, Dallas, TX, February 17, 2003.

### **Jungil Lee**

Glueball Hunting and Exclusive Charmonium-Pair Production at Belle

ANL-HEP Lunch Seminar, May 27, 2003.

Exclusive Double-Charmonium Production in  $e^+e^-$  Annihilation

Triangle Nuclear Theory Colloquium (TNT), Raleigh, NC, May 13, 2003.

Hunting for Gluonia in  $e^+e^-$  Annihilation

CLEO Collaboration Meeting, Cornell University, Ithaca, NY, April 11, 2003.

Exclusive Double-Charmonium Production in  $e^+e^-$  Annihilation

Department of Physics, Cornell University, Ithaca, NY, April 10, 2003.

Exclusive Double-Charmonium Production in  $e^+e^-$  Annihilation

Department of Physics, JLAB, Newport News, VA, March 16-23, 2003.

Exclusive Double-Charmonium Production in  $e^+e^-$  Annihilation

Department of Physics, University of Kentucky, Lexington, March 7, 2003.

### **Harry J. Lipkin**

Neutrino Oscillations--How States with Different Masses Can Be Coherent

Workshop on Trends in Neutrino Physics, Argonne, IL, May 12-16, 2003.

Implications of a DK Molecule Model and Other Tetraquark Models for the Charmed-Strange Resonance at 2.32 GeV

Department of Physics, University of Maryland, College Park, May 8, 2003.

Experimental Challenges for QCD—The Past and the Future

Physics Department, University of California, Irvine, March 11, 2003.

Neutrino Oscillations and Coherence. Friends of Boris Day

Invited talk presented at the KITP Neutrino Workshop, UC-Santa Barbara, March 6, 2003.

### **Brandon Murakami**

Ancillary Abelian Symmetry Solution to the AMSB Slepton Problem

Invited talk presented at SUGRA 20, Boston, MA, March 20, 2003.

Ancillary Abelian Symmetry Solution to the AMSB Slepton Problem

PHENO 2003, U Wisconsin, Madison, May 5, 2003.

Anomaly Mediated Supersymmetry Breaking and the Ancillary U(1) Formalism

Fermilab, Batavia, IL, April 24, 2003.

Ancillary Abelian Symmetry Solution to the AMSB Slepton Problem

The 11<sup>th</sup> Annual International Conference on Supersymmetry and Unification of the Fundamental Interactions (SUSY 2003: Supersymmetry in the Desert), Tucson, AZ, June 7, 2003.

Anomaly-Mediated Supersymmetry Breaking: Wonders and Slepton Solutions

High Energy Physics Division Lunch Seminar, Argonne, IL, March 11, 2003.

### **Jim Norem**

Dark current and x ray measurements of an 805 MHz pillbox cavity

Particle Accelerator Conference, Portland OR, May 12 - 16, 2003

Measurement of beam driven hydrodynamic turbulence

Particle Accelerator Conference, Portland OR, May 12 - 16, 2003

Mechanisms limiting high gradient rf cavities

Particle Accelerator Conference, Portland OR, May 12 - 16, 2003

RF Backgrounds in the Muon Ionization Cooling Experiment.

NuFact 03 Columbia University, June 5-11, 2003

### **Geraldine Servant**

Radionactive Universe

8<sup>th</sup> Itzykson Meeting—"Which Model for the Primordial Universe?", Saclay, France, June 19, 2003.

Constraints on Models with TeV Compactification Scale from Cosmology

6<sup>th</sup> European Meeting—From the Planck Scale to the Electroweak Scale (Planck 2003), CSIC, Madrid, Spain, May 30, 2003.

Constraints on TeV Extra Dimensions from Primordial Cosmology

PHENO 2003, U Wisconsin, Madison, May 6, 2003.

Dark Matter and New Physics

Physics Division, Michigan State University, East Lansing, April 29, 2003.

Radion Cosmology

EFI, University of Chicago, IL, April 23, 2003.

Constraints on Theories with Extra Dimensions from Radion Cosmology  
Physics Division, University of Wisconsin, Madison, April 10, 2003.

Dark Matter and New Physics  
CEA/Saclay, Paris, France, January 29, 2003.

### **Carlos Wagner**

Electroweak Baryogenesis in the MSSM  
Workshop on Baryogenesis, U Michigan, Ann Arbor, June 2003.

Precision Electroweak Data, Unification of Couplings and Collider Phenomenology  
11<sup>th</sup> Annual International Conference on Supersymmetry and Unification of the  
Fundamental Interactions (SUSY 2003: Supersymmetry in the Desert), Tucson, AZ, June  
5-10, 2003.

Supersymmetry and the Matter-Antimatter Asymmetry  
Department of Physics, Texas A&M University, College Station, May 21, 2003.

Physics of Extra Dimensions  
Argonne National Laboratory Theory Meeting, Argonne, IL, April 14, 2003.

Electroweak Baryogenesis and Low Energy Supersymmetry  
Plenary talk, SUGRA 20, Boston, MA, March 17-18, 2003.

Extra Dimensions  
LDRD Symposium, Argonne National Laboratory, IL, March 2003.

Supersymmetry, the Baryon Asymmetry and the Origin of Mass  
Department of Physics, University of Chicago, IL, February 20, 2003.

Electroweak Baryogenesis and Low Energy Supersymmetry  
Aspen Winter Conference on Particle Physics--At The Frontiers of Particle Physics,  
Aspen Center for Physics, CO, January 19-25, 2003.

### **Cosmas Zachos**

Membranes and Consistent Quantum Nambu Mechanics  
Invited talk at the 8<sup>th</sup> International Wigner Symposium, New York, May 28, 2003.

Deformation Quantization, Superintegrability, and Nambu Mechanics  
Enrico Fermi Institute, University of Chicago, IL, January 8, 2003.

## **VI. HIGH ENERGY PHYSICS COMMUNITY ACTIVITIES**

### **Edmond L. Berger**

Scientific Program Committee, V<sup>th</sup> Rencontres du Vietnam, Hanoi, Vietnam, August 6-11, 2004.

Co-Chair, Aspen Winter Conference on Particle Physics, “Where we are and Where we are going”, Aspen Center for Physics, CO, February 1-7, 2004.  
(<http://gate.hep.anl.gov/berger/Aspen04>)

International Advisory Committee, HADRON 2003, Aschaffenburg, Germany,  
August 31—September 6, 2003.

Scientific Organizing Committee and Convener of the Session on the Polarized Gluon Density,  
Fourth Circum-Pan-Pacific Symposium on High Energy Spin Physics, University of  
Washington, Seattle, August 4-7, 2003.

Organizing Committee, 8th Conference on the Intersections of Particle and Nuclear Physics  
(CIPANP 2003), New York, May 19-24, 2003.

Co-Organizer, Argonne Theory Institute on Trends in Neutrino Physics, High Energy Physics  
Division, Argonne, IL, May 12-16, 2003.

Organizer, Argonne Lab-Wide Theory Afternoon, April 14, 2003.

Leader, North American Node, Quarkonium Working Group QWGNET Proposal to the  
European Community to fund a Marie Curie Research Training Network on Heavy  
Quarkonium, 2003.

Scientific Program Organizing Committee, XXXVII<sup>th</sup> Rencontres de Moriond, QCD and High  
Energy Hadronic Interactions, Les Arcs, Savoie, France, March 22-29, 2003.

Scientific Advisory Board, Argonne Theory Institute, 2003—  
(<http://www.anl.gov/OPA/theoryinstitute/index.html>)

Search Committee, Argonne/University of Chicago Joint Appointment in Particle Physics, 2002-  
2003.

Member, American Linear Collider Working Group, 2002—

Member, Committee on International Scientific Affairs, American Physical Society, 2003—

Member, Andrew Gemant Award Committee, American Institute of Physics, 2002—

Adjunct Professor of Physics, Michigan State University, East Lansing, MI, 1997—present.

Member, Coordinated Theoretical-Experimental Project on QCD (CTEQ) Collaboration

### **Geoffrey T. Bodwin**

Convener, Production Section, Quarkonium Working Group QWNET Proposal to fund a Marie Curie Research Training Network on Heavy Quarkonium, 2003—

Member, Local Organizing Committee, Second International Workshop on Heavy Quarkonium, Fermilab, 2003—

Member, Quarkonium Working Group, 2002—

Member, Working Group on Heavy Flavors, Workshop on Hard Probes in Heavy Ion Collisions, CERN, 2001—

### **Wei Gai**

Committee: Scientific Advisory and Organizing Committee, Advanced Accelerator Concepts Workshops, Oxnard, CA 2002, and Stony Brook, NY, 2004.

### **Maury Goodman**

Member Particle Data Group

International Advisory Committee, Neutrino 2004 conference (Paris)

Nominations Committee, Forum on Physics and Society of the American Physical Society

Investments Committee of the American Physical Society

Program Committed of the Weak Interactions and Neutrinos Workshop, WIN 2003, Lake Geneva Wisconsin, October 2003

Organizing Committee, Workshop on Trends in Neutrino Physics, Argonne, May 12-16, 1003.

Chairman of the Organizing Committee, 2<sup>nd</sup> NuMI Off-Axis Experiment Detector Workshop at Argonne National Laboratory, April 25-27, 2003

Organizing Committee, Workshop on Future Low-Energy Neutrino Experiments, April 29-May 2, 2003, Tuscaloosa, Alabama

Editor, Long-Baseline Newsletter

### **Harry Lipkin**

Member, International Advisory Committee, HADRON 2003, Aschaffenburg, Germany, August 31--September 6, 2003.

### **James Norem**

Member of Muon Collaboration Technical Committee

### **Carlos Wagner**

Co-organizer, Argonne Workshop on Branes and Generalized Dynamics, Argonne, IL, October 20-24, 2003.

Head, Theory Committee, Argonne National Laboratory, 2003--

Organizer, Baryogenesis Workshop, U. Michigan, Ann Arbor, June 9-27, 2003.

Co-organizer, Argonne Workshop on Trends in Neutrino Physics, Argonne, IL, May 12-16, 2003.

Search Committee, Argonne/U Chicago Joint Faculty Position, 2002--2003.

Head, Theory Group, HEP Division, Argonne National Laboratory, September 2002—

Associate Professor, Lecturer for Courses on Supersymmetry and Advanced Electrodynamics, U Chicago, IL, 2000--2003.

**Cosmas Zachos**

Principal Organizer, Argonne Workshop on Branes and Generalized Dynamics, Argonne, IL, October 20-24, 2003.

Member, International Advisory Board of the 8<sup>th</sup> International Wigner Symposium, New York, May 27-30, 2003.

Member, International Advisory Board of the (Next) Conference on Differential Geometric Methods in Theoretical Physics, 2003.

Member, Advisory Panel, J. Phys A: Math Gen (IOP).

## VII. HEP DIVISION RESEARCH PERSONNEL

### *Administration*

Price, L.

Hill, D.

### *Accelerator Physicists*

Conde, M.

Norem, J.

Gai, W.

Power, J.

Yusof, Z.

### *Experimental Physicists*

Ayres, D.

Musgrave, B.

W. Ashmanskas

Nodulman, L.

Blair, R.

Proudfoot, J.

Byrum, K.

Repond, J.

Cadman, R.

Reyna, D.

Chekanov, S.

Spinka, H.

Derrick, M.

Stanek, R.

Fields, T.

Talaga, R.

Goodman, M.

Tanaka, M.

Joffe-Minor, T.

Thron, J.

Krakauer, D.

Underwood, D.

Kuhlmann, S.

Wagner, R.

LeCompte, T.

Wicklund, A.

Magill, S.

Xia, L.

May, E.

Yokosawa, A.

Yoshida, R.

### *Theoretical Physicists*

Berger, E.

Servant, G.

Bodwin, G.

Sinclair, D.

Campbell, J.

Wagner, C.

Chiang, C. W.

White, A.

Jiang, J.

Zachos, C.

Lee, J.

Murakami, B.

### ***Engineers and Computer Scientists***

Dawson, J.  
Drake, G.  
Grudzinski, J.  
Guarino, V.  
Gieraltowski, J.

Hill, N.  
Karr, K.  
Kovacs, E.  
Malon, D.  
Schlereth, J.  
Vaniachine, A.

### ***Technical Support Staff***

Adams, C.  
Ambats, I.  
Anderson, S.  
Cox, G.  
Cundiff, T.  
Farrow, M.  
Franchini, F.  
Kasprzyk, T.

Konecny, R.  
Matijas, Z.  
Nephew, T.  
Reed, L.  
Haberichter, W.  
Rezmer, R.  
Skrzecz, F.  
Wood, K.

### ***Laboratory Graduate Participants***

Loizides, J.  
Miglioranzi, S.

Jing, C.  
Morrissey, D.  
Wang, H.

### ***Visiting Scientists***

Kovacs, E. (Theory)  
Krueger, K. (STAR)  
Liu, W. (AWA)

Lipkin, H. (Theory)  
Ramsey, G. (Theory)  
Uretsky, J. (Theory)